UNIVERSIDADE D
COIMBRA

Duarte Miguel Coelho Silva

Asymetric Baryo/Dark Genesis

Dissertação no âmbito do Mestrado em Física Nuclear e de Partículas orientada Professor Doutor João Pedro Trancoso Gomes Rosa e apresentada ao Departamento de Física da Faculdadede Ciências e Tecnologia da Universidade de Coimbra.

outubro de 2021

Abstract

In this work, we propose a model for which a comparable cosmological dark and baryonic matter energy density naturally arises. Based on Supersymmetry, we developed a model where dark matter has an identical gauge structure and unification conditions at high energies as the Standard Model. We generalize the Affleck-Dine mechanism for Baryogenesis to be also responsible for the generation of Dark matter's number density, the Dark-genesis. We show that in these two sectors the ratio of the number densities and masses almost counter-balance each other, resulting in comparable energy densities in a natural way. We achieve this goal without requiring a mass or number coincidence between the sectors. This model may give rise to an asymmetric reheating, evading constrains imposed by Primordial Big Bang Nucleosynthesis and the Cosmic Microwave Background. We propose the dark-neutron as a dark matter candidate, capable of replicating the approximately spherical distributions, as presented by evidence of dark matter in galaxies. The viability conditions of the model are discussed, imposing a subdominant abundance of the Lightest Supersymmetric Particle (LSP). This scenario predicts comparable baryon and dark matter isocurvature perturbations that can be tested with CMB anisotropies and 21 cm line observations.

Keywords: Dark Matter, Baryogenesis, Asymmetric Reheating, Unification, Supersymmetry

Resumo

Neste trabalho, propõe-se um modelo no qual densidades comparáveis de matéria escura e bariónica emergem naturalmente. Baseado em Supersimetria, é criado um modelo em que a matéria escura tem uma estrutura de gauge e condições de unificação a altas energias idênticas àquelas do Modelo Padrão. Generaliza-se o mecanismo de Affleck-Dine para a Bariogénese, de forma a ser também responsável pela "génese da matéria escura". Mostra-se que estes sectores podem tem massas e densidades populacionais que contrabalançam uma com a outra de forma a criar densidades de energia comparáveis nos dois sectores, sem necessitar de alguma coincidencia de massa ou número. Este modelo poderá dar lugar a um Reheating assimétrico, escapando às condições impostas pela Nucleossíntese Primordial e pela Radiação Cósmica de Fundo. Apresentamos como candidato à matéria escura o neutrão-escuro, capaz de replicar as distribuições aproximadamente esféricas apresentadas pela evidência de matéria escura nas galáxias. São apresentadas as condições de viabilidade do modelo, impondo uma abundância subdominante da LSP, a partícula supersimétrica mais leve. Medições do espectro de potência das perturbações de isocurvatura bariónica a partir de observações futuras da linha de 21cm do Hidrogénio poderão vir a ser úteis, após comparação com o espetro das perturbações de isocurvatura de matéria apresentadas na Radiação cósmica de fundo. Estas duas observações poderão trazer informações cruciais na testagem do modelo apresentado neste trabalho.

Palavras-Chave: Matéria Escura, Bariogénese, Reheating Assimétrico, Unificação, Supersimetria

I want to dedicate this work to my father, my mother and my sister, the giants who have always carried me on their shoulders.

Agradecimentos

Gostava de começar por agradecer à Fundação para a Ciência e Tecnologia (FCT) por ter financiado através do projecto "Tidal deformability of neutron stars" de 09/2019 até 08/2020. Também tenho a agradecer ao Departamento de Física (DF) e, em particular, à Prof. Dra. Constança Providência por me ter incluído em um dos seus grupos de investigação (CFisUC), por me ter permitido usar um dos gabinetes, por me ter emprestado um cartão do departamento e pela disponibilidade oferecida para ajudar os seus estudantes. Sinto-me privilegiado por ter tido a oportunidade de estudar num ambiente familiar onde professores, investigadores e funcionários fazem qualquer visitante sentir-se bem vindo. Posso dizer que, durante estes anos, vi o DF como uma segunda casa.

Sinto-me grato por ter tido o Prof. Dr. João Rosa como orientador. Em tempos menos favoráveis, foi notável o conhecimento, inspiração e ideias que me transmitiu. Penso que o tema de investigação que me propôs não podia ter sido mais acertado, uma vez que tive a oportunidade de estudar a maioria dos temas que me trouxeram para a física em 2015. Um especial agradecimento à dedicação e preocupação oferecida na revisão deste trabalho e por me ter integrado no seu grupo de trabalho.

Por último, quero deixar um agradecimento especial à minha família e amigos. Ao meu pai por toda a sabedoria e lições que me tem vindo a transmitir, à minha mãe pelo seu carinho incondicional, à minha irmã por constantemente me expandir os horizontes. Ao meu avô João† por me ter explicado porque não se deve ter 1000 fichas triplas ligadas à mesma tomada, à minha avó Maria pela sua força de vontade e pelas suas orações, ao meu avô António† pelas tardes a jogar às Damas e à minha avó Manuela† por me arrumar sempre o quarto dos brinquedos. Às amizades que criei no curso: à Joana pela motivação nos momentos mais difíceis, pelos jantares fora e pausas do estudo e, claro, pelas aulas de (g)astronomia; à família "El Bagaço" quero vos agradecer por todas as histórias, inventadas ou vividas, criadas ao longo destes anos. Vocês deram um significado especial a tudo isto. Obrigado!

Contents

List of Figures

List of Tables

Chapter 1

Introduction

Cosmology is the branch of physics that studies the origin, composition, evolution and fate of the universe on large scales (> 100 Mpc). Although it is arguable that the beginning of this area can be traced back to any time in the history of humanity, when there was a very thin line between physics and philosophy, it is well accepted that cosmology as we it know today had its origins in the beginning of the 20th century, after Einstein, Friedmann, Hubble and many others revolutionized the way we look at the sky. Today's comprehension of cosmology is based on the *Standard Model of particle physics* (SM) and *General Relativity* (GR).

The Standard Model is the most accepted model of particle physics and describes the three remaining forces of nature: the electromagnetic, the strong and the weak forces. Every particle physics interaction arises by imposing certain space-time and internal symmetries (gauge symmetries). It describes the universe's matter content as composed by fundamental "matter-"particles, and forces as the interchange of particles known as bosons, which naturally arise from the gauge symmetries. However, the Standard Model is just an effective theory at low energies and high energy phenomena may require some extensions. One of the possible extensions is supersymmetry (SUSY), which implies the existence of new massive particles that may be observable in the near future in particle colliders at the TeV scale ($M_S \sim 1000$ GeV), which is thought to be the supersymmetry breaking scale. Another relevant extension is believed to happen at very large scales $M_{GUT} \sim 10^{16}$ GeV, where the three SM forces unify into a single one.

General relativity is our most accepted theory of gravitation. It was first published by Einstein and describes gravity as a manifestation of the curvature of spacetime caused by the presence of energy. Compared to the preceding Newtonian gravity, this theory not only was able to calculate to a better accuracy some aspects of the solar system's planetary dynamics (such as the famous perihelion precession of Mercury) but also predicted the existence of Black Holes and the bending of light trajectories due to the presence of gravitational fields, firstly observed by Arthur Eddington and his team in 1929. Presently, in order to agree with cosmological observations, General Relativity predicts that the universe should be mainly composed of (non-relativistic) matter ($\sim 30\%$) and a mysterious fluid that causes the universe to expand in an accelerated fashion, the so-called *Dark Energy* ($\sim 70\%$).

The Standard Model, together with General Relativity, have conceived the (inflationary) Big Bang theory, the most accepted theory of the cosmological history of the universe. This theory tells us that the universe has been expanding and cooling down since the very beginning, when it was very hot and dense. The successes of this theory are immense. For instance, it has been remarkable in explaining the light element (such as hydrogen, helium and deuterium) abundances in the universe, the origin of the *Cosmic Microwave Background* and its anisotropies, and the formation of galaxies. However, what happened

at high energy scales $M \gtrsim 1000$ GeV or, equivalently, in the first 10^{-10} seconds is still a mystery in cosmology. Although one could be misled to think that such a small time-scale has nothing interesting to offer, it is in this epoch that many of the present cosmological problems took place, such as baryogenesis, dark(matter)genesis, the grand unification of the SM forces and quantum gravity.

Observational evidence shows that only roughly 15% of the universe's matter density is made of baryons i.e. structures composed by standard model particles . Roughly 85% of the universe's matter density corresponds to an unknown form of matter know as *dark matter*. This lifts two questions: 1) what is dark matter made of and 2) why are the densities of dark (ρ_d) and baryonic (ρ_b) matter comparable ($\rho_d/\rho_b \sim 5 \sim \mathcal{O}(1)$)? The second question is a coincidence that could, in principle, be solved if the two sectors had a particle-generating mechanism in common. Some models have addressed the second question by generating comparable number densities in both sectors. However, the coincidence is in the energy $\rho_b = n_b m_b$, not in the number densities, and we would go from an energy-coincidence problem to a mass-coincidence problem:

$$\frac{\rho_d}{\rho_b} = \frac{n_d}{n_b}\frac{m_d}{m_b} = \mathcal{O}(1)\frac{m_d}{m_b} \tag{1.1}$$

In this work, we address these two questions. Based on supersymmetry, we will describe a model for dark matter with an identical gauge group structure and unification conditions at high energies as the Standard Model. We will generalize the concept behind the Affleck-Dine mechanism, an existing mechanism proposed for baryogenesis, to be also behind the dark-genesis. We will see that in these two sectors have number densities are almost inversely proportional to the corresponding supersymmetry breaking scale, which can be very different in the two sectors. We will see that the mass of the stable particles in each sector is also related to the same scale, but in an almost-proportional way. As a result, the masses and number densities will almost counter-balance each other, resulting in a very natural $\mathcal{O}(1)$ factor between energy densities.

In Chapter 2, we will firstly present the appropriate model for large scale cosmology after a brief introduction to general relativity and to observational motivations. In a second moment we will discuss the implications of the equilibrium thermodynamics in the evolution of the universe and we end the chapter with evidence for the existence of dark matter. In Chapter 3 we will describe some relevant aspects of the Standard Model and introduce the *Minimal Supersymmetric SM* (MSSM). Some candidates dark matter proposed in the literature are discussed at the end of this chapter.

In Chapter 4, we discuss how an epoch of accelerated expansion at the beginning of the universe may solve some problems arising in the standard cosmology model. At the end of the chapter, we explain how inflation may provide useful information for high energy physics. In Chapter 5, we approach the conditions for baryogenesis and we present a summary of proposed mechanisms. Finally, we reach this chapter's main objective of explaining the Affleck-Dine mechanism, some analyses that we have done and its application to the MSSM and baryogenesis. In Chapter 6, we present our model for dark and baryo-genesis, some of its cosmological implications and, at the end of the chapter, we present how it can be tested as new observational evidence becomes available. In Chapter 7, we exhibit our concluding remarks and future work perspectives.

Through the course of this work, we will be using the $c = \hbar = k_B = 1$ units:

$$[\text{Energy}] = [\text{Temperature}] = [\text{Mass}] = [\text{Time}]^{-1} = [\text{Length}]^{-1}$$

Chapter 2

Standard Cosmology

"Our whole universe was in a hot and dense state, then nearly fourteen billion years ago expansion started."

— Big Bang Theory Theme

The present standard cosmological paradigm is that the universe evolved from a state of very high temperature and energy density, and began a period of adiabatic expansion - the *Big Bang theory*. As the universe cooled, elements like hydrogen and helium were formed and matter clumped together to form galaxies, stars and planets. This expansion has left some relics that are observable today such as the Cosmic Microwave Background (CMB), the Large Scale Structure (LSS), the baryon number asymmetry and dark matter. Since the universe has been through such high energies, recent cosmological observations [12] might provide crucial information to our understanding of the nature of particle physics, gravity and cosmology.

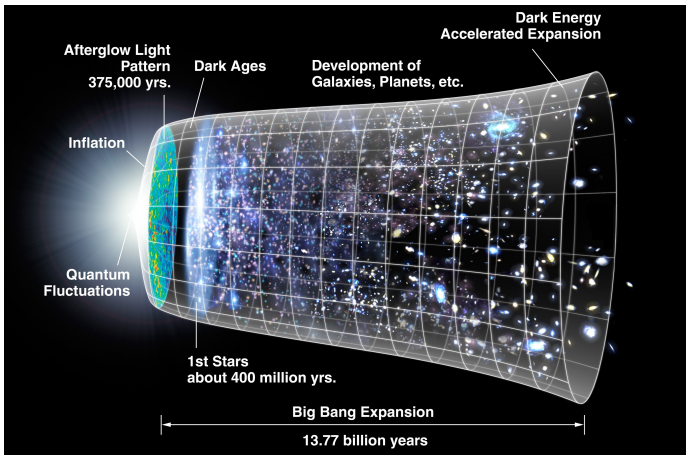

Figure 2.1: The Hot Big Bang Model [1]

2.1 Some Cosmological Observations

This section is dedicated to the discussion of a set of cosmological observations relevant for the subsequent work.

Expanding Universe

One of the most important observations in the history of cosmology is that the universe expanding. This observation was first made by Edwin Hubble [13] and its student Milton Humason while measuring the Doppler shift of our neighbour galaxies ($d < 2$ Mpc). He noticed that the distance to some galaxy and the redshift of its light were proportional:

$$v = Hd \tag{2.1}$$

where the proportionally "constant" is actually time dependent, and is called the *Hubble parameter*. Subsequent observations have verified this fact (Figure 2.2) serving as proof that the universe is expanding (distances get stretched in time just like the distance between two points drawn on a balloon as it is inflated). The Hubble parameter is then related to the rate of change of the scale factor[1] $a(t)$ as:

$$H(t) = \frac{\dot{a}(t)}{a(t)} \tag{2.2}$$

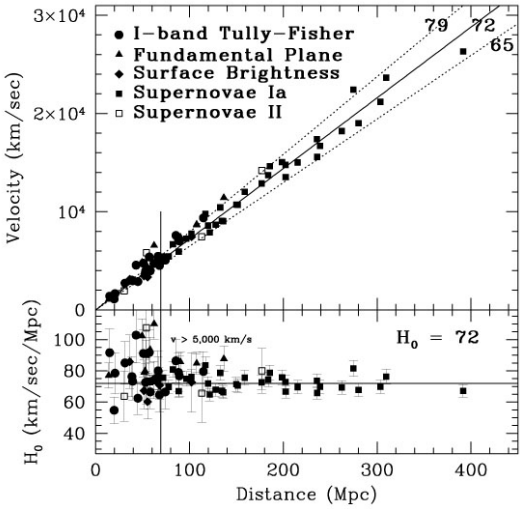

Figure 2.2: Evidence for expansion [2]

The present Hubble parameter measurements place $H_0 = 67.4 \pm 0.5$ kms^{-1}Mpc^{-1} [3] and using the fact that the inverse of the Hubble parameter sets the scale for the age of the universe (Section 2.2), we get $t \sim H_0^{-1} = 13.797 \pm 0.023$Gyr.

Furthermore, it has been measured that the expansion is currently accelerating. As we will see in Section 2.2, this characteristic cannot be produced by ordinary matter and is an indication that some exotic fluid that counteracts gravity should be present in the universe. This fluid is called *dark energy* and is usually associated to vacuum energy (or equivalently, the cosmological constant). Its precise nature represents one of the biggest mysteries of contemporary cosmology.

Cosmic Microwave Background

The Cosmic Microwave Background (CMB) is a Big Bang relic from the time when the temperature of the universe was roughly $T \sim 3000$K ($T \sim 0.1$ eV). At this time, the temperature became low enough so that electrons and protons could become bounded into hydrogen and helium atoms - the *recombination*. Until this time, the universe was so dense that every photon emitted would rapidly be absorbed. As the universe expanded, some photons started to escape - the *decoupling*. These are the photons we observe today in the CMB, emitted at the time of decoupling when the temperature was around $T \sim 3000$ K. As the universe expanded, their wavelength got stretched and today are observed at a

[1] The scale factor is a dimensionless multiplicative factor that accounts for how a distance changes as the space expands. Ex: $d(t_0) = \Delta x \rightarrow d(t) = a(t)\Delta x$.

temperature of 2.725 K. This effect was predicted in 1948 by Alpher, Bethe and Gamow [14] and was discovered by accident by Arno Penzias and Robert Wilson. This discovery was paramount to the validation of the Hot Big Bang model.

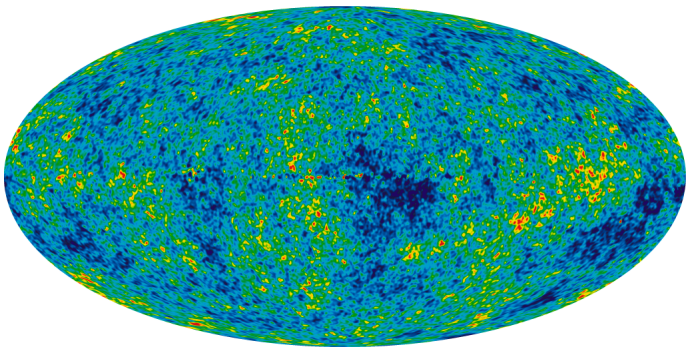

Figure 2.3: $T = 2.7255 \pm 0.0006$ K [3]

The CMB is uniform up to temperature fluctuations of the order $\Delta T/T \sim 10^{-5}$. This fact reveals that photons and matter were in *thermal equilibrium* at the time of decoupling and serves as evidence for the *large-scale isotropy and homogeneity* of the observable universe. The degree of isotropy is so remarkable that even regions which appear to not have ever been in causal contact share the same temperature, which brings up a problem known as *the Horizon Problem* (Section 4.1).

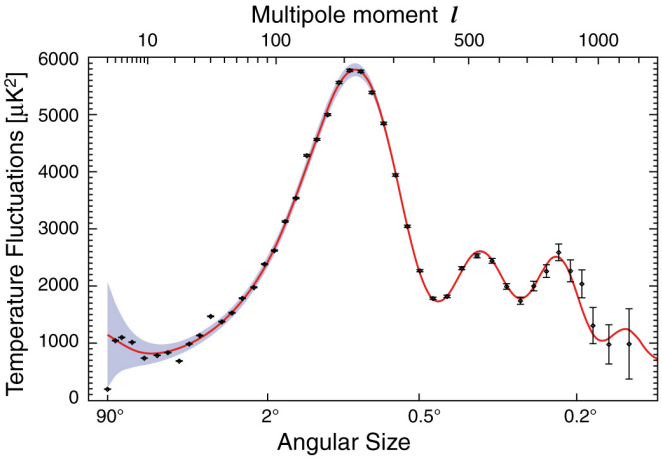

Figure 2.4: The CMB angular spectrum [1].

The statistical properties of the anisotropies[2] provide crucial information on the determination of the universe's curvature from the position of the first peak (at $\theta \sim 1^o$), on explaining the origins of large-scale structure from the evolution of matter perturbation [15] and also puts bounds on the composition of the universe at the time the CMB was emitted.

In particular, the location of the first peak ($l \sim 225$) suggests that the universe is nearly flat [3] and its density is very close to the *critical density* (Section 2.2):

$$\rho_c = 1.88 \times 10^{-29} h^2 \text{gcm}^{-3} \qquad h = 0.704 \pm 0.025 \tag{2.3}$$

Neutrinos are not easy to detect, however, they contribute to entropy and energy density. The CMB bounds the number of light neutrino species to $N_\nu = 2.97^{+0.17}_{-0.17}$ [3].

[2] As an example, Figure 2.4 is obtained by dividing the sky in l+1 regions and measuring the correlations between them, more information provided by Daniel Baumann in [10].

2.2 Standard Model of Cosmology

General Relativity

For a long time, the study of gravity was ruled by Newton's theory of Gravitation, which stated that every massive (m_1) object would exert an instantaneous attractive *force* on the surrounding massive (m_2) objects, proportional to the product of their masses ($F_g \propto m_1 m_2$). However, in 1915 after publishing his famous work on *special relativity*, Einstein came to change the interpretation of gravity with the theory of *general relativity*. He proposed, based on the *Einstein's equivalence principle*, that gravity is not a force, but a manifestation of the *curvature* of the background spacetime that affects every object in the same way.

Einstein's Equivalence principle - the rest mass and the gravitational mass of any object are equal $m_r = m_g$. In local regions of spacetime, it is impossible to distinguish between being in an accelerated frame or in the presence of a uniform gravitational field of the same strength.

- Gravity induces the same acceleration to objects, regardless of their masses.
- In small regions, spacetime should appear flat to a local inertial observer.

In this sense, gravity should not be treated as a force, but as a manifestation of some feature of the background.

In this theory, spacetime may have some complicated curved geometry, being approximately flat in the neighbourhood of every point. The appropriate mathematical structure to describe this spaces is a *differential manifold*, M, equipped with a *metric*, $g_{\mu\nu}$, an object that describes its geometry and gives a notion of distances. The line element is written as:

$$ds^2 = g_{\mu\nu} dx^\mu dx^\nu \tag{2.4}$$

With the requirement that this theory should reduce to Newtonian gravity at low energies, Einstein arrived at a formula known as *Einstein's equations*:

$$\boxed{R_{\mu\nu} - \frac{1}{2} g_{\mu\nu} R + \Lambda g_{\mu\nu} = 8\pi G T_{\mu\nu}} \tag{2.5}$$

where $R_{\mu\nu}$, R, $T_{\mu\nu}$ and Λ are the Ricci tensor, Ricci scalar, the Stress-Energy tensor and the *cosmological constant*, respectively. These equations can be obtained from the action principle by varying the action (Eq. 2.6) with respect to the metric tensor.

$$S = S_H + S_{\text{matter}} = \int \sqrt{-g} \Big(\frac{R - 2\Lambda}{16\pi G} + \mathcal{L}_{\text{matter}} \Big) d^4x \tag{2.6}$$

where the first term is the contribution from the curvature of spacetime, known as Einstein-Hilbert's action and the second term is the Lagrangian of the matter fields.

Back to Einstein's equations (Eq. (2.5)), the left-hand side depends on the metric and its derivatives. On the right-hand side, $T_{\mu\nu}$ contains contributions from all forms of energy density, such as matter and radiation, and is related to the action by:

$$T_{\mu\nu} = -2 \frac{1}{\sqrt{-g}} \frac{\delta S_{\text{matter}}}{\delta g^{\mu\nu}} \tag{2.7}$$

The cosmological constant term is equivalent to a vacuum energy behaving as an isotropic perfect fluid (Section 2.2) and it is often absorbed in the Stress-Energy Tensor. Knowing the stress-energy tensor and symmetries of a system, Einstein's equations give a set of differential equations that can be solved for the metric.

The Cosmological Principle

We may now apply General relativity to the observable universe. To a good approximation, the universe on large scales is well described by the *cosmological principle*. This is the assumption that the energy distribution of our universe is spatially isotropic and homogeneous on large scales ($\gtrsim 300h^{-1}$ Mpc [16]). Notice that, since the universe is expanding, the time coordinate does not share the same symmetry.

The mathematical meaning of isotropic and homogeneous spaces is obtained from the notion of a *maximally symmetric space* [17], i.e., a space whose metric is invariant under translations and rotations[3]. With the above symmetries in mind, let us consider spacetime as a $M = \mathbb{R} \times \Sigma$ manifold, where $\mathbb{R}$ represents time and Σ represents our maximally symmetric 3-space.

$$ds^2 = -dt^2 + a(t)^2\Big[\frac{dr^2}{1-kr^2} + r^2 d\Omega^2\Big] \tag{2.8}$$

where $a(t)$ is the scale factor, which is proportional to the distance between objects as the universe expands. The sign of $k \in \{-1, 0, 1\}$ is directly related to the local geometry of space (hyperbolic, flat, spherical). As supported by experimental evidence and as explained by inflation (chapter 4), the observed flatness motivates the choice $k = 0$.

The Friedmann equations

Now that we have applied the symmetry conditions for the large scale structure, the evolution of the metric and, in particular, of the scale factor can be obtained from Einstein's equations (Eq.(2.5)). After computing the Christoffel symbols (see, for example, [17]), it is straightforward to calculate the Ricci tensor and the Ricci scalar and check that the off-diagonal elements vanish:

$$R_{00} = -3\frac{\ddot{a}}{a} \qquad R_{ii} = g_{ii}(a\dot{a} + 2\dot{a}^2 + 2k) \tag{2.9}$$

$$R = g^{\nu\mu}R_{\nu\mu} = 6\Big[\frac{\ddot{a}}{a} + \Big(\frac{\dot{a}}{a}\Big)^2 + \frac{k}{a^2}\Big] \tag{2.10}$$

Now turning to the Stress-Energy tensor, each component, $T_{\mu\nu}$, the information about the flux of the p_μ-component of the four-momentum in the direction x_ν [18]: T_{00} is the energy density (ρ); $T_{0i} = T_{i0}$ is related to heat condution (in the direction x_i); T_{ij} is the p_i momentum flux in the x_j direction and, in particular, the diagonal components, T_{ii}, are the pressure (p) and the off-diagonal T_{ij} ($i \neq j$) are related to the viscosity of the fluid.

In an isotropic and homogeneous background, it is reasonable to assume that every contribution to the Stress-Energy tensor of Eq. (2.5) can be regarded as an ideal fluid. An *ideal fluid* is defined as an isotropic fluid that is not viscous ($T_{ij} = 0$ if $i \neq j$) and does not conduct heat ($T_{0i} = T_{i0} = 0$) in its frame of reference. As a consequence, its Stress-Energy tensor may be fully defined in terms of its energy density (ρ) and pressure (p)

$$T_{00} = \rho \qquad T_{ii} = g_{ii}p \tag{2.11}$$

[3] More detail on maximally symmetric spaces, as well as the full derivation of the Friedman-Robertson-Walker metric (2.8) is given in [17].

Regarding the cosmological constant as an ideal fluid of energy density $\rho_\Lambda = \Lambda/(8\pi G)$, the $\mu = \nu = 0$ component of the Einstein's equation, (Eq. (2.5)) gives the *1st Friedmann equation*:

$$\boxed{H^2 = \frac{8\pi G}{3}\sum_{i\neq k}\rho_i - \frac{k}{a^2}} \tag{2.12}$$

where $H = \dot{a}/a$ is the Hubble parameter. As a consequence of isotropy, the three $\mu = \nu = i$ components of Eq.2.5 yield identical equations, the *2nd Friedmann equation*:

$$\boxed{\frac{\ddot{a}}{a} = -\frac{4\pi G}{3}\sum_{i\neq k}(1+3w_i)\rho_i} \tag{2.13}$$

where we assumed the present fluids' pressure is well defined in terms of the energy density by its *equation of state* (EoS):

$$p_i = w_i\rho_i \quad \text{(no sum)} \tag{2.14}$$

Critical density and the ΛCDM

The *Critical density* is the density of a perfectly flat universe ($k = 0$):

$$\rho_c(t) = \frac{3H(t)^2}{8\pi G} \tag{2.15}$$

This concept is useful to simplify our notation. Now, instead of speaking of densities of the different species, we can simply speak about fractions of the total energy density, also known as the *abundance*:

$$\Omega_i = \frac{\rho_i}{\rho_c} \tag{2.16}$$

Equation (2.12) can be rewritten as:

$$\sum_{i\neq k}\Omega_i + \Omega_k = 1 \quad , \quad \Omega_k = -\frac{k}{a^2} \tag{2.17}$$

The sum of all density parameters must be equal to the unity. In particular, $\Omega_k = 0$ corresponds to a flat universe. The presently best accepted fit to experimental observations consists of a model known as the *Lambda-CDM* (ΛCDM). In this model, the universe's energy density accommodates four kinds of fluids: *matter* - non relativistic particles; *radiation* - relativistic particles; *dark energy* - a mysterious fluid frequently associated to a cosmological constant (or vacuum energy); and *curvature* - it is not a fluid, but it is convenient to regard it as one. Recent observations of the CMB and LSS [19, 20] indicate that curvature and radiation contributions to the present energy density are negligible. Thus, the universe's density is very close to the critical density, dominated by dark energy and matter (Figure 2.2).

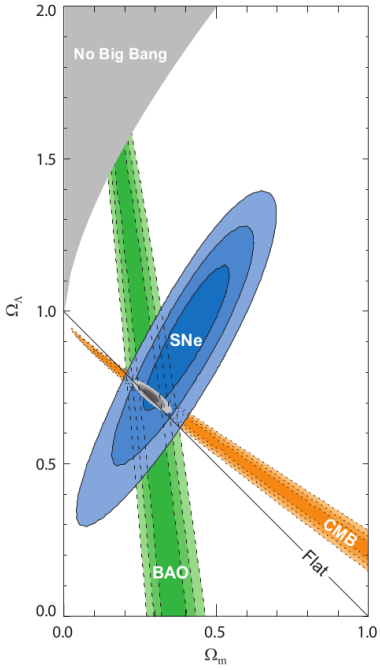

Figure 2.5: Concordance between observations on the ΛCDM model [4].

Density Parameter	Observed
Ω_Λ	0.6911 ± 0.0062
Ω_m	0.3089 ± 0.0062
Ω_r	~ 0.0004
Ω_c	0.0008 ± 0.0040

Table 2.1: Observed density parameters.

Dynamics of fluids in the Universe

Equations (2.12) and (2.13) tell us how the scale factor behaves according to the local energy density. Depending on the species that dominate the energy density, the scale factor evolves differently. As supported by cosmological observations, we are mainly interested in species that behave as matter, radiation or dark energy.

By combining the Friedmann equations, we may obtain the evolution of energy densities of a general fluid species[4]. The solutions to this equation give the evolution of the energy density of some fluid of EoS w in terms of the scale factor:

$$\boxed{\frac{\dot{\rho}}{\rho} = -3H(1+w)} \rightarrow \rho = \rho_0 \left(\frac{a_0}{a}\right)^{3(1+w)} \tag{2.18}$$

If this fluid is composed by:

- **Matter** of mass $m \sim E$ - the energy density is related to the number density of particles by $\rho(a) = m \times n(a)$. As the universe expands, the number density (particles per unit volume) should evolve in inverse proportion to the volume ($V \propto a^3$), thus we expect that $\rho_m \propto a^{-3}$ and $\boxed{w_m = 0}$.
- **Radiation** - the energy is related to the corresponding (de Broglie) wavelength as $E \propto \frac{1}{\lambda}$. The number density is inversely proportional to the volume. The expansion of space stretches the wavelength as $\lambda \propto a$, thus $\rho_r \propto a^{-4}$ and $\boxed{w_r = 1/3}$.
- **Dark energy** - as the universe expands, more vacuum is created, thus the energy density does not get diluted and remains constant $\rho_\Lambda \propto a^0$ and $\boxed{w_\Lambda = -1}$.

By inputting Eq.2.18 into Eq.2.12 for some general dominant specie of fluid, we obtain the evolution of the scale factor and the Hubble parameter. The more relevant solutions are

[4] It is also possible to obtain it from the conservation of energy $\nabla_\mu T^\mu_0 = 0$.

summarized in Table 2.2:

$$a(t) \propto \begin{cases} t^{\frac{2}{3(1+w)}} & , w \neq -1 \\ e^{H_0 t} & , w = -1 \end{cases} \tag{2.19}$$

$$H(t) = \begin{cases} \dfrac{2}{3(1+w)t} & , w \neq -1 \\ H_0 & , w = -1 \end{cases} \tag{2.20}$$

Fluid Species	w	$\rho(a)$	$a(t)$	$H(t)$	$H(a)$
Radiation	$1/3$	a^{-4}	$t^{1/2}$	$(2t)^{-1}$	a^{-2}
Matter	0	a^{-3}	$t^{2/3}$	$2/3t^{-1}$	$a^{-3/2}$
Curvature	$-1/3$	a^{-2}	t	$3t^{-1}$	a^{-1}
Cosmological Constant	-1	ρ_0	$e^{H_0 t}$	H_0	H_0

Table 2.2: Characteristics of the universe in different epochs. The inverse of the Hubble parameter sets the time scale for most of the universe history.

With the present measured concentration of cosmological fluids (Figure 2.2) and Eq. (2.18) it is possible to obtain the evolution of the density parameters, Ω_i, as a function of the scale factor, $a(t)$. If we assume that the universe has been expanding since the beginning and with the same composition, Figure 2.6 shows that radiation and matter were once the dominant part of the energy density, when the scale factor was smaller. By the arguments above, the Big Bang model dictates that the universe began with a *radiation-dominated era*, followed by a *matter-dominated era* and, recently we have entered a *dark energy-dominated era*.

It is interesting to note that we live just in the right time such that matter and vacuum energy have comparable magnitudes (Figure 2.6). If this picture were a little bit different, with vacuum energy dominating earlier, gravitational collapse and galaxy formation could not have occurred and we would not be here to testify. This is the so-called *cosmic coincidence*[21], an unsolved fine tuning problem[5].

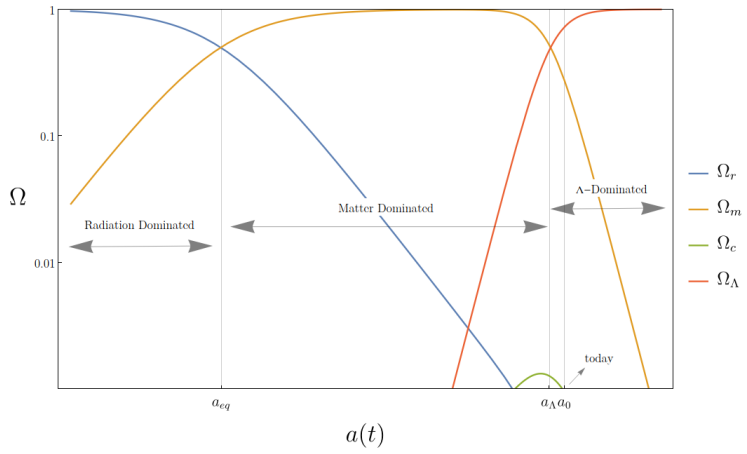

Figure 2.6: Evolution of density parameters as a function of the scale factor. Defining today's scale factor as $a_0 = 1$, matter-radiation equality occurred at $a_{eq} \sim 3.7 \times 10^{-4}$ and matter-lambda equality at $a_\Lambda \sim 0.75$.

[5] i.e., a problem related to an extremely unnatural choice of initial conditions that could evolve to the conditions we observe today.

2.3 Thermodynamics of an expanding universe

Observations of the CMB show that the universe has a very homogeneous temperature. This fact is taken as evidence that photons and matter had enough time to reach thermodynamic equilibrium long before *photon decoupling*.

Thermodynamically, the universe is well described as an expanding isolated system[6] that evolved predominantly in a condition of local thermodynamic equilibrium. Departures from this state gave rise to observable relics as the CMB, the baryon number (Chapter 5) and, the abundance of light elements, and predicts the not-yet-observed Cosmic neutrino Background (CνB). This section is dedicated to the discussion of the thermodynamic evolution of the universe and the analysis of the thermal equilibrium condition.

Equilibrium

Let us define some of the different states of equilibrium:

- **Kinetic equilibrium** - The sum of all forces on every region of the system vanishes, the regions will not move, contract or expand.

  In the case that the system is isolated, there will be no external forces and the pressure, p, becomes homogeneous throughout the system.

- **Chemical equilibrium** - Every chemical interaction in the system happens at the same rate as its inverse process.

$$A + B \rightarrow C + D \tag{2.21}$$

  which is equivalent to saying that the chemical potentials of the intervening species satisfy:

$$\mu_A + \mu_B = \mu_C + \mu_D \tag{2.22}$$

- **Thermal equilibrium** - There is no net flow of heat ($\delta Q = 0$) in any direction and the temperature, T, is homogeneous throughout the system.

- **Thermodynamic equilibrium** - When a system is both in kinetic, chemical and thermal equilibrium. In this state the entropy is maximal, thus, this is the natural state an isolated system of interacting particles is expected to evolve to.

Equilibrium Thermodynamics

Now it is time to introduce the *distribution function*, $f(\vec{x}, \vec{p}, t)$. For a system in equilibrium, this distribution is related to the probability of having a particle at time t with momentum $\vec{p}$ (do not confuse with pressure, p) and at the location $\vec{x}$. The distribution function of a homogeneous and isotropic bosonic fluid in equilibrium is given by the *Bose-Einstein distribution (−)* and for the case of a fermionic fluid, the phase space occupancy is given by the *Fermi-Dirac distribution(+)*:

$$f(\vec{p}) = \frac{1}{e^{\frac{E-\mu}{T}} \pm 1} \tag{2.23}$$

The number density, energy density and pressure of these fluids are related to their phase space occupancy and the particle's internal degrees of freedom, g, by:

[6] A system that does not exchange heat or matter with its neighbourhood.

$$n = g \int \frac{d^3\vec{p}}{(2\pi)^3} f(\vec{p}) \tag{2.24}$$

$$\rho = g \int \frac{d^3\vec{p}}{(2\pi)^3} E(\vec{p}) f(\vec{p}) \tag{2.25}$$

$$p = g \int \frac{d^3\vec{p}}{(2\pi)^3} \frac{|\vec{p}|^2}{3E(\vec{p})} f(\vec{p}) \tag{2.26}$$

where $E(\vec{p}) = \sqrt{|\vec{p}|^2 + m^2}$ is the energy of some mass m particle and momentum $\vec{p}$ in the fluid. In a similar fashion of Section 2.2, let us consider how the number and energy densities behave for *relativistic* and *non-relativistic* species, in the approximation $|\mu| \ll T$:

- Relativistic particles ($T \gg m$)

  In this limit, $E \sim |\vec{p}|$, thus:

$$n_r = \frac{g}{\pi^2} \zeta(3) T^3 \times \begin{cases} 1 & \text{if Bosons} \\ 3/4 & \text{if Fermions} \end{cases} \tag{2.27}$$

$$\rho_r = \frac{\pi^2}{30} g T^4 \times \begin{cases} 1 & \text{if Bosons} \\ 7/8 & \text{if Fermions} \end{cases} \quad \text{and} \quad p_r = \rho_r/3 \tag{2.28}$$

  where ζ is the Riemann Zeta function. Notice that, through a different reasoning, we obtained that the pressure and the energy density of a relativistic species are related by $p = \frac{1}{3}\rho$, as argued in Section 2.2. If a relativistic fluid is made of different species, namely fermions and bosons, its energy density can be written in the compact form:

$$\boxed{\rho_r = \frac{\pi^2}{30} g_*(T) T^4} \tag{2.29}$$

  where $g_*(T)$ is the *effective number of relativistic degrees of freedom* at the (photon) temperature T:

$$g_*(T) = \sum_{\text{bosons}} g_i \left(\frac{T_i}{T}\right)^4 + \frac{7}{8} \sum_{\text{fermions}} g_i \left(\frac{T_i}{T}\right)^4 \tag{2.30}$$

  and T_i is the temperature of each species.

- Non-relativistic particles ($m \gg T$)

  In this limit, the energy can be expanded to first order, $E \approx m + \frac{|p|^2}{2m}$. The term in the denominator becomes dominated by the exponential, so we can write

$$f(\vec{p}) \simeq \frac{1}{e^{E(\vec{p})/T} \pm 1} \simeq e^{-\frac{m}{T} - \frac{|\vec{p}|^2}{2mT}} \tag{2.31}$$

  The integrals can be handled by integrating the angular part (in spherical coordinates) and using the result from Eq. (A.2) to integrate the radial part:

$$n_m = g \left(\frac{mT}{2\pi}\right)^{3/2} e^{-m/T} \tag{2.32}$$

$$\rho_m = nm \tag{2.33}$$

$$p_m = nT \tag{2.34}$$

Notice that we can write the pressure in terms of the enegy density as $p = \rho \times \frac{T}{m}$, since the species is non-relativistic, $\frac{T}{m} \ll 1$, and we recover once again the equation of state $p = 0$, as argued in Section 2.2.

Entropy

Consider the first law of thermodynamics

$$dU = -PdV + TdS \tag{2.35}$$

The entropy density of a system in thermal ($T \sim const$) and kinetic equilibrium ($p \sim const$), is obtained simply by integration the first law of thermodynamics and dividing by the volume:

$$s = \frac{\rho + p}{T} \tag{2.36}$$

In particular, for a relativistic species ($p = \rho/3$):

$$s = \frac{4}{3}\frac{\rho}{T} = \frac{2\pi^2}{45} g T^3 \times \begin{cases} 1 & \text{if Bosons} \\ 7/8 & \text{if Fermions} \end{cases} \tag{2.37}$$

For a non relativistic species ($p = 0$), the entropy is exponentially damped as the temperature decreases (see Eq. (2.32)). Neglecting the non relativistic contributions, for a system composed of bosons and fermions, we can write the total entropy density as:

$$\boxed{s = \frac{2\pi^2}{45} g_*^S(T) T^3} \tag{2.38}$$

where g_*^S is the *effective number of relativistic degrees of freedom contributing to the entropy*:

$$g_*^S(T) = \sum_{\text{bosons}} g_i \left(\frac{T_i}{T}\right)^3 + \frac{7}{8} \sum_{\text{fermions}} g_i \left(\frac{T_i}{T}\right)^3 \tag{2.39}$$

Note that this quantity should differ from g_* (Eq. (2.30)) whenever there is some species decoupled from thermal equilibrium ($T_i \neq T$). However, as Figure 2.7 shows, the difference is almost negligible and it is not a bad approximation to regard these functions as constant at temperatures far from decoupling thresholds.

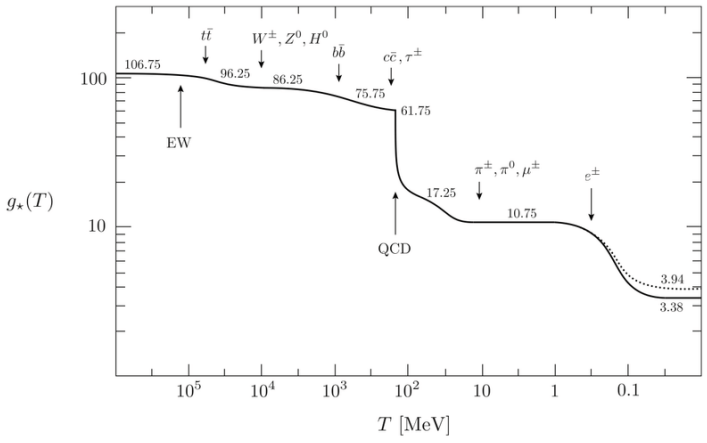

Figure 2.7: Dependence on the temperature of the effective number of relativistic degrees of freedom for the particle content of the Standard Model [5].

Now, for the case of an isentropic expansion, the total entropy in a comoving volume is conserved, $S = a^3 s = const$, which implies:

$$g_*^S T^3 a^3 = const. \rightarrow T \propto a^{-1} \tag{2.40}$$

i.e., away from decoupling thresholds ($g_*^S \simeq const.$), the temperature redshifts with the expansion as a^{-1}.

$$\frac{n}{s} \propto \frac{g_*(T)}{g_*^S(T)} \sim const. \tag{2.41}$$

As a consequence, relativistic species in thermal equilibrium have its number density-to-entropy ratio conserved as long as the expansion remains isentropic.

Conditions for Thermal Equilibrium

In the previous section we derived how the entropy and energy density evolve for matter and radiation in thermodynamic equilibrium. Now let us consider the universe as a system of interacting particles without any assumption about its state of equilibrium and see if we can build a better notion of thermal equilibrium in the light of particle physics and cosmology. This is described by the *Boltzmann equation*, which tells us how the distribution function of some species, $f(\vec{p})$, evolves in terms of its annihilation/creation interaction rates. In an FRW spacetime, it can be written as [22]:

$$\frac{dn}{dt} + 3\frac{\dot{a}}{a}n = \frac{g}{(2\pi)^3}\int C[f(\vec{p})]\frac{d^3\vec{p}}{E} \tag{2.42}$$

where $C[f(\vec{p})]$ is the collision operator, which contains the contributions from every interaction. For our purposes, let us suppose the dominant part of the collision term is due to two-particle collisions. We may then write[7]:

$$\dot{n}_i + 3Hn_i = -\langle\sigma_A|v_i|\rangle[n_i^2 - (n_i^{EQ})^2] \tag{2.43}$$

where σ_A is the total interaction cross section, $|v_i|$ is the mean velocity of the particles involved and n_i^{EQ} is the number density of particle-i in equilibrium. Notice that any difference between n_i and n_i^{EQ} in the right-hand side, the left-hand side will make the system evolve in order to cancel it[8]. Let us rewrite Eq. (2.43) as:

$$\dot{n}_i + \left[3H + \Gamma_i\hat{\Delta}n_i\right]n_i = 0 \tag{2.44}$$

For simplicity and without loss of generality, suppose $\hat{\Delta}n_i \sim \mathcal{O}(1)$. We have two interesting cases:

1. $\Gamma_i \gtrsim H$: the interactions occur quickly enough such that the system remains in thermal equilibrium $n_i \simeq n_i^{EQ}$ (Eq. (2.27)/(2.32));
2. $H \gtrsim \Gamma_i$: the system expands too fast, interactions do not occur quickly enough and it departs from equilibrium. The number density no longer evolves towards n_i^{EQ}, simply decreasing with expansion as $n \propto a^{-3}$. This departure from thermal equilibrium is known as *freeze-out*. If there is no production of entropy ($s \propto a^{-3}$), the number-to-entropy ratio becomes conserved:

$$\frac{n}{s} = const. \tag{2.45}$$

[7] For a more detailed discussion, we refer the reader to [22]

[8] Assuming the right-hand side term is not negligible

This result has very important implications for cosmology, in particular, for baryogenesis. For example: If in the early universe there is some mechanism that creates a baryon asymmetry and then decouples, there will be a remnant baryon density red-shifting as $n_B \propto a^{-3}$. If, at some time, the total entropy of the universe becomes constant, the n_B/s ratio will be preserved with expansion.

Finally, it is interesting to analyse the ratio between Γ and H for gauge-mediated interactions of strength α mediated a mass m_A gauge boson in a radiation-dominated universe (see [15]):

$$\frac{\Gamma_i}{H} = \begin{cases} \alpha^2 M_p \dfrac{T^3}{m_A^4} & m_A \gtrsim T \\ \alpha^2 \dfrac{M_p}{T} & m_A \ll T \end{cases} \tag{2.46}$$

As an example, it is expected that the weak force decouples from thermal equilibrium at some temperature below the $W^{\pm}$ and Z^0 bosons masses, potentially leaving a relic abundance of neutrinos, the so called Cosmic Neutrino Background (CνB). On the other hand, interestingly for temperatures just below the Planck mass ($T \gtrsim \alpha^2 M_p$), the thermal equilibrium condition appears to break down[9]. The bright side is that the thermodynamical equilibrium description appears to be a reasonable assumption for a large range of temperatures ($m_A \lesssim T \lesssim \alpha^2 M_p$).

2.4 Big Bang Nucleosynthesis

One of the most successful predictions of the Hot Big Bang model is the present abundance of the light elements. As discussed in Section 2.3, as the universe expanded and cooled down, some interactions froze and a relic density of some species was left. Primordial Big Bang Nucleosynthesis (BBN) is based on this reasoning, where protons and neutrons were in equilibrium by weak-force mediated processes and then, at $T \sim 1$ MeV, these interactions froze and a relative abundance of neutrons and protons $n_n/n_p \sim 1/7$ was formed[10]. At $T \sim 0.3$ MeV, the temperature was low enough so that neutrons and protons could combine to form stable light elements such as deuterium, helium-3, helium-4 and lithium-7. This mechanism, which studies the evolution of the nuclear number densities, accurately describes the light-element distributions (for a detailed discussion we refer to introductory literature [22, 15]). However, in order to have such successful predictions, the universe should have had an excess of baryons with respect to anti-baryons, which is usually quantified by the baryon-to-photon ratio, $\eta = \dfrac{n_b - n_{\bar{b}}}{n_\gamma}$ [3]:

$$5.8 \times 10^{-10} \leq \eta \leq 6.5 \times 10^{-10} \tag{2.47}$$

This asymmetry should have been produced before BBN, by some mechanism called *baryogenesis* (Chapter 5). Additionally, BBN bounds the relativistic degrees of freedom at $T \sim 1$ MeV to [12]:

$$g_*(T \sim 1 \text{ MeV}) = 10.69 \pm 1.1 \tag{2.48}$$

which is consistent with the photon, the electron, the positron, 3 neutrino species and possibly an additional degree of freedom. However, CMB constrains the effective number of relativistic degrees of freedom at $T \simeq 0.26$ eV to [12]:

$$g_*(T \sim 0.26 \text{ eV}) \simeq 3.36 \pm 0.08 \tag{2.49}$$

[9] Assuming that our approximation remains valid.

[10] At the time weak-force processes freeze-out, $n_n/n_p \sim 1/6$. Before the synthesis of light elements begins, some neutrons decay and the ratio reduces to $n_n/n_p \sim 1/7$.

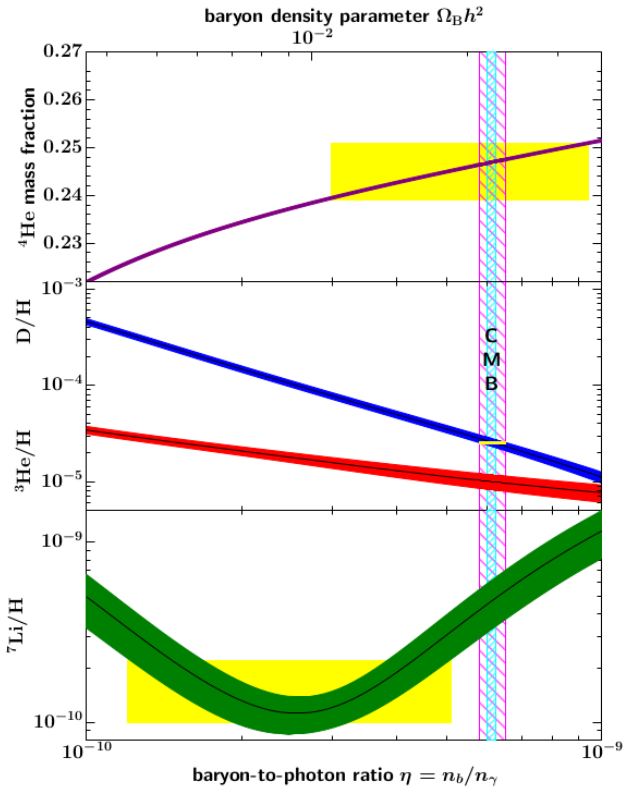

Figure 2.8: The concordance between the CMB (vertical bar) measurements, the observed mass fraction of the light elements (yellow rectangles) and the BBN mass fractions as a function of the baryon-to-photon ratio, η. The inconsistency observed in lithium serves as possible evidence for new physics. [3]

any additional degrees of freedom should be non-relativistic or decoupled and at a lower temperature at the time CMB was emitted. Additionally, CMB anisotropies impose bounds on the baryon-to-photon ratio, since the amplitude of the acoustic peaks in Figure 2.4 has a strong dependence on η (see [11]), giving:

$$\eta = (6.14 \pm 0.25) \times 10^{-10} \tag{2.50}$$

The concordance between BBN and CMB is remarkable (Figure 2.8). As a result, the bound in the present baryon abundance reads [3]:

$$0.021 \leq \Omega_b h^2 \leq 0.024 \quad \rightarrow \quad 0.035 \leq \Omega_b \leq 0.052 \tag{2.51}$$

i.e. baryonic matter contributes at most to 5% of the universe's energy density today. Since ΛCDM tells us that $\Omega_m \sim 0.30$, it suggests that there is some non baryonic and non-relativistic fluid that makes up around 25% of the energy density of the universe, which is usually known as *Cold Dark Matter* (CDM).

Since entropy is a quantity that has been conserved for almost the whole of the universe's history (Eq. (2.41)), it is also useful to define the *baryon-to-entropy* ratio as:

$$\eta_S = \frac{n_b - n_{\bar{b}}}{s} \tag{2.52}$$

which is related today with the baryon-to-photon ratio by $\eta_S \sim \eta/7.04$, thus:

$$8.4 \times 10^{-11} \leq \eta_S \leq 9.1 \times 10^{-11} \tag{2.53}$$

2.5 Dark Matter

The combination of the information from BBN and ΛCDM shows us that ordinary matter makes up only $\sim$ 15% of all the non-relativistic matter density observed. The remaining 85% is known as dark matter and its origin is currently a mystery in cosmology. Also, there is important observational evidence for dark matter that has been obtained from various methods. Let us review the observations from rotation curves of galaxies and weak-lensing techniques. A list of dark matter candidates is given later, in Section 3.3.

Rotation Curves of Galaxies

In principle, a good estimate for the matter density could be obtained by measuring the average mass of galaxies and multiplying it by the number density ($\rho_{LUM} = n\langle M\rangle$). The (observed) rotational velocity of a galaxy is related to its (inferred) mass by Kepler's 3rd Law:

$$v = \sqrt{\frac{GM(r)}{r}} \tag{2.54}$$

What happens is that if we assume that the majority of the mass of the galaxy should be concentrated on its luminous part, we end up finding that luminous matter accounts for less than 1% of the critical density, $\Omega_m < 0.01$.

However, after the 21cm line was discovered, astronomers observed that the velocity of the rare objects far from the luminous centre started flattening (Figure 2.9), indicating that somehow the mass of the galaxy kept increasing $M(r) \propto r$. From these observations, this increment may be explained by a spherical distribution of dark matter. Thus, Dark matter is a form of matter that predominantly interacts gravitationally (at least for long-range interactions). The approximately spherical distribution, rather than in a disk, indicates that any self interactions should be very weak.

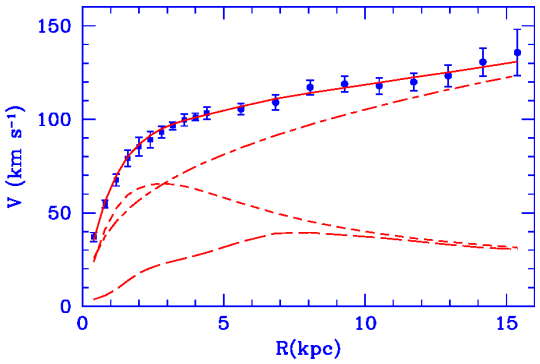

Figure 2.9: Blue dots: observations of velocities of rotation of the galaxy M33 as function of the radius. Continuous line: The best fit to observed data has the contributions from a dark matter halo (dashed-dotted line), a luminous matter disk (short-dashed line) and a gas contribution (long-dashed line) [6]

Weak-Lensing

A flagrant example of the presence of dark matter in galaxies has been given by the Bullet cluster. Weak-lensing reconstructions of the gravitational distribution of mass shows a large displacement when compared to the distribution of luminous objects, suggesting that the greatest part of the cluster mass is non-luminous.

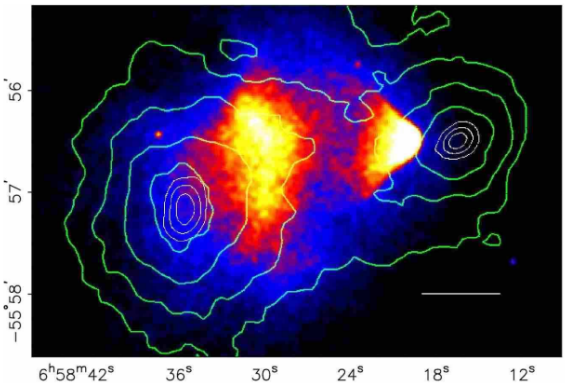

Figure 2.10: Observations of the Bullet cluster show a flagrant example where the luminous matter and the reconstruction from weak-lensing techniques (green lines) do not coincide [7].

Chapter 3

Standard Model of Particle Physics and Beyond

> *"One Ring to rule them all, One Ring to find them, One Ring to bring them all, and in the darkness bind them."*
>
> — J. R. R. Tolkien

3.1 The Standard Model of Particle Physics

The *Standard Model* (SM) describes our current understanding of particle physics. It has remarkably passed strict tests and has been very successful in explaining and predicting experimental physical phenomena. In this model, a limited number of spin-1/2 fermions make up the most fundamental building blocks of matter. Three fundamental forces are carried by spin-1 gauge bosons: Electromagnetism, a long-ranged force carried by the massless photon and associated with an electric charge; Strong force, a short-ranged interaction responsible for binding protons and neutrons into atomic nuclei, carried by massless gluons and associated with a colour charge; and the Weak-force, also short-ranged, responsible for nuclear β-decay, carried by the three massive $W^{\pm}$ and Z^0 gauge bosons. Fermions are further subdivided into two subcategories: the Leptons have no colour charge; the Quarks have colour charge are and bound with each other to form colourless structures known as Baryons (3-quark bound states qqq) and Mesons (quark-antiquark bound states $q\bar{q}$).

Internal Symmetries

The Standard Model has a very elegant mathematical structure [23, 24, 25, 26]. By Noether's theorem, conservation laws are directly related to some underlying invariance (i.e. symmetry) of the system. The Standard Model Quantum Field theory (QFT) is no exception. The introduction of the gauge (local) invariance principle (invariance under continuous local-phase transformations where a field ψ in the fundamental representation of the group transforms as $\psi \to \psi' = e^{i\vec{\alpha}(x)\cdot\vec{T}}\psi$, $\vec{T}$ is a basis for the adjoint representation of the group and $\vec{\alpha}(x)$ is a local parameter) to Quantum Electrodynamics ($U(1)_{em}$), Quantum Chromodynamics ($SU(3)_C$) and Electroweak Theory ($SU(2)_L \times U(1)_Y$) enabled physicists to obtain a deeper understanding of the nature of particle physics.

The Standard Model is based on two distinct symmetries:

1. Space-time: It is invariant under the Poincaré group transformations (translations, rotations and boosts).

2. Internal: Transformations of some field into another (eg. gauge groups) that commute with space-time transformations.

$$\mathcal{P} \oplus G_{int} \to SM \tag{3.1}$$

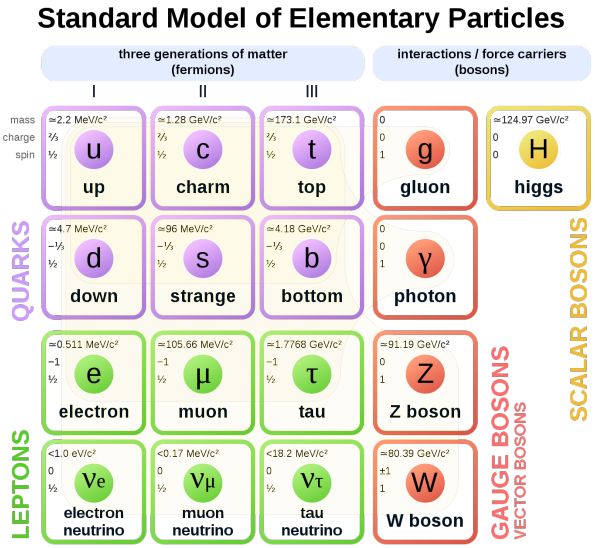

Figure 3.1: The Standard Model particle content is composed by 3 generations of Quarks and Leptons, the force carriers Gauge Bosons and the Higgs Boson, responsible for Electroweak-symmetry breaking [8, 3].

With respect to internal symmetries, the Standard Model is a QFT model invariant under transformation of the $SU(3)_C \times SU(2)_L \times U(1)_Y$ group (see [27]). This invariance constrains the interaction terms, implies the existence of 12 massless gauge boson that mediate the interactions (8 gluons, 3 W-bosons and one B-boson) and treats fermions that behave similarly under the action of some force as belonging to the same multiplet representation.

However, this symmetry is not exact at low energies. In order that fermions and weak-force gauge bosons acquire mass, the $SU(2)_L \times U(1)_Y$ gauge symmetry should be spontaneously broken by interactions with the Higgs field through the *Higgs Mechanism* [23], which is believed to have taken place in the early universe, after the temperature dropped below the *Electroweak Scale* ($\Lambda_{EW} \sim 250$ GeV).

$$SU(3)_C \times SU(2)_L \times U(1)_Y \xrightarrow{\text{Higgs M.}} SU(3)_C \times U(1)_{em} \tag{3.2}$$

Spontaneous Symmetry Breaking

An interesting property of scalar fields is that they can acquire non-zero vacuum expectation values without breaking Lorentz invariance. This property may trigger spontaneous symmetry breaking processes such as the Higgs mechanism. For simplicity, let us consider the complex scalar field Lagrangian:

$$\mathcal{L} = \partial_\mu \phi^\dagger \partial^\mu \phi - \mu^2 \phi^\dagger \phi - \lambda (\phi^\dagger \phi)^2 \tag{3.3}$$

$$= \partial_\mu \phi^\dagger \partial^\mu \phi - V(\phi^\dagger, \phi) \tag{3.4}$$

We are interested in the $\lambda > 0$ case[1]. For $\mu^2 > 0$, the ground state is $|\phi| = 0$ and the Lagrangian is invariant under global phase transformations such as $\phi \to \phi e^{i\alpha}$. Now, suppose that for some reason, the mass term suddenly becomes $\mu^2 < 0$. The minimum of the potential becomes degenerate and ϕ obtains a vacuum expectation value (VEV):

[1] In order for the potential to be bounded from below, λ must be positive.

$$|\phi|^2 = v^2 = -\frac{\mu^2}{2\lambda} \quad , \quad \langle 0|\phi|0\rangle = ve^{i\theta} \tag{3.5}$$

for some $\theta \in [0, 2\pi[$. The relevant fields in QFT are excitations around the ground state. The SSB phenomenon makes the degree of freedom θ massless, which is known as a *Goldstone* boson. In order to proceed, we should redefine our field as oscillations around the new minimum:

$$\phi(x) = (v + h(x))e^{i\theta} \tag{3.6}$$

Rewriting the Lagrangian in terms of Eq. (3.6), it becomes evident from odd-order terms on $h(x)$ that the new ground state is no longer invariant under global phase transformations. This phenomenon is know as *spontaneous symmetry breaking* (SSB).

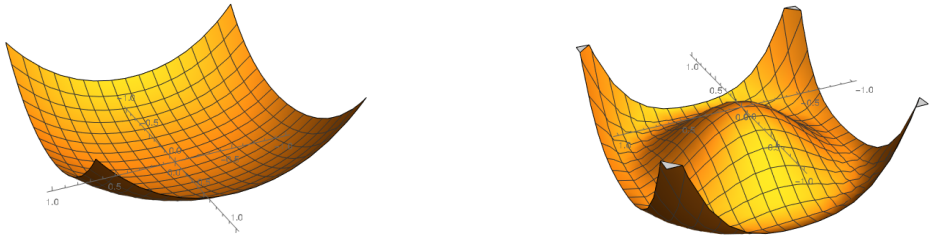

(a) $\mu^2 > 0$ (b) $\mu^2 < 0$

Figure 3.2: In spontaneous symmetry breaking, the origin becomes unstable and the minimum becomes degenerate.

If the broken symmetry is a gauge symmetry, there is an additional interesting implication:

$$\mathcal{L} = \mathcal{D}_\mu\phi^\dagger\mathcal{D}^\mu\phi - \mu^2\phi^\dagger\phi - \lambda(\phi^\dagger\phi)^2 - \frac{1}{4}F_{\mu\nu}F^{\mu\nu} \tag{3.7}$$

where $\mathcal{D}_\mu = \partial_\mu - igA_\mu(x)$ is the covariant derivative. Due to the gauge-scalar field mixing in the kinetic term, mass terms for the gauge bosons ($v^2g^2A_\mu A^\mu$) appear in the new Lagrangian. The massive gauge boson has now three degree of freedom and, the additional degree of freedom has been absorbed from the Goldstone boson. If this scalar couples to fermions, similar terms may arise too.

A well known example is the Higgs mechanism where the Electroweak symmetry spontaneously breaks into Electromagnetism (Eq. (3.2)). The corresponding scalar field is the Higgs $SU(2)_L$ doublet. Fermions, and the $W\pm$ and Z bosons acquire masses in this way (see [28]). Within the Standard Model, temperature corrections result in a positive effective mass squared at large temperatures. If there is some source of negative mass term, as the temperature decreases, SSB may occur and trigger the Higgs mechanism. The source of this negative mass term is unexplained by the Standard Model.

Other Symmetries

Incidentally and as a consequence of gauge invariance, the renormalizable[2] terms of the Lagrangian are invariant under $U(1)$ *global transformations* of the form:

[2] Terms whose coupling constant, g, has a positive or zero mass dimension ($[g] \geq 0$).

$$\psi \to \psi' = e^{i\alpha \hat{N}_{B/L}} \psi \tag{3.8}$$

$$\hat{N}_B = \frac{1}{3} \sum_q (\hat{n}_q - \hat{n}_{\bar{q}}) \tag{3.9}$$

$$\hat{N}_L = \sum_l (\hat{n}_l - \hat{n}_{\bar{l}}) \tag{3.10}$$

where $\hat{N}_{B/L}$ is the baryon/lepton quantum number operator [3] and n_i the indexed specie quantum number operator ($a^\dagger a$). This invariance, in particular, implies the conservation of Baryon number (B), Lepton number (L) and any linear combination such as $B-L$ and $B+L$.

Additionally, there are three relevant discrete symmetries a set of interactions might have: **T** or Time Reversal ($t \to -t$); **P** or Parity Transformations ($\vec{x} \to -\vec{x}$); **C** or Charge Conjugation (particle $\to$ anti-particle). Evidence shows that Strong and Electromagnetic interactions are symmetric under those transformations. However, Weak interactions do violate P and C, since they only involve left-handed[4] particles and right-handed anti-particles.

Renormalization

After Quantum Field theories first appeared, some quantum corrections gave divergent contributions to the mass and coupling constant terms. The issue was that the theories needed to be renormalized (for more details, see [29]).

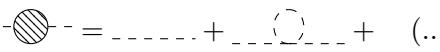

(3.11)

There is no unique way to deal with those divergences. The first step is choosing a *regularization method* (e.g. momentum cut-off or dimensional regularization) in order to understand the nature of each divergence. The theory is said to be *renormalizable* if the number of divergent irreducible diagrams is finite. A *non-renormalizable* theory has infinite, which are caused by terms in the Lagrangian with a coupling constant that has a negative mass dimension. To renormalize a theory, one must choose a *renormalization scheme*.

The MS-bar scheme solves the problem by first splitting the Lagrangian into *physical* terms (observable) and *counter-terms* (unobservable) terms. For example, the 2-point correlation function, $G^{(2)}$, is given by:

$$G^{(2)}(p) = \sim\!\sim\!\sim + \sim\!\otimes\!\sim + \sim\!\otimes\!\sim \tag{3.12}$$

Usually, there is one counter-term for each divergent irreducible diagram. And then, MS-bar sets that at some scale, M (the renormalization scale), the quantum corrections to the correlation functions, $G^{(n)}$, should cancel with the counter-term contributions.

$$G^{(2)}(p)|_{p^2=M^2} = \sim\!\sim\!\sim \tag{3.13}$$

$$G^{(4)}(p_i)|_{s=t=u=M^2} = -ig = \tag{3.14}$$

[3] $\hat{N}_B|q\rangle = 1/3|q\rangle$; $\hat{N}_L|q\rangle = 0$; $\hat{N}_B|l\rangle = 0$; $\hat{N}_L|l\rangle = |l\rangle$. The opposite baryon/lepton number is attributed to antiquarks and anti-leptons. Other particles have $\hat{N}_{B/L}|p\rangle = 0$.

[4] The particle is said to be left-handed if its spin is anti-parallel to the momentum; it is right-handed if the spin is parallel to the momentum.

Physical processes (correlation functions) should not depend on the renormalization scheme or scale we choose. The Callan-Symanzik equation arises as a consequence of the arbitrary choice of the renormalization scale.

$$\Big[M\frac{\partial}{\partial M}+\beta_i\frac{\partial}{\partial\beta_i}+n_i\gamma_i\Big]G^{(n_1,n_2,(...))}(x_1,...,x_n;M,g_i)=0 \tag{3.15}$$

where n_i is the number of fields i involved and γ_i the corresponding anomalous dimension. β_i is the beta function of g_i, which measures how the coupling constants change as the renormalization scale varies:

$$\beta_i = M\frac{\partial g_i}{\partial M} \tag{3.16}$$

The Standard Model is a renormalizable theory[5], since a finite number of counter-terms is needed to renormalize the theory to all orders in perturbation theory. For this theory, there are three beta functions, one for each gauge group coupling constant:

$$\beta_i(g)=-\frac{g_i^3}{(4\pi)^2}\Big[\frac{11}{3}C_2(G_i)-\frac{4}{3}\sum_f C(r_f)-\frac{2}{3}\sum_s C(r_s)\Big] \tag{3.17}$$

where $C_2(G_i)$ is the quadratic Casimir operator for the adjoint representation and $C(r_f)/C(r_s)$ is the Casimir operator for the fermion/scalar field representation r_f/r_s. Thus, the beta-functions depend on the gauge group of each interaction:

- For $G=U(1)_Y$, fields in the adjoint representations have $C_2(G)=0$ and it is common to normalize the hypercharge so that $C(r_f)=\frac{3}{5}\Big(\frac{y_f}{2}\Big)^2$, thus:

$$\beta_1(g)=-\frac{g^3}{(4\pi)^2}b_1 \quad , \quad b_1=\frac{1}{10}\sum_f y_f^2-\frac{1}{20}\sum_s y_s^2 \tag{3.18}$$

- For $G=SU(N)$, $N\geq 2$, fields in the adjoint representations have $C_2(G)=N$, for fields in the fundamental and anti-fundamental representation $C(N)=C(\bar{N})=\frac{1}{2}$, and for the singlet representation $C(1)=0$, thus:

$$\beta_N(g)=-\frac{g^3}{(4\pi)^2}b_N \quad , \quad b_N=\frac{11}{3}N-\frac{2}{3}n_f-\frac{1}{3}n_s \tag{3.19}$$

Solving these equations for the corresponding *fine-structure constants* ($\alpha_i=g_i^2/(2\pi)$), we are led to:

$$\alpha_i^{-1}(Q)=\alpha_i^{-1}(m_Z)+\frac{b_i}{2\pi}\ln\left(\frac{Q}{m_Z}\right) \tag{3.20}$$

where Q is the energy scale of the interaction. This gives the Standard Model's *running coupling constants* . This expression is valid to first order as long as b_i is constant and for $\alpha_i(Q)<1$. In Figure 3.3 is represented the evolution at high energies, with b_i given by Eq. (3.22). It is interesting to note two details: the most obvious, that at high energies, the coupling constants seem to become identical. This fact might suggest that at a scale of

[5] This is, in the absence of gravity. Extensions where gravity is included are non-renormalizable due to the inclusion of non-renormalizable terms suppressed by powers of M_p.

10^{15-16} GeV, there is some form of Strong-Electro-Weak unification. The second detail is that the strong force becomes stronger at lower energies, even becoming non-perturbative $\alpha_3(Q) > 1$, which is believed to be related to the quark confinement. The scale at which the strong force becomes non-perturbative is known as Λ_{QCD}. Solving Eq. (3.20) for Λ_{QCD} and $\alpha_3(\Lambda_{QCD}) = 1$, it is given approximately by:

$$\Lambda_{QCD} \sim m_Z \exp\Big[-\frac{2\pi}{b_3}(\alpha_3^{-1}(m_z) - 1)\Big] \sim \mathcal{O}(200 \text{ MeV}) \tag{3.21}$$

An exact computation of this quantity depends on the renormalization scheme and the approximation order. We are mainly interested in this quantity's order of magnitude $\mathcal{O}(200$ MeV), so that the approximation used serves its purpose.

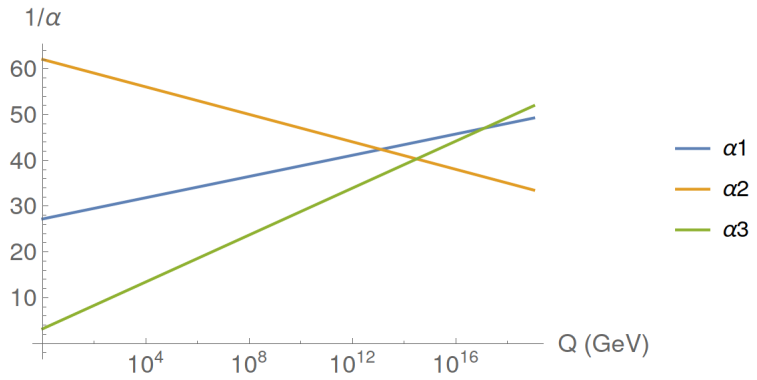

Figure 3.3: Running coupling constants for the SM particle content. The initial conditions are imposed at the scale $\Lambda = m_Z \sim 91$ GeV: $\alpha_1^{-1}(m_Z) \simeq 59.1$, $\alpha_2^{-1}(m_Z) \simeq 29.6$ and $\alpha_3^{-1}(m_Z) \simeq 8.4$, according to experimental measurements.

$$b_N^{SM} = \begin{cases} -41/10 & , N = 1 \\ 19/6 & , N = 2 \\ 7 & , N = 3 \end{cases} \tag{3.22}$$

Beyond the Standard Model

Despite the success of the Standard Model, there are still some gaps to be filled. It is believed that a new extension to higher energies is needed in order to answer questions such as:

1. Why is the SM gauge group $SU(3)_C \times SU(2)_L \times U(1)_Y$?
2. Should the coupling constants unify at high energy scales?
3. Why are there 3 quark and lepton families? And what causes the mass hierarchy?
4. What is the origin and nature of dark matter and dark energy?
5. What generates the baryon asymmetry of the universe?
6. What is the origin of the Higgs boson mass?
7. How to incorporate gravity within the theory?

In this sense, the Standard Model should be regarded as a low-energy effective theory. An extension of the Standard Model may be theorised by implementing some new, or a larger symmetry. The possible choices are reduced by the Coleman-Mandula theorem (see [30]). Under reasonable assumptions, it states that the most general Lie algebra applicable to a relativistic QFT is the one generated by the Poincaré group and the one generated by internal symmetries generators combined in a trivial way (as Eq. 3.1). As a consequence, two particles of different spin cannot belong to the same gauge multiplet.

Grand Unified Theories (GUT) propose that $SU(3)_C \times SU(2)_L \times U(1)_Y$ may be the result of larger gauge group with unified Strong and Electroweak forces, spontaneously broken at high energies ($M_{GUT} \sim 2 \times 10^{16}$ GeV). Finally, as energies approach the Planck mass ($M_p = \sqrt{8\pi G}^{-1} \sim 10^{18}$ GeV), non-renormalizable terms induced by gravity become relevant and the Standard Model loses its predictive power. This is a strong indication that new physics may appear at these scales, described by a theory of *quantum gravity*.

3.2 Minimal Supersymmetric Standard Model

Supersymmetry (SUSY) consists in the idea that force and matter fields are interchangeable while maintaining the theory invariant (*fermion* $\leftrightarrow$ *boson*). Today, the principle of supersymmetry is widely used in several theoretical models such as quantum gravity and grand unification. In general, in supersymmetric extensions of the SM, SM particles belong to a super-multiplet together with their supersymmetric partners (see [30]). Particles in the same super-multiplet are indistinguishable, except for their spin representation.

The *Minimal Supersymmetric Standard Model* (MSSM) is the simplest extension of the SM where Supersymmetry is added as an additional symmetry. In the MSSM, the super-multiplets are composed of two particles differing by 1/2 spin. In the standard nomenclature, fermion's partners are named adding the prefix "$s-$" to the fermion name (electron $e \rightarrow$ *selectron* $\tilde{e}$). Boson's partners are named adding the suffix "$-ino$" to the name of the boson (photon $\gamma \rightarrow$ *photino* $\tilde{\gamma}$).

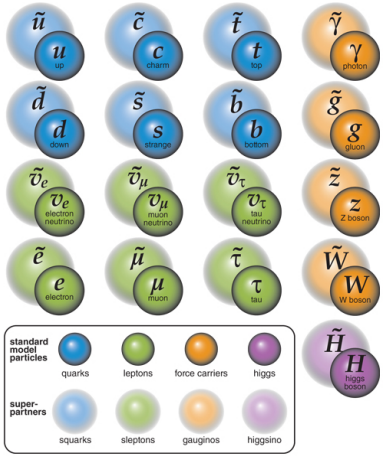

Figure 3.4: The MSSM particle content [9].

The existence of a new Higgsino gives rise to gauge anomalies, which can be cancelled if there is another one with opposite Hypercharge. Due to this fact, the MSSM requires the existence of two Higgs doublets (H_u and H_d) and their corresponding Higgsinos. Now, in the Higgs mechanism, each Higgs boson acquires its vev (v_u and v_d), the up family receives its masses from the H_u, while the down-family and the electron-family receive masses from the H_d, which are given by:

$$m_u = y_u v_u \quad m_d = y_d v_d \quad m_e = y_e v_d \tag{3.23}$$

where v_u and v_d must obey $v = \sqrt{v_u^2 + v_d^2} \sim 246$ GeV and y_u and y_d are the Yukawa coupling constants, which measure the coupling strength of the fermions with the respective Higgs boson. With only one constraint, we gained a new parameter, frequently denoted by $\tan\beta = v_u/v_d$.

Since it transforms bosons into fermions, changing spin, Supersymmetry generators do not commute with the ones from the Poincaré group. It seems that the Coleman-Mandula theorem could rule these theories out. However, SUSY generators obey anti-commutation, rather than commutation relations. The combination of this set of generators form a superalgebra, i.e., a generalized concept of algebra that includes anti-commutative symmetry generators. This is enough to evade one of the assumptions and "survive" the implications of the theorem. Poincaré, gauge and SUSY generators along with their (anti)commutation relations form a super-algebra. This extension might be regarded as a generalization of the Poincaré group to a spacetime with anti-commuting degrees of freedom, labelled by Grassmann numbers - a *superspace*. The SUSY generators are associated to a translation along the new coordinates [31, 30].

In the MSSM, the interaction terms in the Lagrangian are obtained from the renormalizable superpotential. This object is a mass dimension 3 complex valued function constructed by combination of the MSSM superfields into gauge-invariant, R-parity invariant (defined later in this section) and renormalizable monomials:

$$W_{MSSM} = y_u^{ij}\bar{u}_i Q_j \cdot H_u - y_d^{ij}\bar{d}_i Q_j \cdot H_d - y_e^{ij}\bar{e}_i L_j \cdot H_d + \mu H_u \cdot H_d \tag{3.24}$$

where the i, j indices correspond to the generation and the colour indices are omitted for simplicity. The parameter μ is related to the Higgs mass term and should not be much larger than the electroweak scale. The fields are in the left-chiral representation, where upper-case superfields stand for $SU(2)_L$-doublets and lower-case for fields $SU(2)_L$-singlets, some examples being:

$$Q = \begin{pmatrix} \tilde{u}_L \\ \tilde{d}_L \end{pmatrix} \qquad L = \begin{pmatrix} \tilde{\nu}_L \\ \tilde{e}_L \end{pmatrix} \qquad \bar{e} = \tilde{e}_R^* \qquad \bar{d} = \tilde{d}_R^* \tag{3.25}$$

For the purposes of this work, we are mainly interested in the scalar part of the interaction terms (as written in the above equation), which is equivalent to regarding the superfields as their scalar part ($\Phi = \phi$). The scalar potential of the theory is obtained from the F and D-terms:

$$\mathcal{V} = F_i^\dagger F_i + \frac{1}{2}\sum_N g_N^2 D_{\alpha,N} D_N^\alpha \tag{3.26}$$

where the sum is made over repeated indices and over gauge groups and their generators, t_N^α. The F- and D-terms are given by:

$$F_i = -\left(\frac{\partial W}{\partial \phi_i}\right)^\dagger \quad , \quad D_N^\alpha = \phi_i^\dagger t_N^\alpha \phi_i \tag{3.27}$$

Hierarchy Problem

One of the strongest motivations for Supersymmetry is the weak-scale hierarchy problem [32, 31]. With the eminence of new physics appearing at the Planck scale, why are the Higgs mass and Electroweak scale is so low? Unlike fermion and gauge fields, there is no

chiral or gauge symmetry forbidding mass terms for scalar fields. If there is new physics at some large cut-off scale M, it could introduce quadratic corrections to the Higgs mass via:

- Scalar field loops:

$$\sim |y_s|^2 \int^M d^4k \frac{1}{k^2 - M_H} \sim |y_s|^2 M^2 \tag{3.28}$$

- Fermion and anti-fermion loops:

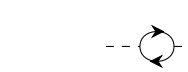

$$\sim (-1)|g_f|^2 \int^M d^4k \frac{1}{k^2 - M_H} \sim -|g_f|^2 M^2 \tag{3.29}$$

The fact that there might be new physics near $M_P \sim 10^{18}$ GeV and that the Higgs boson mass is as low as $M_H \sim 125$ GeV is intriguing. Any large scale contributions would drive the Higgs mass to much larger values. The natural solution is that the above contributions cancel each other. With the particle content of the Standard Model, this is not the case. However, with the Minimal Supersymmetric SM, each fermion field has a scalar partner with the same coupling constants and vice-versa. This results in a perfect cancellation of quadratic corrections, only leaving a mild logarithmic dependence on the cut-off scale.

Soft SUSY Breaking and Hidden Sector

Although supersymmetry promises a very elegant solution, there is an elephant in the room: these new particles have never been observed or produced in experiments. Nature might be supersymmetric, however, if this symmetry is spontaneously broken at some high-energy scale, such that s-particles gained masses large enough to escape our experiments.

From the (anti)commutation laws of the SUSY algebra (see [31]), a positive energy density is a sufficient condition for SUSY-breaking:

$$\langle 0|\hat{H}|0\rangle \neq 0 \rightarrow Q_i|0\rangle \neq 0 \tag{3.30}$$

In particular, SUSY breaks if the scalar potential $\mathcal{V}$ (Eq.3.26) is non-zero. This symmetry could, for instance, be spontaneously broken by some F- or D-term v.e.v.. However this source of SUSY-breaking implies the existence of low-mass s-particles or some gauge symmetry breaking, both of which are phenomenologically incompatible (as discussed in [32, 31]). Alternatively, SUSY-breaking may be caused by mass and Yukawa terms induced directly on the scalar potential from some extra-MSSM mechanism. There are plenty of renormalizable terms:

- Gaugino Masses: $-\frac{1}{2}(M\tilde{g}^a \cdot \tilde{g}^a + M_2\tilde{W}^a \cdot \tilde{W}^a + M_1\tilde{B} \cdot \tilde{B})$
- Squark masses: $-m_{ij}^2\tilde{Q}_i^\dagger \cdot \tilde{Q}_j - m_{ij}^2\tilde{\bar{u}}_i^\dagger\tilde{\bar{u}}_j - m_{ij}^2\tilde{\bar{d}}_i^\dagger\tilde{\bar{d}}_j$
- Slepton masses: $-m_{ij}^2\tilde{L}_i^\dagger \cdot \tilde{L}_j - m_{ij}^2\tilde{\bar{e}}_i^\dagger\tilde{\bar{e}}_j$
- Higgs mass terms: $-m^2H_u^\dagger \cdot H_u - m^2H_d^\dagger \cdot H_d - (bH_u \cdot H_d + h.c.)$
- Triple scalar couplings: $-a_u^{ij}\tilde{\bar{u}}_i\tilde{Q}_j \cdot H_u + a_d^{ij}\tilde{\bar{d}}_i\tilde{Q}_j \cdot H_d + a_e^{ij}\tilde{\bar{e}}_i\tilde{L}_j \cdot H_d + h.c.$

For the case of the present SUSY-breaking, the mass and Yukawa terms are related to some scale m_{susy}. SUSY breaking is thought to occur in some hidden sector, where some field X (which does not have direct couplings to the MSSM) acquires an F-term. The breaking is communicated to the MSSM through large mass M_ψ messenger fields ψ and gives rise to terms proportional to (see Figure 3.5):

$$m_{susy} \sim \lambda \frac{F_X}{M_\psi} \tag{3.31}$$

Figure 3.5: Hidden sector SUSY-breaking

One might think that this breaking should become negligible at scales $\Lambda > m_{susy}$ and SUSY restored. However, as we have seen before, in the course of the universe's history, the energy density was not exactly null and sometimes even changed its sources. Thus, it is possible that SUSY has been broken by various mechanisms since the early universe. We will return to this subject later in this work.

R-parity

In the construction of the MSSM, we have required the theory to be symmetric under R-parity. The reason behind this imposition is to forbid L or B-violating terms:

$$W_{\Delta L=1} = \lambda_e^{ijk} L_i \cdot L_j \bar{e}_k + \lambda_L^{ijk} L_i \cdot Q_j \bar{d}_k + \mu_L^i L_i \cdot H_u \tag{3.32}$$

$$W_{\Delta B=1} = \lambda_B^{ijk} \bar{u}_i \bar{d}_j \bar{d}_k \tag{3.33}$$

In particular, these terms provide new decay channels for the proton, which have never been observed by experiment. Thus, the coupling strengths of these terms are strongly restricted by experiment. One way to address this problem is simply imposing B and L-conservation. However, there are non-perturbative electroweak processes, known as Sphalerons, that become relevant at high energies and are known to conserve only $B - L$ (Section 5.1). R-parity is a weaker condition. It implies the conservation of B and L in renormalizable terms, although allowing non-renormalizable terms that do not conserve it.

$$R = (-1)^{2s+3(B-L)} \rightarrow R = \begin{cases} 1 & \text{"SM particles"} \\ -1 & \text{"super partners"} \end{cases} \tag{3.34}$$

This symmetry is multiplicatively conserved and implies that an interaction between an odd-number of s-particles results in an odd-number of s-particles. As we will see in section 3.3, this implies the existence of a new dark matter candidate.

Strong-Electro-Weak Unification

Through the reasoning described in the last section, the new scalars and fermions within the MSSM will enter the loops and influence the beta functions. The decoupling theorem [33] ensures that the contribution of these particles is suppressed below the energy corresponding to their mass. It is a reasonable approximation to assume that all s-particles

start contributing to the running at the same scale M_{susy}. Thus, the evolution of α_i is given by:

$$\alpha_i^{-1}(Q) = \begin{cases} \alpha_i^{-1}(m_Z) + \dfrac{b_i^{sm}}{2\pi} \ln\left(\dfrac{Q}{m_Z}\right) & , Q < M_{susy} \\ \alpha_i^{-1}(M_{susy}) + \dfrac{b_i^{mssm}}{2\pi} \ln\left(\dfrac{Q}{M_{Susy}}\right) & , Q > M_{susy} \end{cases} \tag{3.35}$$

and is shown in Figure 3.6. The three coupling constants converge very accurately if one assumes $M_{susy} \sim 1 - 10$ TeV. This might be just a meaningless coincidence, but, if experiments find evidence of s-fermions or gauginos at the TeV-scale, it may be a strong clue that the MSSM is the result of a larger symmetry that has been spontaneously broken at the scale $M_{GUT} \sim 2 \times 10^{16}$ GeV. It is common to set the unification conditions at:

$$\alpha_1^{-1}(M_{GUT}) = \alpha_2^{-1}(M_{GUT}) = \alpha_3^{-1}(M_{GUT}) \sim 25.6 \tag{3.36}$$

Just like coupling constants, other Lagrangian parameters also change with scale, in particular masses. There are also analogous unification conditions for these parameters. A very interesting result from MSSM and unification at M_{GUT} comes from the running mass-squared of H_u. Thanks to the large Yukawa coupling of the top quark, it is actually possible for the squared-mass to become negative and trigger Electroweak symmetry breaking at the correct scale (as analysed, for example, in [31]).

For the reasons presented above, we will in this work consider the MSSM and keep in mind the SUSY-breaking scale is likely to be at $M_{susy} \sim 1 - 10$ TeV, at least in our "visible" sector as we will later discuss (Chapter 6).

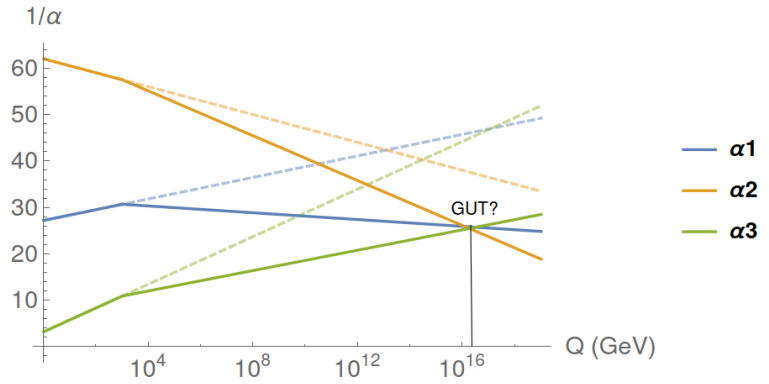

Figure 3.6: Running coupling constant for the MSSM (solid line) vs. SM (dashed lines) particle content. The initial conditions are imposed at the scale $\Lambda = M_Z \sim 91$ GeV: $\alpha_1^{-1}(M_Z) \simeq 59.1$, $\alpha_2^{-1}(M_Z) \simeq 29.6$ and $\alpha_3^{-1}(M_Z) \simeq 8.4$

$$b_N^{mssm} = \begin{cases} -33/5 & , N = 1 \\ -1 & , N = 2 \\ 3 & , N = 3 \end{cases} \tag{3.37}$$

Flat Directions

A particular feature of the MSSM is the existence of many scalar fields. *Flat directions* are non-trivial trajectories in scalar field configuration space along which the scalar potential (Eq. (3.26)) is zero. This can be seen by counting degrees of freedom (d.o.f.).

The MSSM contains 49 complex d.o.f. in its scalar fields and the conditions for the scalar potential to vanish are:

$$F_i = -\Big(\frac{\partial W}{\partial \phi_i}\Big)^\dagger = 0 \qquad D^\alpha = \phi_i^\dagger t^\alpha \phi_i = 0 \tag{3.38}$$

For $SU(3) \times SU(2) \times U(1)$, there are 12 D-term conditions (one for each generator). With the gauge conditions, there are 37 d.o.f. remaining. If the F-term conditions are restrictive enough, the fields are restricted to $\phi_i = 0$. If not, there will be some d.o.f.s remaining and the potential along some directions will be flat or approximately flat. This allows fields to acquire v.e.v.s while maintaining the potential unchanged.

As an example, consider the following configuration of the Q, L and $\bar{d}$ scalar fields:

$$Q_1^\alpha = \frac{1}{\sqrt{3}}\begin{pmatrix}\phi\\0\end{pmatrix} \qquad L_1 = \frac{1}{\sqrt{3}}\begin{pmatrix}0\\\phi\end{pmatrix} \qquad \bar{d}_2^\alpha = \frac{1}{\sqrt{3}}\phi \tag{3.39}$$

where the upper index α stands for the colour charge and the lower index for the quark/lepton generation. The D-term conditions are:

$$\begin{aligned} D_{U(1)_Y} \supset \;& Q^\dagger \hat{Y} Q + L^\dagger \hat{Y} L + \bar{d}^\dagger \hat{Y} \bar{d} \\ \to & \frac{1}{3}(Y_Q + Y_L + Y_{\bar{d}})\phi^\dagger \phi = 0 \end{aligned} \tag{3.40}$$

$$\begin{aligned} D^a_{SU(2)_L} \supset \;& Q^\dagger \frac{\tau^a}{2} Q + L^\dagger \frac{\tau^a}{2} L \\ \to & \frac{1}{6}((\tau^a)_{11} + (\tau^a)_{22})\phi^\dagger \phi = 0 \end{aligned} \tag{3.41}$$

$$\begin{aligned} D^a_{SU(3)_C} \supset \;& Q^\dagger \frac{\lambda^a}{2} Q + \bar{d}^\dagger \frac{\lambda^a}{2} \bar{d} \\ \to & \frac{1}{6}((\lambda^a)_{\alpha\alpha} - (\lambda^a)_{\alpha\alpha})\phi^\dagger \phi = 0 \end{aligned} \tag{3.42}$$

Notice that the D-term conditions are satisfied for $\phi \neq 0$. It is straightforward to see that this direction is F-flat too. The F-term corresponding to the H_d gives $F_{H_d} = y_d^{12} Q_1 \bar{d}_2 \sim 0$, since $y^{ij} \sim 0$ for $i \neq j$. The remaining terms are trivially zero, since they include fields with vanishing vev.

A common way to characterise flat directions is by constructing the gauge-invariant monomial, $X_m = \Phi_1 \cdots \Phi_m$, composed by the relevant superfields. In particular for the above example, $X = Q_1 L_1 \bar{d}_2$ ($m = 3$) and its scalar part is parametrized by a scalar field $X = \phi^m$. Notice that one quanta of this flat direction carries $B = 1/3 + 0 - 1/3 = 0$ and $L = 0 + 1 + 0 = 1$. Similarly, other flat directions also carry some $U(1)$ charge.

Now, this direction's flatness may be disturbed by non-renormalizable terms and soft SUSY-breaking:

- **Non-renormalizable terms** in the superpotential induced by some scale M (Planck or GUT) physics become relevant at high enough energies

$$W = W_{MSSM} + \sum_{n>3} \frac{\lambda}{M^{n-3}} \Phi^n \tag{3.43}$$

Non-renormalizable terms introduce new conditions to the flat directions. Since, in order to have vanishing F-term the flat direction must have some free degrees of freedom, every MSSM flat direction is eventually lifted by some non-renormalizable term of order n [34]. This induces a scalar potential caused by the non-zero F-terms of the form[6]:

$$\mathcal{V}(\phi) \supset \frac{|\lambda|^2}{M^{2n-6}}(\phi^\dagger\phi)^{n-1} \tag{3.44}$$

Notice that this potential term is $U(1)$-invariant, preserving the number-charge carried by the flat direction.

- **Soft SUSY-breaking terms** contribute to the scalar potential, breaking SUSY. The flat direction is lifted if any of these terms depends on any of its fields. For the example above:

$$-m_{ij}^2\tilde{Q}_i^\dagger\cdot\tilde{Q}_j - m_{ij}^2\tilde{L}_i^\dagger\cdot\tilde{L}_j - m_{ij}^2\tilde{\bar{d}}_i^\dagger\tilde{\bar{d}}_j \to V(\phi) \supset -(m_Q^2+m_L^2+m_{\bar{d}}^2)\phi^\dagger\phi \tag{3.45}$$

- **Supergravity** (SUGRA) is one of the approaches that relates supersymmetry with general relativity. This theory emerges from promoting the SUSY transformations to local transformations, implying the existence of a spin-2 gauge boson, the graviton, and its partner, the spin-3/2 gravitino. Supergravity induces corrections to the scalar potential of the form (with $D^\alpha = 0$):

$$\mathcal{V} \supset e^{K/M_p^2}\Big[\underbrace{D_iW(K^{-1})_{ij}D_j^*W^*}_{F_iF^{*i}} - \frac{3}{M_p^2}|W|^2\Big] \tag{3.46}$$

where $D_iW = W_i + K_iW/M_p^2$ and the index i stands for the derivative with respect to the field ϕ_i. The term K is the Kahler potential, a real function of the superfields and its conjugates of mass dimension 2. This is the object responsible to generating the kinetic terms for the SUGRA Lagrangian, its minimal form being $K = \mu\Phi_i^\dagger\Phi_i$. For a review on Supergravity we refer the reader to [35].

The dynamics of flat directions plays a central role in the Affleck-Dine Mechanism for Baryogenesis [36] to be discussed in Section 5.3. A summary of the MSSM renormalizable flat directions and the terms that lift them is available in Appendix A.2, the full study is provided by [34].

3.3 Dark Matter Candidates

As far as we know, Cold Dark Matter (CDM) should be some massive, long-lived [37] species that predominantly interacts gravitationally with ordinary matter. As mentioned in Section 2.5, its nearly spherically-uniform distribution in galaxies suggests that any long-range interactions should be weak or absent. These conditions leave room for a broad list of theoretical candidates. Some of the most relevant in the context of particle physics are:

[6] Actually, this is just the dominant term. Terms from supergravity are suppressed by higher powers of M. Other terms may come from couplings to fields other than the ones in the flat direction, which have $\langle\Phi\rangle = 0$ and become negligible in the scalar potential.

- **Axions** - A particle first postulated in 1977, related to the spontaneously breaking of a hypothetical $U(1)$ Peccei-Quinn symmetry [38], with the objective of solving the strong CP-problem. In invisible axion models [39], these particles are long lived $SU(2)_L \times U(1)_Y$ singlets with small masses of the order 10^{-5} eV $< m_A < 10^{-3}$ eV. A large abundance of axions is thought to have been produced in the early universe, originated from a boson condensate. With the above range of masses and with a large abundance, the axion is an important candidate that may account for the Ω_{cdm} observed.

- **Thermal WIMPs** - A very wide class of particles with masses above the GeV scale that only interact gravitationally and possibly via some weak-scale force. Most commonly, the abundance of this particles is attributed to a departure from thermal equilibrium (Section 2.3) in the early universe, leaving a relic density that may account for cold dark matter.

- **Lightest Supersymmetric Particle (LSP)** - In the MSSM, the superpotential W_{MSSM}, is constructed assuming the theory is R-parity symmetric. As a consequence, the reaction product of an initial state containing an odd/even number of s-particles must have also an odd/even number of s-particles. Hence, the decay of lightest s-particle (LSP) into ordinary particles is forbidden. This is, if R-parity is respected, the LSP should be stable and may potentially account for the CDM density parameter. Examples of LSP candidates are the *gravitino* (supersymmetric partner of the graviton in SUGRA models) and the *neutralino* (a mass eigenstate resulting from mixing of the Bino, the neutral Wino and the neutral Higgsinos created after the electroweak symmetry breaking [31]).

These are just three of a large list of candidates. In principle, most of these candidates could be produced via some mechanism unrelated to Baryogenesis. Since Baryonic and Dark matter have comparable densities:

$$\frac{\rho_b}{\rho_d} \sim \frac{m_b}{m_d}\frac{n_b}{n_d} \sim \frac{1}{5} \tag{3.47}$$

it seems an unlikely coincidence that the number densities and masses of baryonic and cold dark matter have conspired in order to ensure the observed density ratios. Perhaps if dark and baryonic matter arise from a common mechanism, comparable energy densities would follow. However, if the two mechanisms are unrelated, it seems to be a strange coincidence. As mentioned in the introduction, this issue is the main focus of this work (Chapter 6).

Chapter 4

Inflation and Cosmological Perturbations

"There is no dark side of the moon, really. As a matter of fact it's all dark."

— Gerry O'Driscoll, *Eclipse*

As we discussed in Chapter 2, the Big Bang theory has been remarkable in explaining several cosmological observations. However, this theory has its shortcomings. Namely, it requires extremely fine-tuned initial conditions that might be obtained simply by chance (anthropic principle) or may be an attractor solution from some dynamical mechanism. The disadvantage of relying on chance is that any initial condition must be put "by hand", whereas in a dynamical model the initial conditions become a prediction. In the inflationary cosmological model [40], the universe went through a period of near-exponential expansion (*quasi-de Sitter universe*, $H \sim$ const.) driven by the dynamics of a scalar field, the *inflaton*. This model naturally establishes the fine-tuned initial conditions at early times.

4.1 Standard Cosmology Problems

Let us briefly review some of the Hot Big Bang shortcomings and see how Inflation can deal with them (for a more detailed analysis we refer to [10]).

1. **The Horizon Problem** - The light we observe in the CMB comes from roughly 10^5 causally disconnected regions [10]. How can it be so homogeneous?

   With Inflation: If the presently observable universe was initially in causal contact and underwent a period of accelerated expansion, it would eventually become bigger than the particle horizon[1].

2. **The Flatness Problem** - At early times, any slight deviation from flatness would grow with expansion. $\Omega_k \sim 0$ is an unstable fixed point and today's observation would require an extreme fine-tuned choice of initial conditions $\Omega_k(M_p) < \mathcal{O}(10^{-60})$.

   With Inflation: In a quasi-de Sitter universe, the density parameter evolves as $\Omega_k \propto a^{-2}$. If the period of inflation lasts long enough, the $\Omega_k = 0$ solution becomes a stable fixed point, i.e, for generic initial conditions before inflation, the system will naturally evolve into a flat universe.

3. **Formation of Structure** - Standard cosmology cannot explain how galaxies and voids could have formed and the origin of the large scale anisotropies on the CMB.

   With Inflation: if Inflation is driven by a scalar field, it exhibits quantum fluctuations. These give rise to inhomogeneities in the energy density and curvature (section 4.3)

[1] Region of causal contact.

on superhorizon scales, which grow during inflation. After this period, the energy density and curvature perturbations cause some regions to be more dense than others, evolving into galaxy formation.

4. **Unwanted Relics** - Grand Unified Theories predict the existence of very massive and stable states that might have been produced in the early universe at high temperatures and should be observable today.

   With Inflation: In a period of accelerated expansion, any initial number density of massive states gets rapidly diluted ($n \propto a^{-3}$). If the temperature of the universe after inflation is not high enough to thermally produce these relics, their number density becomes negligible.

Thus, Inflation becomes an attractive solution for the fine-tuning problems we find on the Hot Big Bang Model.

4.2 Scalar Field Inflation

In principle, as we have seen in section 2.2, a period of accelerated expansion could be achieved if a cosmological constant dominates the universe's energy density. However, since this kind of fluid does not redshift or decay, a transition into the standard cosmology would not follow. In order to accommodate a period of Inflation in the early universe history, the energy density of the universe should be dominated by some fluid that mimics the behaviour of a cosmological constant and then decays away. This dynamics can be obtained from the evolution of a real scalar field, the *inflaton*. In order to see how, consider the action of the inflaton:

$$S_I = \int \sqrt{-g}\Big(-\frac{1}{2}\partial_\mu I \partial^\mu I - V(I)\Big) d^4x \tag{4.1}$$

Varying the action with respect to the metric tensor for an FRW spacetime (see [15]), the energy density and pressure of a scalar field is obtained from the $0,0$ and i,i components of the stress-energy tensor (Eq. (2.7)), respectively:

$$\begin{aligned} T_{00} = \rho_I &= \frac{1}{2}\dot{I}^2 + V(I) + \frac{(\nabla I)^2}{2a^2} \\ T_{ii} = p_I &= \frac{1}{2}\dot{I}^2 - V(I) - \frac{(\nabla I)^2}{6a^2} \end{aligned} \tag{4.2}$$

The equation of motion comes from the conservation of the energy (Eq. (2.18)) and is given by:

$$\ddot{I} + 3H\dot{I} + \partial_I V = 0 \tag{4.3}$$

where, assuming homogeneity, we have neglected the gradient-dependent terms. From Eq. (4.2), we see that if one component of the energy density dominates, the ratio of inflaton's pressure and energy density becomes well defined by a constant equation of state. In particular, notice that if the potential energy dominates over the kinetic energy, the inflaton behaves as a cosmological constant ($w = -1$). The period of accelerated expansion required by inflation may be achieved if a) the inflaton field is initially displaced from its potential minimum and moves very slowly $\dot{I}^2 \ll V(I)$ and b) the field acceleration is negligible compared to the velocity ($\ddot{I} \ll 3H\dot{I}$). These are know as the *slow-roll* conditions and, while they are satisfied, the field is *overdamped* and its mass term $m_I^2 = V''(I)$ is negligible. The equations of motion are simplified to:

$$3H\dot{I} \simeq -\partial_I V \tag{4.4}$$

$$H^2 \simeq \frac{V(I)}{3M_p^2} \tag{4.5}$$

During this epoch, the potential and the Hubble parameter are almost constant. As required, the scale factor evolves as:

$$a(t) \sim a(t_i)e^{Ht} \tag{4.6}$$

In general, the inflaton potential should be very flat, in order for these conditions to be met. This generically implies that, the interactions between the inflaton and other fluids should be very weak during inflation. In order to solve the Horizon and Flatness problems, inflation should have expanded the scale factor by a factor of $a(t_e)/a(t_i) = e^{N_e}$, where $N_e = 50 - 60$ is the number of e-folds. This is enough to ensure that the presently observable universe was within the particle horizon during inflation. Since the universe's temperature red-shifts with expansion, at the end of inflation the universe is cold.

In order to end inflation and exit to the standard cosmology, the inflaton must decay and the temperature of the universe must increase, in order to create the initial conditions for BBN. This is provided by *reheating*, a period where the inflaton decays into relativistic particles, increasing the temperature of the universe. Firstly, in order for this period to take place, the slow roll conditions must be broken, causing the end of inflation. It occurs if the potential steepens and the field acquires velocity (Eq. (4.4)), for example as in Figure 4.1. Note from Eq. (4.2) that when $V(I) \sim \dot{I}^2/2$, the field becomes pressureless, now behaving as non-relativistic matter ($w = 0$). This happens if the field starts oscillating about a the true minimum of its potential since, by the Virial theorem applied to a harmonic oscillator, $\langle V \rangle \sim \langle \dot{I}^2/2 \rangle$. In this period, the energy density is dominated by inflaton oscillations around the minimum of the potential ($m_I^2 = V''(I)$).

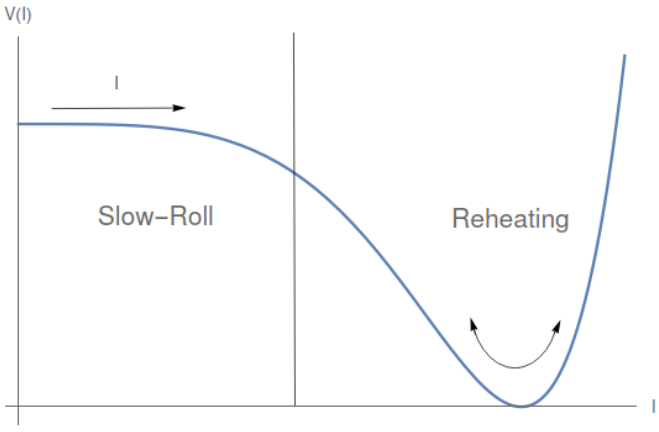

Figure 4.1: An example of potential for the inflaton: $V(I) = V_0\Big(1 - \frac{\gamma}{n}\Big(\frac{I}{M_p}\Big)^n\Big)^2$

The initial conditions of a radiation-dominated universe are set after the inflaton decay (at some rate Γ_ϕ[2]) into lighter particles. This dynamics is obtained from the Boltzman

[2]The general Γ_ϕ has been put in by hand. However, terms of this form follow from the Action Principle, after including the appropriate interaction terms.

equation (Eq. (2.44)) and is given by the system:

$$\begin{aligned}\dot{\rho}_\phi + 3H\rho_\phi &= -\Gamma_\phi \dot{\phi}^2 \\ \dot{\rho}_r + 3H\rho_r &= \Gamma_\phi \dot{\phi}^2 \\ H^2 &= \frac{8\pi G}{3}(\rho_r + \rho_\phi)\end{aligned} \tag{4.7}$$

Any decaying channels will cause the inflaton oscillations to be damped (specially after $H \lesssim \Gamma_\phi$) and *reheating* begins (see [41]). In this period, the inflaton's energy density is transferred into relativistic particles, increasing the temperature of the universe ($T \propto \rho_r^{1/4}$) and its entropy. When $\rho_r \gtrsim \rho_\phi$, radiation starts dominating the energy density, signalling the begining of the radiation era of standard cosmology. The *reheating temperature*, T_R, is defined as the temperature at the time the radiation energy density starts becoming dominant, $\rho_r = \rho_\phi$ (using Eq. 2.29), it is the temperature standard cosmology begins at:

$$T_R \sim g_*^{-1/2}(M_p \Gamma_\phi)^{1/2} \tag{4.8}$$

where ϕ_e is the field value at the time inflation ends and $M_p = (8\pi G)^{-1/2}$ is the reduced Planck mass. High reheating temperatures lead to overproduction of relics, such as gravitinos and monopoles, that could over-close the universe. Although the maximum reheating temperature is model dependent, typical constraints read [36, 15, 42]:

$$10 \text{ MeV} < T_R < 10^9 \text{ GeV} \tag{4.9}$$

4.3 Cosmological Perturbations

In the preceding section, we focused on the dynamics of the inflaton at the classical level. Extending the reasoning to include quantum fluctuations of the inflaton field, inflation also provides a natural explanation to the anisotropies shown in the CMB. The main source of CMB anisotropies is produced by the inflaton's quantum fluctuations. These are called the *adiabatic* or *curvature perturbations*, and are dominant because the inflaton's fluctuations cause perturbations in the energy density which, by Einstein's equations (Eq. (2.5)), are transmitted to perturbations in the background curvature. There may be other subdominant components known as *non-adiabatic* or *isocurvature perturbations* and is caused by quantum fluctuations of subdominant fluids during inflation. These perturbations produce shifts from the dominant adiabatic component. Let us study the evolution of a generic field ϕ that has a time-dependent homogeneous part, $\bar{\phi}$ and spacetime-dependent perturbations, $\delta\phi$:

$$\phi(\vec{x}, t) = \bar{\phi}(t) + \delta\phi(\vec{x}, t). \tag{4.10}$$

As in the classical case, the equation of motion follow from Eq. (4.2) and Eq. (2.18), now including the gradient terms:

$$\delta\ddot{\phi} + 3H\delta\dot{\phi} - \frac{1}{a^2}\nabla^2\delta\phi + V''(\bar{\phi})\delta\phi = 0 \tag{4.11}$$

to linear order. The analysis is simplified (see [15]) if we rewrite the time derivatives in terms of the conformal time $d\tau = dt/a(t)$, and then rewrite the perturbation in terms of its rescaled Fourier modes ($\chi_k = a(t)\delta\phi_k$):

$$\delta\phi(\vec{x}, \tau) = \int \frac{d^3k}{(2\pi)^3} e^{ik\cdot x} \frac{\chi_k(\tau)}{a(\tau)} \tag{4.12}$$

The mean and variance of the field fluctuations are given by (for a more detailed derivation, see [15, 43]):

$$\langle \delta\phi \rangle = 0 \quad , \quad \langle \delta\phi^2 \rangle = \int \frac{d^3k}{(2\pi)^3} H^2\tau^2 |\chi_k|^2 \tag{4.13}$$

During inflation $a''/a = 2/\tau^2$ and the conformal time is given by $a''/a = 2/\tau^2$. The equation of motion for χ_k in the de-Sitter space reads:

$$\chi_k'' + \left(k^2 - \frac{2}{\tau^2}\right)\chi_k = 0 \tag{4.14}$$

and has an exact analytic solution. By renormalization and an appropriate choice of vacuum (see [10]), this equation has the following particular solution:

$$\chi_k = \left(1 - \frac{ik^{-1}}{\tau}\right)\frac{e^{-ik\tau}}{\sqrt{2k}} \tag{4.15}$$

Before proceeding, let us discuss the physical meaning of the comoving time. Writing the FRW metric (Eq. (2.8)) in terms of the conformal time and considering null-geodesics ($ds^2 = 0$) in the radial direction ($d\Omega = 0$), we obtain:

$$ds^2 = a(t)^2\left(-d\tau^2 + \frac{dr^2}{1-kr^2}\right) \rightarrow d\tau = \pm\frac{dr}{\sqrt{1-kr^2}} \tag{4.16}$$

from the equation above (Eq. (4.16)), the flat space case ($k = 0$), it is easy to see that the conformal time is ($\pm$) the distance a massless particle travels (notice the constant k in this equation has nothing to do with the wave number k in the main discussion). The *comoving horizon* $\Delta\tau$ is the maximum distance a photon ($ds = 0$) can travel between t_i and t_f as:

$$\tau_i - \tau_f = \int_{t_i}^{t_f} \frac{dt}{a(t)} \tag{4.17}$$

Thus, for $t_i = 0$ and during the inflation $\tau = -(aH)^{-1}$. τ is the *particle horizon* and defines the maximum radius of a region in causal contact at a certain time t.

Let us consider the two limiting cases of Eq. (4.15):

- For $k^{-1} \gg \tau$, the perturbation mode wavelength is bigger than the horizon - *super-horizon scales*

$$\chi_k \simeq \frac{-i}{\sqrt{2k^3}\tau} \quad \rightarrow \quad |\delta\phi_k| \simeq \frac{H_I}{\sqrt{2k^3}} \tag{4.18}$$

  and on superhorizon scales, the mode amplitude is time-independent.

- $k^{-1} \ll \tau$, the perturbation mode wavelength is smaller than the horizon - *sub-horizon scales*

$$\chi_k \simeq \frac{e^{-ik\tau}}{\sqrt{2k}} \quad \rightarrow \quad |\delta\phi_k| \simeq H_I\tau\frac{e^{-ik\tau}}{\sqrt{2k}} \tag{4.19}$$

  and on subhorizon scales, the fluctuations oscillate.

Notice that $\tau = (aH_I)^{-1}$, decreasing exponentially during inflation. This means that modes that are sub-horizon at the beginning of inflation, become super-horizon after some e-folds, freezing their amplitude. On the other hand, after inflation ends, the particle

horizon starts increasing (e.g. for radiation dominated $\tau \propto t^{1/2}$). Thus, after inflation, the perturbation modes re-enter the horizon (Figure 4.2) and start oscillating.

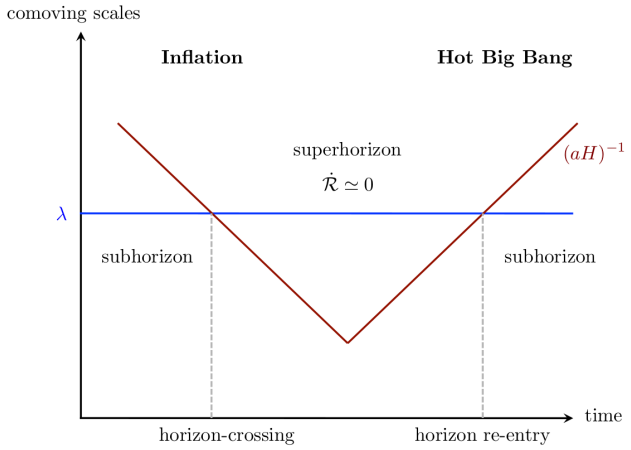

Figure 4.2: During inflation, perturbation modes (blue line) become superhorizon, i.e., larger than the particle horizon (red line). These modes eventually re-enter the horizon and become subhorizon after inflation, when the expansion slows down [10].

These perturbations are encoded in the universe's energy distribution. As an example, the CMB shows the anisotropies of the photon fluid's at the time of recombination. In particular, since at this time the energy density is dominated by matter and, because photons are in thermal equilibrium with baryons, the temperature anisotropies show us how matter was distributed at the time of recombination. The spectrum is commonly analysed after expanding it in a series of spherical harmonics [10]. Small l modes correlations contain valuable information about the Sachs-Wolfe effect [3]. This is, redshift caused to CMB photons from the interaction with gravitational potentials (e.g. galaxies) along their path, before observation. For large l, i.e, large k, the correlation spectrum peaks and troughs, shown in Figure 2.4, reproduce the oscillatory dynamics of sub-horizon perturbation modes.

Massive perturbations

In the previous subsection, we have considered the evolution of fluctuations for the case of massless fields ($V''(\phi) = 0$). In chapter 6, we will be interested in the perturbations due to massive fields. In this case, $V''(\phi) = m_\chi$ and Eq. (4.14) has an additional term. Let us rewrite it as (see [43]):

$$\chi_k'' + \left[k^2 - \frac{2}{\tau^2}\left(\nu_\chi^2 - \frac{1}{4}\right)\right]\chi_k = 0 \quad \text{with} \quad \nu_\chi = \sqrt{\frac{9}{4} - \left(\frac{m_\chi}{H_I}\right)^2} \tag{4.20}$$

Since the parameter ν_χ may be real or imaginary, depending on the mass m_χ, this equation has two regimes. In the regime $m_\chi < 3H/2$, the super-horizon modes are given by:

$$|\phi_k| \simeq \frac{H_I}{\sqrt{2k^3}}\left(\frac{k}{aH_I}\right)^{3/2-\nu_\chi} \tag{4.21}$$

For the case where $m_\chi > 3H/2$, ν_ϕ becomes imaginary and the solution has the form [43]:

$$|\phi_k| \simeq \left(\frac{H}{2\pi}\right)\left(\frac{H}{m_\chi}\right)^{1/2}\left(\frac{k}{aH}\right)^{3/2} \tag{4.22}$$

Notice that if the mass of the mode is not negligible, the amplitude is significantly redshifted by expansion.

Power Spectrum

A very important observable for the analysis of CMB anisotropies is the power spectrum. The super-horizon perturbation modes provide the relevant contributions for this observable.

$$\langle \delta\phi^2 \rangle \simeq \int \frac{d^3k}{(2\pi)^3} \mathcal{P}_\phi(k) = \int \Delta^2_\phi(k) d\ln k \tag{4.23}$$

where $\mathcal{P}_\phi$ is defined as the *power spectrum* and Δ_ϕ the *dimensionless power-spectrum*, defined as:

$$\mathcal{P}_\phi(k) = \frac{H^2}{2k^3} \quad , \quad \Delta^2_\phi(k) = \frac{k^3}{2\pi^2}\mathcal{P}_\phi(k) \tag{4.24}$$

During inflation, the inflaton perturbations caused homogeneities in the energy density and curvature. These perturbation modes exited the horizon and their amplitude froze. The curvature perturbations are obtained from the perturbed FRW-metric. In order to ensure that our quantities do not depend on the coordinate choice, we must work with gauge-invariant quantities (see [15, 43, 10]), which will be useful to compute the perturbation power-spectrum. The adiabatic part is a characteristic of the background, characterized by the gauge-invariant $\zeta_i = \delta\rho_i/\dot{\rho}_i$. The resulting power spectrum for the gauge-invariant comoving curvature perturbations is given by:

$$\mathcal{P}_\zeta = \left(\frac{H}{\dot{\phi}}\right)^2 \mathcal{P}_\phi(k) \quad , \quad \Delta^2_\zeta(k) = \frac{k^3}{2\pi^2}\mathcal{P}_\zeta(k) \tag{4.25}$$

The adiabatic part is the dominant component and obeys:

$$\frac{\delta\rho_b}{3\rho_b} = \frac{\delta\rho_d}{3\rho_d} = \frac{\delta\rho_\gamma}{4\rho_\gamma} = \frac{\delta\rho_\nu}{4\rho_\nu} \tag{4.26}$$

where the multiplicative factor comes from the different redshift the fluids have. Observations by the Planck satellite have measured the adiabatic component dimensionless power-spectrum to be [44]:

$$\Delta^2_\zeta \simeq 2.2 \times 10^{-9} \tag{4.27}$$

The isocurvature modes are the non-adiabatic components of the perturbations, i.e., any shift from the equality of Eq. (4.26). In particular, the fluid i perturbation with respect to the fluid j is an isocurvature perturbation, characterized by the gauge-invariant S_{ij}:

$$S_{ij} = 3\left(\frac{\delta\rho_i}{\dot{\rho}_i} - \frac{\delta\rho_j}{\rho_j}\right) \tag{4.28}$$

Now, the power-spectrum of adiabatic and non-adiabatic modes are related to the gauge-invariant terms defined above by:

$$\Delta^2_\zeta = \frac{k^3}{2\pi^2}\langle \zeta^2_\gamma \rangle \quad , \quad \Delta^2_I = \frac{k^3}{2\pi^2}\langle S^2_{ij} \rangle \tag{4.29}$$

The strength of isocurvature perturbations is frequently expressed as the ratio:

$$\beta_{iso}(k) = \frac{\Delta^2_I(k)}{\Delta^2_\zeta(k) + \Delta^2_I(k)} \tag{4.30}$$

Observations from Planck establish an upper bound $\beta_{iso}(k_{mid}) < 0.037$ for uncorrelated isocurvature modes, with $k_{mid} = 0.050\ \mathrm{Mpc}^{-1}$. We will return to this formalism in section 6.5.

Chapter 5

Baryogenesis

"Now, you must cut down the mightiest tree in the forest with a.... HERRING!"

— Knights who say "NI!"

The matter content of the universe appears to be essentially made of particles, rather than antiparticles. The observed antiparticles coming from cosmic rays are relatively rare and consistent with antiparticles that were accidentally created by collisions of some particle with the interstellar medium. Additionally, if there were regions mainly constituted by particles and other regions by anti-particles, we would be able to observe the light from regions of matter-antimatter annihilation.

We are led to conclude that the universe matter content is mainly composed of baryons and leptons. In standard cosmology, the baryon number of the universe was tought to be defined by an initial condition. However, in inflationary cosmology, any initial asymmetry gets exponentially diluted by the expansion. Thus, this asymmetry must be generated by some mechanism posterior to inflation. *baryogenesis* is a process that should have happened in the early universe and established the baryon number (B) asymmetry required for the success of the primordial nucleosynthesis.

5.1 Sakharov's Conditions

To accomplish this goal, whatever the mechanism is, it should follow Sakharov's conditions [45] (for a more detailed analysis, see [11]):

1. There should be some source of **B-violation**: This is the most obvious condition, baryogenesis should have some transition that takes some zero baryon number state to a non-zero (B) baryon number state:

$$X \to Y + B \tag{5.1}$$

2. **Departure from Thermal Equilibrium**: Unless the system departs from thermal equilibrium, the inverse and direct transitions will always be equal, producing no net baryon number. Thus, we must require a departure from thermal equilibrium to generate a B-asymmetry:

$$\Gamma(X \to Y + B) \neq \Gamma(Y + B \to X) \tag{5.2}$$

3. **C-violation**: If the process is invariant under charge conjugation, its conjugate process (accomplished by substitution of each particle by its anti-particle) would have the same rate and produce the opposite baryon number. For this reason, we must require C-violation:

$$\Gamma(X \to Y + B) \neq \Gamma(\bar{X} \to \bar{Y} + \bar{B}) \tag{5.3}$$

4. **CP-violation**: Now, suppose that the state B is left handed, B_L. If the process were CP-invariant (C-transformation plus inversion of handedness), we would get:

$$\begin{aligned}\Gamma(X \to Y + B_L) &= \Gamma(\bar{X} \to \bar{Y} + \bar{B}_R) \\ \Gamma(X \to Y + B_R) &= \Gamma(\bar{X} \to \bar{Y} + \bar{B}_L)\end{aligned} \tag{5.4}$$

the four processes combined lead to a vanishing net baryon number production and, therefore, we must also require CP-violation (Eqs.(5.4) to become inequalities).

B-violation in the SM

As mentioned in Section 3.2, B and L-violating processes are known to exist within the Standard Model, via non-perturbative sphaleron processes with $\Delta B + L = \pm 6$.

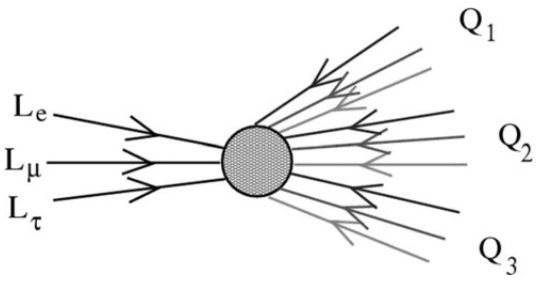

Figure 5.1: In this process, three $SU(2)$-doublet lepton interact (one of each generation), producing three trios of each anti-quark generation. This process violates B and L by 3 units. However, $B - L$ is conserved. [11]

At low energies, this process results from the non-trivial vacuum structure of the broken $SU(2)_L$ gauge symmetry. The vacuum state is discretely degenerate and allows quantum tunnelling processes between states with different $B-L$. The tunnelling amplitude is very small at low energies $\mathcal{A} \sim 10^{-173}$, since the potential barrier between vacuum states is too large. However, for temperatures $T \gtrsim 100$ GeV, these processes may become relevant [11]. Above the electroweak scale, $SU(2)_L$ is unbroken and the barriers between vacuum states disappear, increasing the sphaleron interaction rate. These processes are thought to be in thermal equilibrium up to $T \sim 10^{13}$ GeV.

Since sphaleron processes are in thermal equilibrium in the early universe, any $B + L$ produced is expected to be washed out. On the other hand, $B - L$ seems to be conserved in every known physical process. Thus, $B - L$ is the relevant component that is conserved if Baryogenesis takes place at high energies.

5.2 Examples of mechanisms for Baryogenesis

Before getting into the Affleck Dine mechanism for Baryogenesis, which will be the focus of our discussion, let us first review some of the alternative mechanisms.

Electroweak Baryogenesis

A possible explanation for Baryogenesis that could, in principle, be incorporated within the Standard Model is Electroweak-scale Baryogenesis [46]. If the Electroweak phase transition is first order, the Higgs potential develops a barrier and the transition between the symmetric ($\langle h \rangle = 0$) and broken phase ($\langle h \rangle = v$) occurs via quantum tunnelling. As a consequence, EW-breaking will be inhomogeneous in space, creating *bubble nucleation* bounded by domain walls.

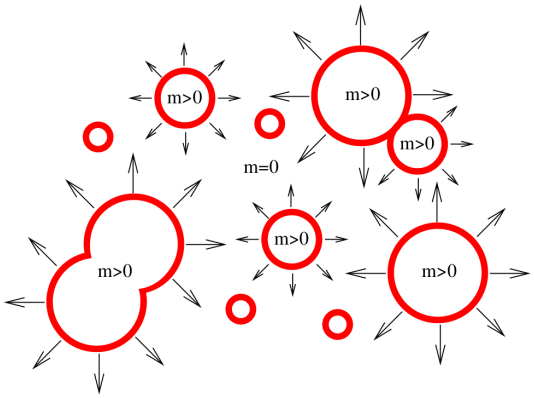

Figure 5.2: In a bubble nucleation process, the phase transition occurs in some regions of space before the others, creating bubbles of broken symmetry.[11]

As the bubble expands, particles in the symmetric phase undergo interactions with the wall, which provide the source of CP-asymmetry, causing a net flux of baryons inside the bubbles. The C-violation source is provided by the $SU(2)_L$ nature of sphalerons. In these models, the rate of sphaleron processes inside the bubble is slow enough so that the created B is not totally washed out. In contrast, outside the bubble the corresponding deficit of B is washed out. By this reasoning, at the end of EW symmetry breaking, we are left with a net B that may account for the observed asymmetry.

Despite having all the ingredients needed to produce baryon number, electroweak baryogenesis within the Standard Model requires the Higgs mass to be less than $m_H \lesssim 30$ GeV, which is ruled out by experiment. In models with additional Higgs doublets such as the MSSM, the 2-Higgs doublet model (2HDM) and Non Minimal Supersymmetric SM (NMSSM), new sources of CP-violation are added and a first order phase transition is more naturally established (see [11] and its references).

GUT Baryogenesis

In the context of Grand Unified Theories (GUT), the MSSM gauge groups are the result of a larger symmetry gauge group such as $SU(5)$ or $SO(10)$. A larger symmetry gauge group comes with an additional number of gauge and Higgs bosons, with masses of the order $M_{GUT} \sim 10^{16}$ GeV. In this mechanism, B-violating processes occur via out-of-equilibrium decays of these bosons into baryons and/or leptons $X \to b + l$. C and CP-violating processes occur if there are two or more of such bosons. The problem with this mechanism resides in the fact that these bosons must have been thermally produced after inflation. This requires very large reheating temperatures, potentially overpopulating the universe with relics such as gravitinos or monopoles [22, 11].

5.3 The Affleck-Dine Mechanism

The Affleck-Dine (AD) Mechanism [47] was firstly proposed in 1985 by Michael Dine and Ian Affleck as a mechanism of Baryogenesis. In this model, the AD-field is a scalar field that parametrizes some non-zero $B-L$ SUSY flat direction and acquires a large vev during inflation. After inflation ends, the complex phase of this field gains a velocity, generating the $B-L$ asymmetry. This mechanism might also be responsible for the production of dark matter. If this is the case, it provides a natural way of explaining their similar density parameters as we will show in Chapter 6. Due to the sphaleron processes, we must keep in mind the relevant $U(1)$ asymmetry we need to produce is a $B-L$. However, for simplicity, we will refer to it as baryon number.

Baryon number production

One of the main characteristics of the AD-mechanism is the connection between a complex phase velocity and the production of baryon number. Consider the following global phase transformation of a complex scalar field:

$$\begin{aligned} \phi &\to e^{i\alpha}\phi \simeq \phi + i\alpha\phi \\ \phi^* &\to e^{-i\alpha}\phi^* \simeq \phi^* - i\alpha\phi^* \end{aligned} \tag{5.5}$$

By the variational principle, the variation of the action in a flat FRW spacetime is given by:

$$\delta S \sim \int d^4x \partial_\mu \Big[\sqrt{-g}(\partial^\mu\phi^*\phi - \partial^\mu\phi\phi^*)\Big] \tag{5.6}$$

Invariance under transformation Eq.5.5 implies the conservation of the number $N^0_\phi = ia^3(t)(\dot{\phi}^*\phi - \dot{\phi}\phi^*)$. If ϕ carries some baryonic charge, β, the baryon number density is given by:

$$n_B = i\beta(\dot{\phi}^*\phi - \phi^*\dot{\phi}) = 2i\beta\dot{\theta}|\phi|^2 \tag{5.7}$$

where, in the last step, we wrote ϕ in the exponential form $\phi = |\phi|e^{i\theta}$ and $\dot{\theta}$ is the complex-phase velocity. In order to secure the 1st Sakharov's condition , we need a source of baryon number violation. This can be achieved if the potential has terms that are not invariant under the transformations of Eq.5.5. Such terms are of the form:

$$V(\phi) \supset \phi^n + \phi^{*n} \tag{5.8}$$

The inflaton and the AD-field

During inflation, the vacuum energy is, by definition, positive and supersymmetry is broken. The SUSY-breaking terms (as the ones presented in section 3.2) are induced by non-renormalizable terms in the superpotential, which can be constructed by the product of invariant monomials (see [34]). Let X be some monomial that characterises a flat direction and whose scalar part may be parametrised as $X = c\phi^m$. This flat direction may be lifted by terms of the form:

$$W = \frac{\lambda}{nM^{n-3}}\phi^n \qquad W = \frac{\lambda}{M^{n-3}}\phi^{n-1}\psi \tag{5.9}$$

where M is some large scale such as M_p or M_{GUT} and ψ is the scalar part of some field that does not belong to the flat direction. In the context of SUSY, this gives an F-term contribution to the scalar potential (F_ϕ and F_ψ, respectively) of the form:

$$\mathcal{V}(\phi) \supset \frac{|\lambda|^2}{M^{2n-6}}(\phi^\dagger\phi)^{n-1} \tag{5.10}$$

which is $U(1)$-invariant, as mentioned on Section 3.2. Now, *SUGRA corrections* (Eq. (3.46)), give rise to two types of terms in the scalar potential of the AD field:

- Terms that appear whether or not the flat direction is lifted by a non-renormalizable or a renormalizable superpotential term. These terms do not depend on the scalar part of the flat direction's superpotential, $W(\phi)$:

$$\mathcal{V}(\phi) \supset e^{K(\phi^\dagger,\phi)/M_p^2}V(I) + K_\phi K^{\phi\bar{\phi}}K_{\bar{\phi}}\frac{|W(I)|^2}{M_p^4} + \Big(K_\phi K^{\phi\bar{I}}D_{\bar{I}}W^*(I)\frac{W(I)}{M_p^2} + h.c.\Big) \tag{5.11}$$

  where $\mathcal{V}(I)$ is the part of the potential corresponding to the inflaton:

$$\mathcal{V}(I) \simeq e^{K(I^\dagger,I)/M_p^2}\Big(F_I^*F^I - \frac{3}{M_p^2}|W(I)|^2\Big) \tag{5.12}$$

  This energy is dominant during inflation and the subsequent matter era. Thus, from the Hubble equation, $\mathcal{V}(I) \sim 3H^2M_p^2$, which gives $D_IW(I) \sim HM_p$ and $W(I) \sim HM_p^2$ [36]. The terms thus have the general form:

$$\mathcal{V}(\phi) \supset H^2M_p^2 f\Big(\frac{|\phi|}{M_p}\Big) \tag{5.13}$$

- Terms that arise if the flat direction is lifted by a non-renormalizable term such as Eq. (5.9). These terms depend on $W(\phi)$:

$$\mathcal{V}(\phi) \supset W_\phi K^{\phi\bar{\phi}}K_{\bar{\phi}}\frac{W^*(I)}{M_p^2} + \Big(\frac{1}{M_p^2}K_IK^{I\bar{I}}K_I - 3\Big)\frac{W(\phi)^*W(I)}{M_p^2} + W_\phi K^{\phi\bar{I}}D_{\bar{I}}W^*(I) + h.c. \tag{5.14}$$

  and give rise to the A-terms:

$$\mathcal{V}(\phi) \supset HM_p^3 f\Big(\frac{\phi^n}{M_p^n}\Big) \tag{5.15}$$

  These terms are very important, since they provide the $U(1)$-violation needed for Baryogenesis.

With the contributions from the terms above, the potential for the flat direction due to the couplings to the inflaton is given by:

$$\mathcal{V}(\phi) = -cH^2(t)|\phi|^2 + \lambda\Big(\frac{aH(t)\phi^n}{nM^{n-3}} + h.c.\Big) + |\lambda|^2\frac{|\phi|^{2(n-1)}}{M^{2(n-3)}} \tag{5.16}$$

where a is complex and λ and c are real parameters of $\mathcal{O}(1)$. With a minimal Kahler term, the last term of Eq. (5.11) is absent and $c < 0$. However, non-minimal Kahler terms become relevant during inflation and the last term is likely to contribute so that $c > 0$. Following the procedure of [36], we shall consider the latter case.

Hidden Sector SUSY-breaking

Similarly to the case of the Inflaton, the hidden sector responsible for soft SUSY breaking at low energies also introduces SUGRA corrections to the flat direction's potential. These terms may be obtained by changing $I \to X$ in Eqs. (5.11) and (5.14). However, the potential is different and may be approximated by $\mathcal{V}(X) \sim |F_X|^2$, giving $D_X W(X) \sim F_X$ and $|W(X)| \sim |F_X|^2/M_X$. Mass terms arise, in analogy with Eq. (5.13) from the exponential term of Eq. (5.11):

$$\mathcal{V}(\phi) \supset \frac{|F_X|^2}{M_p^2}\phi^\dagger\phi \quad \to \quad m_{susy} \sim \frac{F_X}{M_p} + \mathcal{O}(M_p^{-4})f \tag{5.17}$$

These terms are the soft terms induced by the hidden sector SUSY breaking terms mentioned in Section 3.2. There are also new A-terms (capital letter A-terms correspond to Hidden sector SUSY-breaking), the dominant part comes from the first term of Eq. (5.14):

$$\mathcal{V}(\phi) \supset \frac{\lambda}{M^{n-3}}\frac{|F_X|^2}{M_p^2 M_X}e^{-i\alpha}\phi^n + h.c. \sim \lambda\frac{A m_{susy}}{M^{n-3}}\phi^n + h.c. \tag{5.18}$$

where A absorbs the complex phase of $W(\chi)$, α. This terms may also be induced by gauge interactions of the messenger fields with the MSSM. The precise nature of these terms is out of the scope of this work (see [32, 30]), what we should keep in mind is that SUSY-breaking induces these terms which become relevant as soon as the Hubble parameter decreases below m_{susy}.

Dynamics of the AD-field

During inflation, the Hubble parameter may simply be regarded as a constant $H(t) = H_I$.

$$\mathcal{V}(\phi) = -cH_I^2|\phi|^2 + \lambda\Big(\frac{aH_I\phi^n}{nM^{n-3}} + h.c.\Big) + |\lambda|^2\frac{|\phi|^{2(n-1)}}{M^{2(n-3)}} \tag{5.19}$$

If the A-term is non-zero, the $U(1)$ global phase symmetry is broken and there will be n degenerate minima with phase differences of $2\pi/n$ (as shown for $n = 4$ in Figure 5.3a). During this period, for $c \sim \mathcal{O}(1)$, the induced mass on ϕ is comparable to the damping term $m_\phi = V''(\phi_0) = \mathcal{O}(1)H_I \sim 3H_I$. Thus, the motion of the AD-field is critically damped and the field rapidly approaches one of the potential minima for a general set of initial conditions (Figure 5.3b).

$$\ddot{\phi} + 3H_I\dot{\phi} + V'(\phi) = 0 \tag{5.20}$$

At the end of the inflation, the AD-field is at the minimum of the potential, with a large vev.

$$|\phi_0| \sim \Big(\frac{\sigma H_I M^{n-3}}{\lambda}\Big)^{\frac{1}{n-2}} \qquad \arg(\phi) = \theta_I \tag{5.21}$$

where σ is an $\mathcal{O}(1)$ combination of the parameters c, a and n.

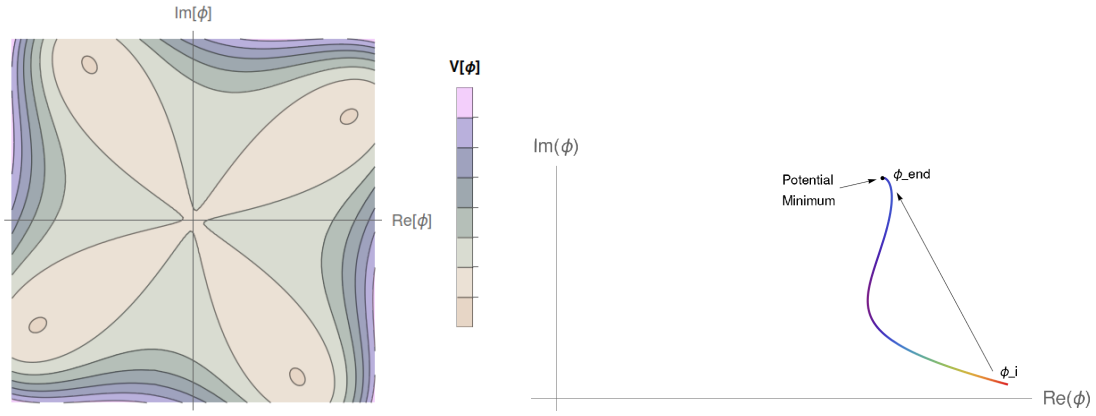

(a) (b)

Figure 5.3: a) For $n = 4$, the potential has 4 discrete minima. The tilt is caused by the complex parameter a phase. b) During inflation and for a general set of initial conditions, the AD field rapidly approaches one of its potential minima.

After inflation ends, the universe enters an inflaton-matter dominated era. Supersymmetry is broken due to the energy density of the inflaton oscillations around the minimum of its potential, $V(I)$. The Hubble parameter is no longer constant, decreasing as $H(t) \sim 2/(3t)$. Since the inflaton still dominates the energy density and while $H(t) \gg m_{susy}$, the $\mathcal{V}(\phi)$ terms do not change significantly:

$$\mathcal{V}(\phi) = -cH(t)^2|\phi|^2 + \left[\frac{aH(t)\lambda\phi^n}{nM^{n-3}} + h.c.\right] + |\lambda|^2\frac{|\phi|^{2(n-1)}}{M^{2(n-3)}} \tag{5.22}$$

As time passes, the minimum amplitude decreases with the Hubble parameter (Eq.(5.23)). The AD-field motion is still critically damped. Thus, it tracks the minimum closely, possibly with small oscillations around it [36]. The phase established at the end of inflation remains unaltered.

$$|\phi_0(t)| \sim \left(\frac{\sigma H(t) M^{n-3}}{\lambda}\right)^{\frac{1}{n-2}} \quad \arg(\phi) = \theta_I \tag{5.23}$$

As the Hubble parameter approaches the SUSY-breaking scale $H(t) \sim m_\phi$, the hidden-sector SUSY-breaking terms mentioned above in this section become relevant.

$$\mathcal{V}(\phi) = (m_\phi^2 - cH^2)|\phi|^2 + \left[\frac{(aH + Am_\phi)\lambda\phi^n}{nM^{n-3}} + h.c.\right] + |\lambda_n|^2\frac{|\phi|^{2(n-1)}}{M^{2(n-3)}} \tag{5.24}$$

where, by Eq. (5.18) m_ϕ, is typically of the order m_{susy}. For the baryonic sector, we take $m_\phi \sim 1$ TeV, as argued in section 3.2.

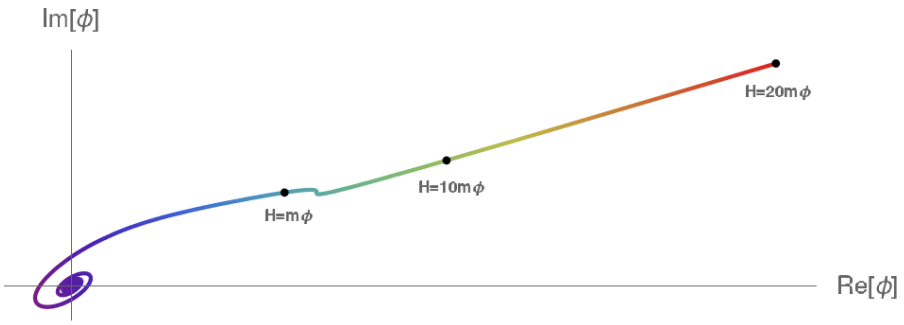

Figure 5.4: An example for $n = 4$. For $H > m_\phi$, the field follows a radial trajectory. At $H \sim m_\phi$, the field is subject to a torque and starts a spiral motion into the origin with conserved $\dot{\theta}$. We have used m

At this time, two relevant processes happen: Firstly, as the new A-terms become relevant ($H \sim m_\phi$), the phase of the minimum starts changing, inducing a non-zero angular velocity $\dot{\theta}$ for the field. Secondly, as $H(t)$ decreases, the induced quadratic mass term eventually becomes positive $\sim m_\phi^2$ and the minimum is now at the origin. Now, the field is under-damped, since the damping $\Gamma = 3H(t)$ term becomes smaller than m_ϕ. The AD-field spirals into the origin, with a fixed angular momentum and a red-shifting amplitude $|\phi| \propto a^{-3/2}$. An example of the AD field dynamics is shown in Figure 5.4.

In synthesis, this mechanism allowed us to produce a conserved angular momentum (per comoving volume) from general initial conditions. Since $n_B = \beta|\phi|^2\dot{\theta}$, if the AD-field carries B, this angular momentum can be associated to the production of a baryon number.

Notice that the phase difference between the A-term and the a-term is our source of CP-violation, as required by Sakharov's conditions (section 5.1). The baryon-number generated depends on this difference, as we have verified numerically (Figure 5.5). This dependence is frequently parametrized by the multiplicative parameter $\sin\delta \sim \mathcal{O}(1)$ [48].

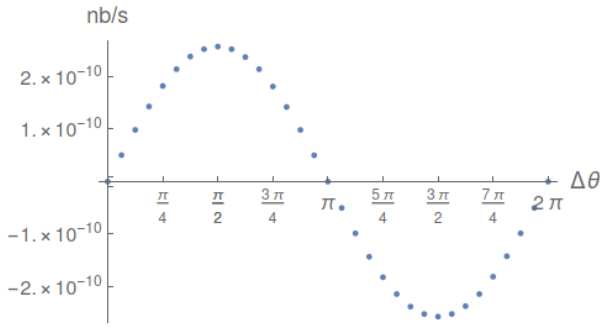

Figure 5.5: Number-to-entropy dependence on the difference $\Delta\theta = \theta_a - \theta_A$. In this example, we have considered a $n = 4$ potential, $M = 10^{-2}M_p$, $T_R = 10^{-7}M_p$, $m_{susy} = 10^{-15}M_p$ and $c = |a| = |A| = |\lambda| = 1$.

Baryon-to-Entropy ratio

Notice that this mechanism occurs during a matter dominated era, before the period of reheating, where the inflaton decays into relativistic particles. The baryon number produced by baryogenesis mechanisms is usually represented as the baryon-to-entropy ratio (Eq. (2.52)). This quantity is constant as long as there is no further production of baryon number or entropy. However, most of the entropy in the universe is produced during reheating.

From Eqs.(2.29) and (2.38), we obtain the relation between entropy and radiation energy density $s = \frac{4}{3}\frac{\rho_r}{T}$. If we assume that the inflaton energy density is fully transferred into radiation at the time of Reheating:

$$\rho_r \sim \rho_I \sim 3H^2 M_p^2 \tag{5.25}$$

Right after $H \sim m_\phi$, both the inflaton and the AD-field are non-relativistic, thus the ratio ρ_ϕ/ρ_I is constant until Reheating. As verified numerically, the ratio at $H = m_\phi$ with $\rho_\phi \sim m_\phi^2|\phi|^2$ (Eq. 5.23) is a good approximation for the subsequent evolution:

$$\frac{\rho_\phi}{\rho_I} \sim \frac{1}{3}\left(\frac{\sigma m_\phi M^{n-3}}{M_p^2}\right)^{\frac{2}{n-2}} \tag{5.26}$$

At Reheating, using the approximations above and the fact that $\rho_\phi = n_\phi m_\phi$:

$$\frac{n_b}{s} \sim n_b \frac{\rho_\phi}{n_\phi m_\phi}\frac{3T}{4\rho_I} \quad \rightarrow \quad \boxed{\frac{n_b}{s} \sim \left(\frac{M^{n-3}}{\lambda M_p^{n-2}}\right)^{\delta_n} T_R m_{susy}^{-1+\delta_n}} \tag{5.27}$$

where we have neglected $\mathcal{O}(1)$ multiplicative factors (such as σ and n_b/n_ϕ) and defined δ_n as:

$$\delta_n = \frac{2}{n-2} \leq 1 \quad , \quad n > 3 \tag{5.28}$$

After reheating, the AD-field eventually decays into quarks and leptons[1], transferring the produced baryon number $(B-L)$ to ordinary matter. Notice that the larger the SUSY-breaking scale, the smaller the baryon-to-entropy ratio. In particular for $n > 4$, this implies that some sector with a large SUSY-breaking scale would produce lower "baryon" abundance. Also, writing Eq. (5.27) as

$$\frac{n_b}{s} \sim \frac{10^{-4}}{\lambda^{\delta_n}}\left(\frac{10^2 M}{M_p}\right)^2 T_R m_{susy}^{-1+\delta_n} M^{-\delta_n}, \tag{5.29}$$

We note that, since δ_n decreases with n, because $m_{susy} < M$ and fixing T_R , M and m_{susy}, the baryon number production is more effective for larger larger n. This result has important implications, as we will discuss in the next chapter. Now, let us analyse how n restricts the space of parameters by imposing the produced baryon-to-entropy is of order 10^{-9} (Eq. (2.53))

- For $n = 4$, baryon-to-entropy does not depend on m_{susy}:

$$\frac{n_b}{s} \sim 10^{-11} \times \left(\frac{M}{10^{-2}\lambda M_p}\right)\left(\frac{T_R}{10^{-9} M_p}\right) \tag{5.30}$$

  In order for a $n = 4$ flat direction to produce the observed baryon-to-entropy ratio, reheating temperatures must be of the order $T_R \gtrsim 10^9$ GeV. These temperatures could have overproduced relics, as in the case of GUT baryogenesis (section 5.2)

- For $n = 6$:

$$\frac{n_b}{s} \sim 10^{-11} \times \frac{1}{\sqrt{\lambda}}\left(\frac{M}{10^{-2} M_p}\right)^3\left(\frac{T_R}{10^{-15} M_p}\right)\left(\frac{10^{-15} M_p}{m_{susy}}\right)^{1/2} \tag{5.31}$$

  In the $n = 6$, the Reheating temperature is low enough $T_R \lesssim 10^6$ GeV to escape the problems presented in the previous case.

[1] Typically fluctuations in the homogeneous AD-field grow and lead to the formation of "Q-balls" [49], i.e. localized AD-field configurations carrying the baryon number, which then decay into SM quarks.

Odd-n and R-parity

In the MSSM, the only $n = 7$ flat direction is the $\Phi^5 = LL\bar{d}\bar{d}\bar{d}$ and the $n = 9$ is the $\Phi^5 = QQ\bar{u}\bar{u}\bar{e}$ which, assuming R-parity is conserved, are lifted by [34]:

$$W_7 \supset \frac{\lambda}{M^4} LLLdddH_u \qquad W_9 \supset \frac{\lambda}{M^6} QuQuQueeH_d \tag{5.32}$$

respectively. Both have the form of the second type of Eq.(5.9), where the ψ field is H_u and H_d. Any A-term (see Eq. 5.14) arising from this superpotential terms would be proportional to $\langle H_u \rangle \ll \phi_0$ (or $\langle H_d \rangle$), making these flat directions subdominant when compared to $n = 6$. For Baryogenesis purposes, in the above conditions, Eq.(5.32) cannot induce the A-terms required on the respective flat direction in order to produce enough baryon number [49].

Chapter 6

Asymetric Baryo- and Dark-genesis

"It pays to keep an open mind, but not so open your brains fall out."

— Carl Sagan

In this section we will study the cosmological consequences of an $SU(3) \times SU(2) \times U(1)$ dark matter model. This simple model is constructed based on the gauge unification principle, where dark matter and visible matter share the same ultraviolet gauge structure and boundary conditions, whereas in the infrared they acquire different properties. We will show how this paradigm may naturally explain some of the dark matter-related issues such as the ρ_d/ρ_b coincidence and how a stable dark neutron may give rise to spherical distributions of dark matter in galaxies, while respecting the BBN and CMB constraints such as the bounds on the number of relativistic degrees of freedom and isocurvature perturbations.

6.1 Model Description

Baryonic/Visible sector: Let us suppose that nature is indeed supersymmetric and that the baryonic/visible part of the matter density in the universe is composed by MSSM particles. The scalars of this sector must have acquired masses of the order $m_{susy} \sim \mathcal{O}(1)$ TeV (breaking Supersymmetry), induced by some hidden sector F or D-term that is communicated through a messenger to the visible sector (as argued on Section 5.3), e.g.:

$$m_S^b \sim \lambda_b \frac{F_\chi}{M} \tag{6.1}$$

where χ is some hidden sector field that acquires the F-term, λ_b the coupling strength between χ and the baryonic-messenger and M is the messenger mass (typically Planck or GUT-scale). By the principle of gauge-coupling unification, we treat $M_{GUT} \sim 2 \times 10^{16}$ GeV as a fundamental scale, which may be common to other sectors. At unification, particle physics becomes invariant under some large gauge group transformation that contains $SU(3)_C \times SU(2)_L \times U(1)_Y$ as one of its subgroups. The coupling constants obey the unification condition:

$$\alpha_i^{-1}(M_{GUT}) \sim 25.6 \quad i = 1, 2, 3 \tag{6.2}$$

The non-relativistic energy density of the visible sector is mainly due to the most stable baryons. In this model, this baryon number density is produced by the Affleck-Dine mechanism, through the decay of the Baryonic AD-field (BAD) into visible sector particles.

Dark sector: In this model, dark matter particles belong to a new sector, which we call the Dark Sector. As required by dark matter evidence, interactions between the visible and dark sectors are predominantly gravitational. We impose that this sector also has

identical $SU(3) \times SU(2) \times U(1)$ gauge structure, particle content and GUT-scale boundary conditions as the visible sector:

$$\alpha_b(M_{GUT}) = \alpha_d(M_{GUT}) \sim 25.6 \tag{6.3}$$

where the indices b and d correspond to baryon and dark, respectively. This is motivated by heterotic superstring theories [50], where particle physics and gravity are coupled together using large groups such as $E_8 \times E_8$ or $SO(32)$. These groups contain two $SU(3) \times SU(2) \times U(1)$ as subgroups:

$$E(8) \times E(8) \supset \Big[SU(3) \times SU(2) \times U(1)\Big] \times \Big[SU(3) \times SU(2) \times U(1)\Big] \tag{6.4}$$

SUSY-breaking is mediated to the dark sector through the dark-messenger fields. As we shall see in the next section, the superpotential non-renormalizable terms (Eq. (5.9)) that lift the flat directions are of the same order n. However, in general, the coupling strength to the hidden sector is different from the one in Eq. (6.1), and so is the induced SUSY-breaking scale.

$$m_S^d \sim \lambda_d \frac{F_\chi}{M} \tag{6.5}$$

In theories with a large number of dimensions, some parameters are sensible to the local geometry of the extra dimensions. In particular, large hierarchies between m_S^d and m_S may arise due to the different sectors being located in different points of the additional dimensions.

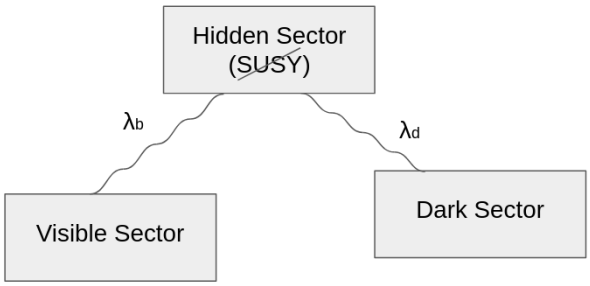

Figure 6.1: In principle, since the coupling constants and masses of messengers may differ, the communication of SUSY breaking to the visible and dark sector is not symmetric, resulting in different m_S scales.

As a result, the SUSY-breaking scale in the dark sector (m_S^d) may be much larger than the TeV-scale and dark scalars become much heavier than in the visible sector. However, as we will see in the next section, despite this large hierarchy we may naturally obtain an $\mathcal{O}(1)$ ratio of densities.

$$\frac{\rho_b}{\rho_d} \sim \frac{m_b}{m_d}\frac{n_b}{n_d} \sim \frac{1}{5} \tag{6.6}$$

Dark fermions, as in the MSSM, acquire masses proportional to the dark electroweak scale and to the Yukawa coupling to the corresponding Higgs boson. Flavon models [51, 52] propose that Yukawa couplings to the Higgs may be explained by some SSB mechanism caused by the vev of one or more pseudo-Goldstone bosons known as flavons. Despite being expected some flavour hierarchy, the mass-splittings in the dark sector need not be the same nor related to the visible sector analogues. However, the SUSY-breaking and electroweak scale ratio (which is related to the running of the squared Higgs mass and the particle content) should be roughly the same, in principle with one $m_q \sim \mathcal{O}(1)\Lambda_{EW}$ dark-quark, in analogy with the top quark.

The number densities of dark-baryons are also produced by an Affleck-Dine mechanism. We call the scalar field that parametrizes the lifted flat direction the dark Affleck-Dine (DAD) field. These are the main assumptions of the model. Let us now proceed to some of the cosmological consequences.

6.2 The ρ_d/ρ_b ratio

General Method

In the visible sector, we know that the greatest part of mass density is dominated by protons and neutrons. Neutrons are just a little bit more massive ($m_p \sim m_n \sim 940$ MeV) and are only stable when in nuclei bound states. These quark-composed particles are the lightest baryons and decay into lighter particles is not allowed due to colour-confinement and baryon number conservation. Thus, we may argue that the matter content of the universe is dominated by the stable baryon of each sector.

As mentioned in Section 3.1, baryons are structures composed of three quarks, a simplified picture since these are just the "valence" quarks. These three quarks coexist along with a sea of gluons, quark-antiquark pairs and other virtual particles which carry most of the baryon's rest energy (see [53]). Most of a baryon mass is dynamically produced by QCD binding energy, with the three quark rest masses contributing to roughly 1% of the total mass. Now, notice that $\Lambda_{QCD} \sim 200$ MeV and the nucleon masses are of the same order of magnitude:

$$m_b \sim 5 \times \Lambda_{QCD} \tag{6.7}$$

it seems reasonable to link this "missing" energy with the quark confinement and the scale at which QCD becomes non-perturbative. As we shall see below, using GUT-scale boundary conditions Eq. (6.3) and by the same reasoning as Eq. (3.21), this scale depends on the dark sector SUSY breaking scale and serve as an estimate for the dark matter particle's mass.

Let us illustrate our reasoning starting by computing Λ_{QCD} for a generic SUSY-breaking scale by studying the running coupling constant α_3, with initial conditions imposed by Eq. (6.3) and assuming a single mass threshold (m_{susy}) i.e. assuming that every supersymmetric particle has a mass at the order of m_{susy} and decouples from the running at energies below this threshold. From now on, we will omit the gauge group index "3" and m_{susy} will be abbreviated to m_S:

$$\alpha^{-1}(Q) = \begin{cases} \alpha^{-1}(M_{GUT}) + \dfrac{b^S}{2\pi} \ln\left(\dfrac{Q}{M_{GUT}}\right) & , M \geq Q > m_S \\ \alpha^{-1}(m_S) + \dfrac{b}{2\pi} \ln\left(\dfrac{Q}{m_S}\right) & , Q < m_S \end{cases} \tag{6.8}$$

Notice that, since we are starting from high energies to low energies, we will be able to study its dependence on m_S. Typically, for the region of parameters b^S and m_S we are interested in, $\Lambda_{QCD} < m_S$. We may rewrite the evolution for $Q < m_S$ as:

$$\alpha^{-1}(Q) = \alpha^{-1}(M_{GUT}) + \frac{b^S}{2\pi} \ln\left(\frac{m_S}{M_{GUT}}\right) + \frac{b}{2\pi} \ln\left(\frac{Q}{m_S}\right) \quad , Q < m_S \tag{6.9}$$

Solving the above expression for $Q = \Lambda_{QCD}$, with $\alpha^{-1}(\Lambda_{QCD}) = 1$, we obtain (e.g. Figure 6.2a):

$$\Lambda_{QCD} \sim M_{GUT}^{\epsilon} m_S^{1-\epsilon} \exp\left(-\frac{2\pi}{b}(\alpha^{-1}(M_{GUT}) - 1)\right) \quad , \quad \epsilon = \frac{b^S}{b} \tag{6.10}$$

where for the MSSM, $\epsilon = 3/7 < 1$ (from Figures 3.3 and 3.6), the Λ_{QCD} dependence on m_S is shown in Figure 6.2b.

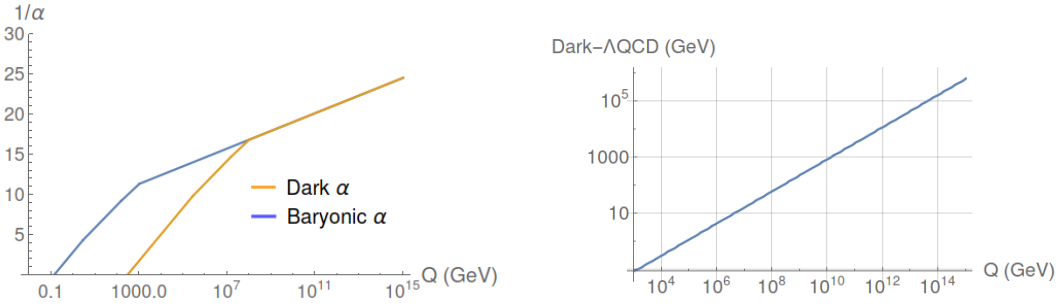

(a) α^{-1} vs. Q (b) Λ_{QCD} vs. m_S

Figure 6.2: a) Example of the coupling constant dependence on the interaction energy-scale, Q, for $m_s^b \sim 10^3$ GeV and $m_s^d \sim 10^8$ GeV. b) A high-energy SUSY-breaking scale gives rise to stable dark-baryons of masses up to $\mathcal{O}(10^6)$ GeV. Notice that the SUSY-breaking scale dependence gets softened by the $1-\epsilon$ power.

Now notice that Eq. (6.10) has an almost-linear dependence on m_S, while Eq.(6.11), obtained in the last Section (Eq. (5.27)), has an almost-inverse dependence on m_S:

$$\frac{n_b}{s} \sim \left(\frac{M^{n-3}}{\lambda M_p^{n-2}}\right)^{\delta_n} T_R m_S^{-1+\delta_n} \tag{6.11}$$

where δ_n was defined in Eq. (5.28) and its values are summarized on Table 6.1. From Eqs. (6.10) and (6.11), a larger SUSY-breaking scale in the dark sector corresponds to heavier particles with a lower number density produced by the AD-mechanism. Thus, the energy density-to-entropy has just a mild dependence on the SUSY-breaking scale:

$$\frac{\rho}{s} \sim \left(\frac{M^{n-3}}{\lambda M_p^{n-2}}\right)^{\delta_n} T_R M_{GUT}^{\epsilon} \exp(\cdots) m_S^{\delta_n - \epsilon} \tag{6.12}$$

Now, as argued in section 6.1, the dominant contribution to the number densities is given by the flat directions with the largest n. As a consequence, the ratio between the visible and the dark sector's energy density is given simply by:

$$\frac{\rho_d}{\rho_b} \sim \mathcal{O}(1) \times \left(\frac{m_S^d}{m_S^b}\right)^{\delta_n - \epsilon} \tag{6.13}$$

If the power $\delta_n - \epsilon$ is small enough, we will be able to explain how two models with very different SUSY-breaking scales, masses and number may naturally present identical energy densities. We see from Figure 6.3, that a $\mathcal{O}(1)$ factor between the energy densities is actually very natural for flat directions lifted by order $n = 6, 7, 9$ non-renormalizable terms, even when $m_s^d \gg m_s^b$. However, as we discussed in section 5.3, within the MSSM the $n = 7, 9$ flat directions are not appropriate for the AD-mechanism. For this reason, we will only consider the dominant $n = 6$ flat direction from now on.

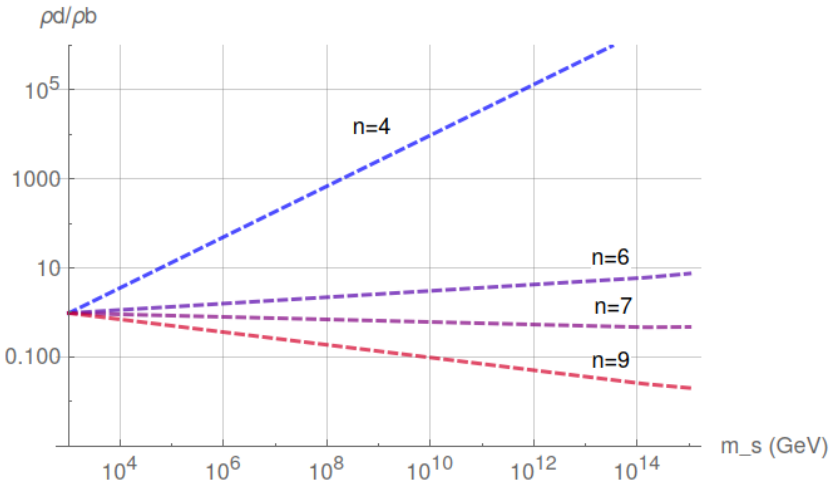

Figure 6.3: Density ratio between the dark and the visible sector caused by $n = 4, 6, 7, 9$ flat directions, as a function of the dark SUSY-breaking scale, m_s^d, using $m_s^b = 1$ TeV.

n	δ_n
4	1.00
6	0.50
7	0.40
9	0.28

Table 6.1: δ_n as a function of n.

More mass thresholds

In the previous subsection we found that the ratio of densities between the visible and dark sector may become mildly dependent on the SUSY-breaking scale as long as the exponent $\delta_n - \epsilon$ is small enough. This result was based on a simplified assumption that only the SUSY-breaking scale mass threshold would be significant for determining Λ_{QCD}. Now we are going to see how this relation changes as we introduce new thresholds. Let us start with the top quark with $m_t \sim \Lambda_{EW}$:

$$\alpha^{-1}(Q) = \begin{cases} \alpha^{-1}(M_{GUT}) + \dfrac{b^S}{2\pi} \ln\left(\dfrac{Q}{M_{GUT}}\right) & , M \geq Q > m_S \\ \alpha^{-1}(m_S) + \dfrac{b}{2\pi} \ln\left(\dfrac{Q}{m_S}\right) & , m_S > Q > \Lambda_{EW} \\ \alpha^{-1}(\Lambda_{EW}) + \dfrac{b^t}{2\pi} \ln\left(\dfrac{Q}{\Lambda_{EW}}\right) & , Q < \Lambda_{EW} \end{cases} \tag{6.14}$$

Now, the top quark decouples at an energy of the order the Electroweak scale and if Λ_{QCD} is below this scale, it will be affected. For $\Lambda_{QCD} > \Lambda_{EW}$, Λ_{QCD} is still given by Eq. (6.10) but, for $\Lambda_{QCD} < \Lambda_{EW}$ we obtain:

$$\Lambda_{QCD} \sim M_{GUT}^{\frac{b^S}{b^t}} m_S^{\frac{b-b^S}{b^t}} \Lambda_{ew}^{1-\frac{b}{b^t}} \exp\left(\frac{2\pi}{b^t}[1 - \alpha^{-1}(M)]\right) \tag{6.15}$$

We now have an extra dependence on the Electroweak scale and it may seem that the almost-linear dependence on the SUSY-breaking scale has been lost. However, we may rewrite $\Lambda_{EW} = \dfrac{\Lambda_{EW}}{m_S} m_S$:

$$\Lambda_{QCD} \sim M_{GUT}^{\frac{b^S}{b^t}} \left(\frac{\Lambda_{EW}}{m_S}\right)^{1-b/b^t} \exp\left(\frac{2\pi}{b^t}[1 - \alpha^{-1}(M)]\right) m_S^{1-\epsilon^t} \tag{6.16}$$

This expression is practically the same, but now with $\epsilon^t = b^S/b^t$ and $(\Lambda_{EW}/m_S)^{1-b/b^t}$. The effect of the latter to ρ_d/ρ_b is negligible since, as argued on section 6.1, the hierarchy

between the electroweak and SUSY-breaking scales should not be too different from the MSSM. The major consequences to the density ratio are related to the change in the $\epsilon \to \epsilon^t$ exponent.

If Λ_{QCD} occurs below lower mass thresholds (such as the bottom, charm,...), identical changes to the above expression would occur. As mentioned in section 6.1, the Yukawa couplings of fermions to the Higgs are not restricted by any unification condition. That is, the mass hierarchies do not need to be the same as in the MSSM (e.g. bottom, charm and τ may have different masse scales). However, the parameters ϵ are just related to the degrees of freedom coupled to the strong interactions (Eq. (3.19)). We present a summary of how the parameter ϵ behaves within the MSSM in Table 6.2.

Last Threshold	b	ϵ	$m_S^d \to \mathcal{O}(5)$
M_{GUT}	3	–	
m_S	7	$3/7 \simeq 0.43$	9×10^{12} GeV
m_t	23/3	$9/23 \simeq 0.39$	2×10^{9} GeV
$m_{b/c/\tau}$	9	$1/3 \simeq 0.33$	1×10^{7} GeV
m_s	29/3	$9/29 \simeq 0.31$	5×10^{6} GeV
$m_{u/d}$	11	$3/11 \simeq 0.27$	–

Table 6.2: Summary of the parameter ϵ according to the thresholds considered. The last column shows the typical dark SUSY-breaking scale so that give a $O(5)$ density ratio between the dark and baryonic sector (using $m_s^b \simeq 1$ TeV).

In Figure 6.4, we present the dark sector SUSY-breaking scale dependence of the density ratios. We see that even including all these mass thresholds, the dark matter and baryonic are still compatible for a wide range of SUSY-breaking scales, and hence for a wide range of masses. Additionally, we have been neglecting $\mathcal{O}(1)$ terms that may differ between the sectors and introduce relevant contributions to the ratio. However, any analysis of this kind would make the conclusions model-dependent.

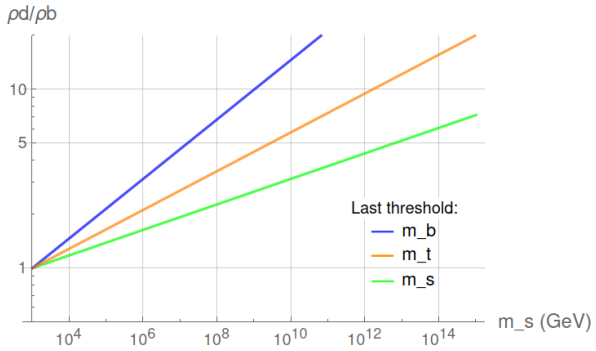

Figure 6.4: Density ratios considering new thresholds contributions. In blue, the bottom/charm quark threshold, m_b, in orange the top quark m_t and in green the dark-SUSY-breaking scale, m_S. The density ratios are plotted with respect to the dark-SUSY breaking scale considering the same mass hierarchies with respect to the SUSY-breaking scale as in the baryonic sector, with $m_S^b \simeq 1$ TeV.

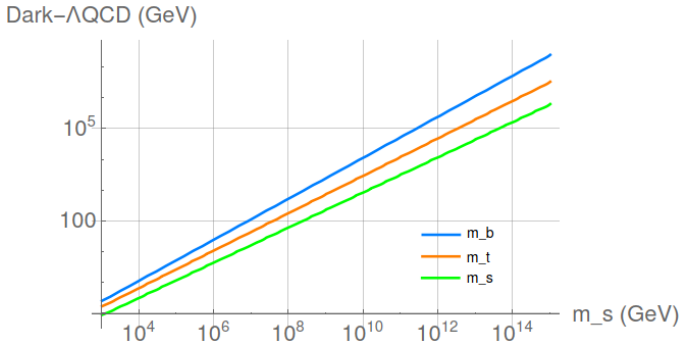

Figure 6.5: Typical baryon masses in the dark sector ($m_d \simeq \Lambda^d_{QCD}$), depending on its SUSY-breaking scale.

In the beginning of this section, we argued that most of baryon's mass is somehow related to Λ_{QCD}. If the dark "up" and "down" Yukawa couplings are such that these quarks become heavier than Λ_{QCD}, the dominant baryon's mass contribution now comes from the quarks' rest mass. In this scenario, the density ratio blows up. However, as in the baryonic sector, we may assume that the dark up and down quarks have masses below Λ^d_{QCD}, not contributing to the baryon mass computation.

6.3 Asymmetric Reheating

In this chapter we have been proposing the existence of a Dark sector which has an identical structure to the MSSM. Under the assumptions of this model, it explains the density ratios observed between dark and baryonic matter.

Now recall that in chapter 2 we presented the BBN and CMB constraints on the number of relativistic degrees of freedom (Eq. (2.48) and Eq. (2.49)). Since the dark sector is so similar to the MSSM, it must have its own relativistic particles e.g. the dark photon and possibly dark neutrinos. The dark photons, in particular, would contribute with two additional relativistic degrees of freedom if it were in equilibrium with the ordinary photons at recombination, which is ruled out by the CMB constraints on g_*. However, since the dark and visible sectors interact so weakly, there is no reason to assume this was the case. By Eq. (2.30), the contributions to Eqs. (2.48) and (2.49) are reduced if the dark sector's temperature is lower than the visible's.

A solution to this issue is provided by an asymmetric reheating, i.e., a period of reheating where the inflaton decays more effectively into one sector than into the other (Eq. (6.17)). In this case, we want the inflaton to transfer most of its energy density into the visible sector's relativistic particles. Since $\rho_r \propto T^4$, the two sectors acquire different temperatures.

$$\begin{aligned}
&\dot{\rho}_I + 3H\rho_I = -\Gamma_I \dot{I}^2 \\
&\dot{\rho}_b + 3H\rho_b = \Gamma_b \dot{I}^2 \\
&\dot{\rho}_d + 3H\rho_d = \Gamma_d \dot{I}^2 \\
&H^2 = \frac{8\pi G}{3}(\rho_d + \rho_b + \rho_I) \\
&\Gamma_I = \Gamma_b + \Gamma_d
\end{aligned} \tag{6.17}$$

where Γ_b and Γ_d are the inflaton decay rates into the baryonic and dark sector, respectively. In order to have an asymmetric reheating, we must have $\Gamma_b \gg \Gamma_d$. In order to understand where this asymmetry might come from, let us analyse the dominant inflaton

decay channels. The simplest decay comes from a coupling between the inflaton (assumed to be an MSSM-gauge singlet) and two scalar fields:

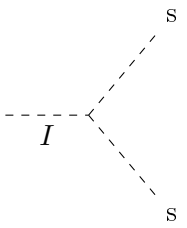

(6.18)

The inflaton decay into fermions is slightly more complicated. Fermions are chiral i.e. a left-handed fermion is charged under $SU(2)_L$ while the right-handed fermion is not. Thus, in order to construct an invariant term, the field that decays must have the same $SU(2)_L$ charge as the fermion. As mentioned in section 4.2, the inflaton, in order to have a flat enough potential slow-roll inflation, should be a singlet under the MSSM gauge group. Thus, the inflaton will never decay directly into fermions. It must decay first into a pair of virtual scalars (as in Eq. (6.18)) which, in turn, decay into two fermion pairs, as shown in Eq. (6.19).

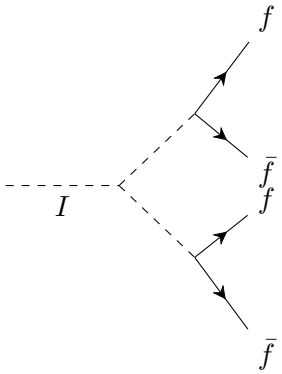

(6.19)

At reheating, the inflaton decays into both sectors through the above decay channels. However, if the SUSY-breaking mass is large enough in the Dark sector, the dark-scalar fields may become heavier than the inflaton. If this is the case, the inflaton can never decay into dark-scalar particles. In particular, the diagram of Eq. (6.18) is kinematically forbidden. Since the scalar fields in Eq. (6.19) are virtual, the inflaton may still decay into dark-fermions, but this decay rate is suppressed by powers of the virtual scalar field's mass-squared. The least suppressed term comes from the decay of Eq. 6.19, which yields:

$$\Gamma_d \propto \frac{m_I^8}{m_s^8} \tag{6.20}$$

This is what causes the asymmetry we needed to have an asymmetric reheating and to escape BBN/CMB constraints on the effective number of relativistic degrees of freedom. A solution to Eqs. (6.17) is shown in Figure 6.6. After reheating, the ratio between densities is equal to the ratio between the decay rates:

$$\frac{T_d^4}{T_b^4} = \frac{\rho_d}{\rho_b} = \frac{\Gamma_d}{\Gamma_b} \tag{6.21}$$

The contributions to the effective degrees of freedom from the dark sector are proportional to T_d^4/T_b^4. Thus, if dark sector SUSY-breaking scale is large enough to cause an asymmetric reheating, this model may pass the g_* tests imposed by CMB and BBN .

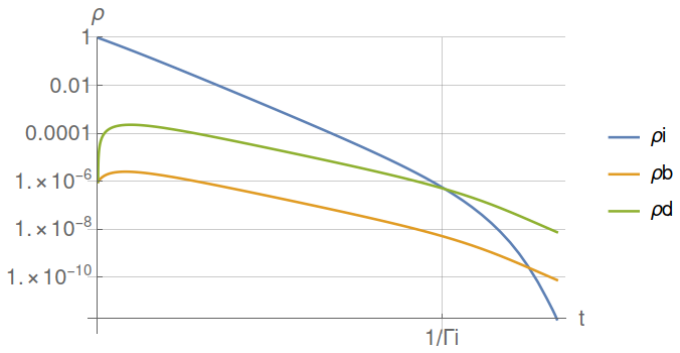

Figure 6.6: The solution to Eqs. (6.17) for $\Gamma_b = 100 \times \Gamma_d$ normalized to $\rho_\phi(0) = 1$.

6.4 Dark Matter Candidates

The Dark Neutron

A very intriguing property of particle physics may be seen when analysing the quark masses. The down-type quarks and the charged leptons have a very similar mass spectrum (Table 6.3). Recall that in section 3.2 we have mentioned that, in the MSSM, quarks and leptons acquire masses proportional to the vev of the corresponding Higgs boson (H_u for the up family or H_d for the down and electron family):

$$m_u = y_u v_u \quad m_d = y_d v_d \quad m_e = y_e v_d \tag{6.22}$$

Since these down-type quarks and charged lepton masses are proportional to the same Higgs vev, v_d, it seems that the corresponding Yukawa couplings follow the same generation patterns. In contrast, the up-family is typically heavier, which seems to be due to a different Higgs vev, v_u which, naturally, may be larger ($v_u > v_d$). What does not seem to be natural is the first generation where, suddenly, the three fermions masses are of the same order. And even worse: the up quark becomes lighter than the down quark.

Family	Gen.I	Gen.II	Gen.III
up	2.2 MeV	1.28 GeV	173.1 GeV
down	4.7 MeV	96 MeV	4.18 GeV
electron	0.5 MeV	105 MeV	1.77 GeV

Table 6.3: Masses of quarks and leptons

Just like the gauge coupling constants, the Yukawa couplings also depend on the energy scale. To first order, the evolution is given by [32]:

$$\begin{aligned}
\frac{dy_{u_i}}{dt} &= \frac{y_{u_i}}{16\pi^2}\left(6y_{u_i}^2 + y_{d_i}^2 - \frac{16}{3}g_3^2 - 3g_2^2 - \frac{13}{15}g_1^2\right) \\
\frac{dy_{d_i}}{dt} &= \frac{y_{d_i}}{16\pi^2}\left(6y_{d_i}^2 + y_{u_i}^2 + y_{e_i}^2 - \frac{16}{3}g_3^2 - 3g_2^2 - \frac{7}{15}g_1^2\right) \\
\frac{dy_{e_i}}{dt} &= \frac{y_{e_i}}{16\pi^2}\left(4y_{e_i}^2 + 3y_{d_i}^2 - 3g_2^2 - \frac{3}{5}g_1^2\right)
\end{aligned} \tag{6.23}$$

where i corresponds to the generation index. We tried to approach the problem by analysing the running of these couplings. The different behaviour of lighter generations could be due to the fact that Yukawa couplings are so small ($\mathcal{O}(10^{-5})$) that the negative

contributions from gauge couplings ($\mathcal{O}(10^{-1})$) would dominate, whereas, in the case of the third generation, $y_t \sim 0.7$ dominates.

We observed that (Figure 6.7) the running of 1st and 2nd generation barely change with the energy scale and we concluded that this is probably not the reason behind the up-mass "anomaly". Even if these Yukawa couplings start the running at a large scale (e.g. M_{GUT}) with $y_u(M_{GUT}) = y_d(M_{GUT})$, the evolution does not depend on the exact condition. Qualitatively, the up quark Yukawa coupling tends to become larger than the down quark's in the infrared, at least to first order.

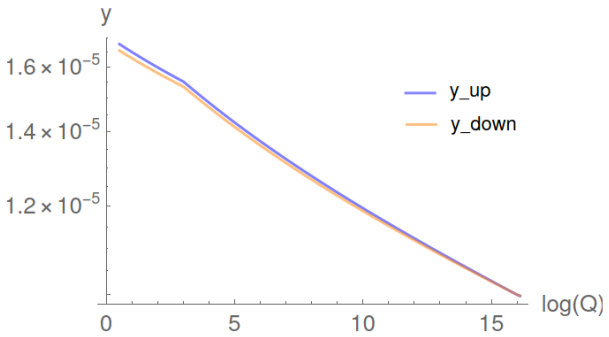

Figure 6.7: The dependence of y_u and y_d on the scale considering $y_u(M_{GUT}) = y_d(M_{GUT}) = 10^{-5}$. We found no evidence for a lighter up-quark caused by the running.

Hoping that a second order approximation would not change this scenario qualitatively, we are led to conclude that we were right at the beginning of this section: having an up-quark lighter than the down-quark does not look natural and it seems this is a special feature of the MSSM. It gets even more interesting if we compare the masses of the proton ($m_{uud} \sim 938.272$ MeV) and the neutron ($m_{udd} \sim 939.565$ MeV). The proton is the most stable baryon by a mass difference of $m_{udd} - m_{uud} \sim 1.293$ MeV, which is smaller than $m_d - m_u \sim 2.5$ MeV. If the up-quark were heavier than the down-quark, it would probably be enough to make the neutron the stable baryon.

Due to the above reasoning, we may envisage scenarios where the dark-up quark is heavier than the dark-down quark, forming stable neutrons. If this is the case, the electromagnetic interaction at large distances becomes negligible. The only interactions are short-ranged or gravitational. In galaxies, the visible sector matter distribution tends to evolve from spherical distributions to form disks due to total angular-momentum conserving collisions between objects. On the other hand, as mentioned in section 2.5, dark matter distributions in galaxies are approximately spherically uniform, it seems that there are roughly no collisions between these objects. Thus, a stable dark neutron in the Dark sector could be a reasonable candidate for dark matter, protected by dark-baryon number conservation.

The LSP

As we have seen in the previous section, our model may easily account for most of the dark matter present in the universe. This may be seen as a success, although, if we don't want to overpopulate the universe with dark matter candidates, we must deal with the remaining relics, such as the LSP. Let us analyse which conditions should be met so that the dark neutron becomes the dominant part of the dark matter abundance.

Firstly, why are we particularly worried about the LSP? Two of the most important conditions used in the construction of our model were Supersymmetry and R-parity. For this model, nature must be supersymmetric in order to use the new scalar fields and flat-directions they provide, as required by the AD-mechanism. R-parity appears when we try

to relate the AD-mechanism with the MSSM flat directions. We have relied on the study by Gherghetta [34], where R-parity and gauge-invariance were taken as primary assumptions in order to construct the set of non-renormalizable superpotential terms that are able to lift the MSSM flat directions. As we mentioned in section 3.2, these two conditions imply the existence of a stable Lightest Supersymmetric Particle (LSP).

Each sector has its own LSP (except if it is the gravitino, since gravity is common to both sectors). Whichever it is, its contribution to the dark matter may be subdominant today. If the dark sector SUSY-breaking scale is large enough, the reheating is asymmetric (section 6.3), the inflaton decays into the super-partners are forbidden resulting in a negligible dark-LSP abundance.

Now, turning to the visible sector, in order to there are two ways the LSP abundance can become negligible. In the first scenario, the LSP remains in thermal equilibrium with ordinary matter after becoming massive. As we have seen in section 2.3, for $T < m_{LSP}$, their equilibrium abundances get exponentially diluted. This dilution occurs via R-parity conserving processes such as $LSP + LSP \rightarrow$ ordinary matter. In the second scenario, the LSP becomes unstable and decays via R-parity violating processes.

There are some restrictions to the second case. Firstly, LSP decays any time after BBN would produce high-energy electromagnetic or hadronic showers. In order not to affect the BBN predictions for light element abundances, observations constrain the lifetime of the unstable LSP to $\tau < \mathcal{O}(10^7)$ s. Additionally, at low energies, as we mentioned in section 3.2, R-parity violation must be small enough so that the visible sector's proton remains stable. In any case, R-parity may be an exact symmetry in the early universe and be spontaneously broken at low energies. The parameter space of R-parity violating terms is large enough to allow this symmetry to be broken in some sector, allowing the LSP to decay, while forbidding proton decays (see [54]). These decays are expected to increase the entropy of the universe. This is not a problem, any increase in the entropy and consequent baryon asymmetry dilution caused by the LSP decay may be compensated by an increase in the initial asymmetry (Eq. (5.31)), requiring a higher reheating temperature, which does not change the density ratios presented above.

Thus, since we assume the dark-neutron dominates the dark matter energy density, in order for our model to be viable, the LSP abundance should be subdominant, which may occur via dilution in the thermal bath or R-parity violating decays.

6.5 DAD and BAD isocurvature perturbations

As shown in section 4.3, during the inflation, quantum fluctuations of subdominant fluids get stretched with expansion and eventually leave the horizon. If those modes are massless, their amplitude stays constant (Eq. (4.18)) until they re-enter the horizon again. However, if those modes have masses of the order of the Hubble parameter $m_\chi \sim H_I$, the perturbation amplitude gets exponentially redshifted with expansion. The AD-fields are two of such fields. Since these fields decay into baryons and dark-baryons, and their quantum fluctuations are uncorrelated, it is expected that a contribution to the uncorrelated matter isocurvature perturbations should arise. Since at the time CMB was emitted, the universe is dominated by matter, these perturbations should be encoded in the temperature spectrum. Interestingly, in the future, we may be able to isolate the baryon isocurvature perturbations by observations of the hydrogen 21 cm line [55]. Comparing with CMB, we may be able to deduce the contribution due to the dark-AD field, which could serve as an important probe of our model.

Mass term for the θ field

If we rewrite the AD-field in the complex-exponential notation $\phi = |\phi|e^{i\theta}$, the kinetic term changes to:

$$\partial_\mu\phi\partial^\mu\phi = \partial_\mu|\phi|\partial^\mu|\phi| + \phi_0^2\partial_\mu\theta\partial^\mu\theta \tag{6.24}$$

where ϕ_0 is given by Eq. (5.21). The AD-field has two degrees of freedom described by the real scalar fields $|\phi|$ and $\chi = |\phi_0|\theta$. The potential during inflation (Eq. (5.19)) as a function of these fields is given by:

$$\mathcal{V}(\phi) = -cH_I^2|\phi|^2 + \lambda\frac{|a|H_I}{nM^{n-3}}|\phi|^n\cos(\theta_a + n\chi/\phi_0) + |\lambda|^2\frac{|\phi|^{2(n-1)}}{M^{2(n-3)}} \tag{6.25}$$

In order to calculate the quantum fluctuation modes amplitude associated to χ and $|\phi|$, we are interested in these fields' masses, which are given by the second derivative of the potential, with respect to the corresponding field:

$$m_\chi^2 = \frac{\partial^2}{\partial\chi^2}V(\chi) \sim \lambda\frac{n|a|H_I}{M^{n-3}}\phi_0^{n-2}\cos(\theta_a + n\chi/\phi_0) \tag{6.26}$$

$$m_{|\phi|}^2 = -2cH_I^2 + \lambda(n-1)\frac{|a|H_I}{M^{n-3}}|\phi|^{n-2}\cos(\cdots) + 2\lambda^2(n-1)(2n-3)\frac{|\phi|^{2(n-2)}}{M^{2(n-3)}} \tag{6.27}$$

replacing ϕ_0 for its value during the inflation Eq. (5.21), the masses become:

$$m_\chi^2 \sim 2n|a|\sigma H^2\cos(n\chi/\phi_0) \tag{6.28}$$

$$m_\phi^2 = (|a|\sigma(n-1) + 2(n-1)(2n-3)\sigma^2)H_I^2 \sim \mathcal{O}(1)H_I^2 \tag{6.29}$$

so that the phase field χ may be lighter than the Hubble parameter during the inflation. As we will see, its fluctuations may be observable through the baryon isocurvature perturbations.

AD-field isocurvature perturbation

Baryon isocurvature perturbations (Eq. (4.28)) are given by:

$$S_{b\gamma} = \frac{\delta\rho_b}{3\rho_b} - \frac{\delta\rho_r}{4\rho_r} = \frac{\delta\eta_b}{\eta_b} \tag{6.30}$$

where the last equality follows from writing $\rho_b \sim m_b n_b$ and $\rho_r \sim sT$. This is, from the baryon-to-entropy ratio we are able to calculate the baryonic isocurvature perturbation. The result is analogous for the case of dark matter. In the previous sections, we have neglected the $\mathcal{O}(1)$ terms. In this section, we are now interested in the isocurvature perturbation produced by the angular degree of freedom. Let us write the baryon-to-entropy ratio as in [48]:

$$\eta_b \sim \left(\frac{M^{n-3}}{\lambda M_p^{n-2}}\right)^{\delta_n} T_R m_{susy}^{-1+\delta_n}\sin(n\theta)\sin(\delta) \tag{6.31}$$

where θ is the AD-field complex phase during the inflation. Evaluating at the end of inflation and from Fig. 5.3b, $\theta = \theta_A$. The isocurvature perturbations are, thus, given by:

$$S_{b\gamma} = \frac{n\cos(n\theta)}{\sin(n\theta)}\Big|_{\theta=\theta_A}\delta\theta \to \Delta_{b\gamma}^2 = n^2\cot^2(n\theta_A)\frac{\Delta_\chi^2}{\phi_0^2} \tag{6.32}$$

Δ^2_χ is obtained from the massive field perturbation amplitude Eq. (4.21) and is given by:

$$\Delta^2_\chi = \frac{H^2}{(2\pi)^2}\left(\frac{k}{aH}\right)^{3-2\nu} \tag{6.33}$$

The power-spectrum of baryon isocurvature modes is thus given by:

$$\Delta^2_{b\gamma} = \frac{n^2\cot^2(n\phi_A)}{(2\pi)^2}\left(\frac{\lambda}{\sigma}\right)^{1/2}\left(\frac{H}{M}\right)^{3/2}\left(\frac{k}{aH}\right)^{3-2\nu} \tag{6.34}$$

where the $cot(n\theta_A) \sim O(1)$ in the physically interesting cases and σ is a combination of the potential parameters a, n and c, as mentioned in section 5.3.

Matter isocurvature perturbation

The total matter isocurvature perturbation is given by:

$$S_{m\gamma} = \frac{\delta\rho_m}{3\rho_m} - \frac{\delta\rho_r}{4\rho_r} \tag{6.35}$$

writing $\rho_m = \rho_d + \rho_b$ and since the dark and visible perturbations come from different AD-fields, they are uncorrelated ($\langle\delta\rho_d\delta\rho_b\rangle = 0$), the dimensionless power-spectrum is given by:

$$\Delta^2_m = \left(\frac{\Omega_b}{\Omega_m}\right)^2\Delta^2_b + \left(\frac{\Omega_d}{\Omega_m}\right)^2\Delta^2_d \tag{6.36}$$

since isocurvature for visible and dark matter are given by the same expression Eq.(6.34), possibly only differing on the mass of the perturbation, m_χ, and other $\mathcal{O}(1)$ couplings:

$$\Delta^2_m = \frac{n^2}{(2\pi)^2}\left(\frac{\lambda}{\sigma}\right)^{1/2}\left(\frac{H}{M}\right)^{3/2}\left[\left(\frac{\Omega_d}{\Omega_m}\right)^2\left(e^{-N_e}\right)^{3-2\nu_d} + \left(\frac{\Omega_b}{\Omega_m}\right)^2\left(e^{-N_e}\right)^{3-2\nu_b}\right] \tag{6.37}$$

Slight differences between the dark and visible masses, m_χ (Eq. (6.28)), make the term of the least massive mode dominate over the other, thus we may have three cases:

$$\Delta^2_m \simeq \left(\frac{\lambda}{\sigma}\right)^{1/2}\left(\frac{H}{M}\right)^{3/2}\left(e^{-N_e}\right)^{3-2\nu} \times f_\Omega \tag{6.38}$$

where

$$f_\Omega \simeq \begin{cases} (\Omega_b/\Omega_m)^2 & , m_{DAD} > m_{BAD} \\ (\Omega_b/\Omega_m)^2 + (\Omega_d/\Omega_m)^2 & , m_{DAD} \sim m_{BAD} \\ (\Omega_d/\Omega_m)^2 & , m_{DAD} < m_{BAD} \end{cases} \tag{6.39}$$

From this we can conclude that in our model, if the isocurvature perturbations in the CMB are only due to baryonic and dark matter, the isocurvature power spectrum (IPS) observed in the CMB and in the 21 cm line spectra should only differ by the factor f_Ω, that relates de abundances.

Parameter Constraints

From the observational data presented in section 4.3, we may restrict the parameter space of the potential terms $V(\phi)$ during the inflation (Eq. (5.19)). The upper bound on isocurvature modes $\beta_{iso}(k_{mid}) < 0.037$ (Eq. (4.30)), with $k_{mid} = 0.050$ Mpc^{-1} translates into the upper bound for baryon isocurvature perturbations of:

$$\Delta^2_{b\gamma} < \frac{8.45\times10^{-11}}{f_\Omega} \tag{6.40}$$

replacing by Eq. (6.34), supposing $\lambda/\sigma \simeq \mathcal{O}(1)$ and solving for ν and m_χ, we obtain:

$$\nu < \frac{1}{2N_e} \ln\left[\frac{8.45\times10^{-11}}{f_\Omega}\left(\frac{M}{H}\right)^{3/2}\right] + \frac{3}{2} \tag{6.41}$$

$$\frac{m_\chi^2}{H_I^2} > \frac{9}{4} - \left(\frac{1}{2N_e} \ln\left[\frac{8.45\times10^{-11}}{f_\Omega}\left(\frac{M}{H}\right)^{3/2}\right] + \frac{3}{2}\right)^2 \tag{6.42}$$

The mass of the modes is related to the potential parameters by Eq. (5.19). The present upper bound for the Hubble parameter is given by:

$$H_I \sim \left(\frac{r}{0.01}\right)^{1/2} \times 10^{13}\ \text{GeV} \tag{6.43}$$

For the case of $N_e = 55$ and $M \sim M_{GUT} \sim 10^3 H$, we obtain:

$$m_\chi^2 > (0.25 - 0.37) H_I^2 \tag{6.44}$$

where the lower bound depends on the value of f_Ω.

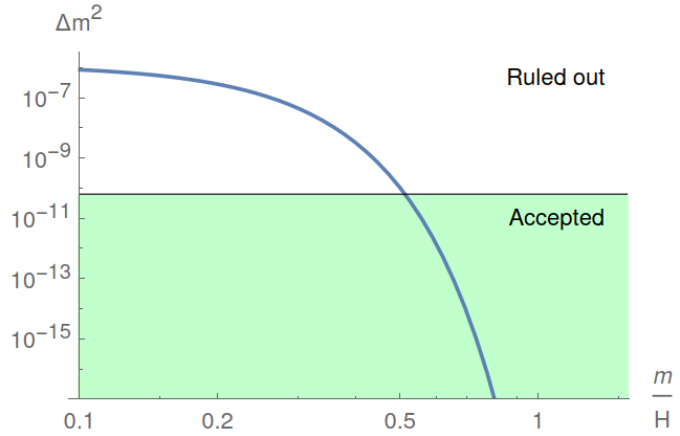

Figure 6.8: Parameter space for the χ field mass. We fixed $M = 10^3 H = M_{GUT}$.

Thus, the modes during the inflation must have masses of the order of the Hubble parameter in order to produce isocurvature perturbations compatible with experiment. Notice from Figure 6.8 that the isocurvature perturbation decreases abruptly as $m_\chi \to H$. Also, we did not bother considering cases where $m_\chi/H > 3/2$ (the solution presented in Eq. (4.21) is not valid for this region) since their amplitude decreases with the scale factor during inflation as $a(t)^{-3} \simeq e^{-3N_e}$ [43].

In summary, the isocurvature perturbations may not be observable if the field is too heavy. The evidence for our model mentioned in the last subsection may not be observed in the near future.

Chapter 7

Conclusions and Future Work

In this work, we have constructed a model of visible and dark matter in order to approach the $\rho_d/\rho_b \sim \mathcal{O}(1)$ density ratio coincidence. This model was constructed based on the gauge unification principle and supersymmetry, where both dark and visible sectors had an identical gauge structure and unification conditions, differing on their supersymmetry breaking scales. In analogy with the baryonic sector, we assumed the dominant part of dark matter is composed of dark-baryons.

In section 6.2, in order to explain the energy densities of (dark) baryons, we combined an Affleck-Dine mechanism for Baryogenesis and associated the strong-force confinement scale (Λ_{QCD}) with the scale of baryon masses in both sectors. We obtained that, while keeping a comparable energy density with the visible sector, the dark sector may have much heavier dark-baryons caused by its very large supersymmetry breaking scale.

In section 6.3, we showed that, even though the dark sector may have relativistic species, these do not violate the strict bounds imposed by BBN and CMB on the effective number of relativistic degrees of freedom. This comes as a result of scalars particles being heavier than the inflaton. In these conditions, reheating is asymmetric and the dark sector acquires a lower temperature, resulting in negligible contributions to the relativistic degrees of freedom, g_*.

In section 6.4, we have argued that in the dark sector the up quark could (and probably should) be heavier than the down quark, making the dark-neutron a new dark matter candidate. The fact that dark matter is mainly made of neutral particles results in weak interactions between particles, naturally explaining the near-spherical distribution presented by this sector. We also presented the conditions for a viable model, in particular, explaining how the LSP could give negligible contributions for the dark fluid.

Finally, in section 6.5, we presented a way to test our model from the isocurvature perturbation it leaves behind after inflation. An accurate measure of the CMB matter-IPS, together with a measure of the baryon-IPS, from future observations of the hydrogen 21cm line, will let us constrain the dark matter-IPS. Observing that these two IPS sources (dark and baryonic) are in fact uncorrelated and predicting correctly their ratio may serve as a smoking gun for the model presented above and provide valuable information to cosmology and particle physics. In particular, crucial clues for Baryogenesis, Inflation, GUT-scale physics and Supersymmetry may follow.

Up to this point, our model seems to describe dark and baryonic matter in a consistent way with observations, but it is not all there is. It is very interesting to see that, after all, dark matter may not be so different from ordinary matter. This critical assumption to our model is actually motivated by string theory models for quantum gravity. In some of these theories, two MSSM-like gauge groups can be embedded within the string theory gauge group. The large hierarchies between the SUSY-breaking scales and Yukawa couplings of both sectors may also be explained by these theories, where these hierarchies come from

both sectors "living" in different points of the additional compact dimensions and these quantities being dependent on the local geometry of this 6-dimensional space.

Since we have focused on making the discussion as general as possible, the model ended up becoming relatively simple. It leaves room for new assumptions and a more detailed analysis may be implemented in order to check for new cosmological consequences. Thus, we are looking forward to approach some scenarios we might have overlooked. We are aware that there are models where the first inflaton decays are non-perturbative. This gives rise to the so-called *preheating* and may give rise to a large production of dark scalars before the reheating. The question of whether or not the preheating changes section's 6.3 conclusions should be addressed in a later work. From section 6.4, we might want to study additional cosmological consequences of the dark neutron as the dark matter candidate. And also a deeper analysis on the LSP candidates, R-parity violating models and conditions for its sub-dominance may be a target of study in the future.

In summary, we have constructed a model for the cosmological evolution of dark and baryonic matter that is consistent with observations and symmetries of high energy physics. A model that can be tested and leaves room for further study.

Appendix A

A.1 Some useful integrals

$$\int_0^{+\infty} \frac{x^n}{e^x - 1} dx = \zeta(n+1)\Gamma(n+1) \tag{A.1}$$

$$\int_0^{+\infty} x^n e^{-x^2} dx = \frac{1}{2}\Gamma\Big(\frac{1+n}{2}\Big) \tag{A.2}$$

$$\frac{1}{e^x + 1} = \frac{1}{e^x - 1} - \frac{2}{e^{2x} - 1} \tag{A.3}$$

A.2 MSSM renormalizable flat directions and couplings

$X = \phi^m$	$B - L$	n
LH_u	-1	4
$QL\bar{d}$	-1	4
$QQQQ\bar{u}$	1	4
$\bar{u}\bar{u}\bar{u}\bar{e}\bar{e}$	1	4
$QLQL\bar{d}\bar{d}$	-2	4
$QQLL\bar{d}\bar{d}$	-2	4
$QQQQ\bar{d}LL$	-1	4
$QLQLQL\bar{e}$	-1	4
$QL\bar{u}QQ\bar{d}\bar{d}$	-1	4
$\bar{u}\bar{u}\bar{u}\bar{d}\bar{d}\bar{d}\bar{e}$	-1	4
$LL\bar{e}$	-1	6
$\bar{u}\bar{d}\bar{d}$	-1	6
$\bar{u}\bar{u}\bar{d}\bar{d}\bar{d}\bar{d}$	-2	6
$LL\bar{d}\bar{d}\bar{d}$	1	7
$QQ\bar{u}\bar{u}\bar{e}$	-3	9

Table A.1: Renormalizable flat directions in the MSSM with non-vanishing $B - L$ and order, n, of the non-renormalizable operator that lifts it.

A.3 MSSM Yukawa couplings

Family	Gen.I	Gen.II	Gen.III	times
up	9×10^{-6}	5.2×10^{-3}	7×10^{-1}	$\sin^{-1}\beta$
down	19×10^{-6}	3.9×10^{-4}	17×10^{-3}	$\cos^{-1}\beta$
electron	2×10^{-6}	4.2×10^{-4}	7.2×10^{-3}	$\cos^{-1}\beta$

Table A.2: Fermion-Higgs Yukawa coupling strengths

Bibliography

[1] NASA/WMAP Science Team, May 2013. https://map.gsfc.nasa.gov.

[2] W. L. Freedman, B. F. Madore, B. K. Gibson, and et al. Final results from the Hubble space TelescopeKey project to measure the hubble constant. *The Astrophysical Journal*, 553(1):47–72, may 2001.

[3] Particle Data Group and et al. Review of Particle Physics. *Progress of Theoretical and Experimental Physics*, 2020(8), 08 2020. 083C01.

[4] M. Kowalski, D. Rubin, and et al. Improved cosmological constraints from new, old, and combined supernova data sets. *The Astrophysical Journal*, 686(2):749–778, Oct 2008.

[5] J. Baur. *Determining the mass of cosmological neutrinos using Lyman-alpha forests*. PhD thesis, 09 2017.

[6] E. Corbelli and P. Salucci. The extended rotation curve and the dark matter halo of m33. *Monthly Notices of the Royal Astronomical Society*, 311(2):441–447, Jan 2000.

[7] D. Clowe, M. Bradač, Gonzalez A. H., and et al. A direct empirical proof of the existence of dark matter. *The Astrophysical Journal*, 648(2):L109–L113, aug 2006.

[8] Standard model of elementary particles. https://en.wikipedia.org/wiki/File:Standard_Model_of_Elementary_Particles.svg.

[9] B. Allanach. Going nowhere fast, Apr 2020. https://www.americanscientist.org/article/going-nowhere-fast.

[10] D. Baumann. Inflation. In *Theoretical Advanced Study Institute in Elementary Particle Physics: Physics of the Large and the Small*, 7 2009.

[11] J. Cline. Baryogenesis. 2006.

[12] N. Aghanim, Y. Akrami, M. Ashdown, and et al. Planck 2018 results. *Astronomy Astrophysics*, 641:A6, Sep 2020.

[13] E. Hubble. A relation between distance and radial velocity among extra-galactic nebulae. *Proceedings of the National Academy of Sciences*, 15(3):168–173, 1929.

[14] R. A. Alpher, H. Bethe, and G. Gamow. The origin of chemical elements. *Phys. Rev.*, 73:803–804, Apr 1948.

[15] J. Rosa. Introduction to cosmology. http://gravitation.web.ua.pt/cosmo.

[16] K. K. S. Wu, O. Lahav, and M. J. Rees. The large-scale smoothness of the universe. *Nature*, 397(6716):225–230, Jan 1999.

[17] S. M. Carroll. *Spacetime and Geometry: An Introduction to General Relativity*. Cambridge University Press, Cambridge, 2019.

[18] B. F. Schutz and Cambridge University Press. *A First Course in General Relativity*. Series in physics. Cambridge University Press, Cambridge, 1985.

[19] P. A. R. Ade, N. Aghanim, and et al. Planck2015 results. *Astronomy Astrophysics*, 594:A13, Sep 2016.

[20] G. Hinshaw, D. Larson, E. Komatsu, and et al. Nine-year wilkinson microwave anisotropy probe (wmap) observations: Cosmological parameter results. *The Astrophysical Journal Supplement Series*, 208(2):19, 09 2013.

[21] I. Zlatev, L. Wang, and P. J. Steinhardt. Quintessence, cosmic coincidence, and the cosmological constant. *Physical Review Letters*, 82(5):896–899, Feb 1999.

[22] E. W. Kolb and M. S. Turner. *The early universe.* Westview Press, 1990.

[23] D. Griffiths. *Introduction to Elementary Particles.* 2004.

[24] I. J. R. Aitchison and A. J. G. Hey. *Gauge Theories in Particle Physics: A Practical Introduction: From Relativistic Quantum Mechanics to QED, Fourth Edition.* Number vol. 1. Taylor & Francis, Oxfordshire, 2012.

[25] G. G. Ross. *Grand Unified Theories.* Benjamin/Cummings Publishing Company, San Francisco, 1985.

[26] J. Fuchs and C. Schweigert. *Symmetries, Lie Algebras and Representations: A Graduate Course for Physicists.* Cambridge Monographs on Mathematical Physics. Cambridge University Press, Cambridge, 2003.

[27] H. Georgi. *Lie Algebras In Particle Physics: from isospin to unified theories.* Frontiers in Physics. Avalon Publishing, New York, 1999.

[28] H. E. Logan. Tasi 2013 lectures on higgs physics within and beyond the standard model, 2017.

[29] M. E. Peskin and D. V. Schroeder. *An Introduction To Quantum Field Theory.* Frontiers in Physics. Avalon Publishing, 1995.

[30] S. Weinberg. *The Quantum Theory of Fields III - Supersymmetry*, volume 3. Cambridge University Press, Cambridge, 2019.

[31] I. Aitchison. Supersymmetry and the mssm: An elementary introduction. 06 2005.

[32] S. P. Martin. A supersymmetry primer. *Advanced Series on Directions in High Energy Physics*, page 1–98, Jul 1998.

[33] T. Appelquist and J. Carazzone. Infrared singularities and massive fields. *Phys. Rev. D*, 11:2856–2861, May 1975.

[34] T. Gherghetta, C. Kolda, and S. P. Martin. Flat directions in the scalar potential of the supersymmetric standard model. *Nuclear Physics B*, 468(1-2):37–58, May 1996.

[35] H. Nastase. Introduction to supergravity, 2012.

[36] M. Dine, L. Randall, and S. Thomas. Baryogenesis from flat directions of the supersymmetric standard model. *Nuclear Physics B*, 458(1-2):291–323, Jan 1996.

[37] B Audren, J. Lesgourgues, G. Mangano, P. D. Serpico, and T. Tram. Strongest model-independent bound on the lifetime of dark matter. *Journal of Cosmology and Astroparticle Physics*, 2014(12):028–028, Dec 2014.

[38] R.D. Peccei and H. Quinn. Cp conservation in the presence of pseudoparticles. *Physical Review Letters - PHYS REV LETT*, 38:1440–1443, 06 1977.

[39] R. D. Peccei. The strong cp problem and axions. *Axions*, page 3–17, 2008.

[40] A. H. Guth. Inflationary universe: A possible solution to the horizon and flatness problems. *Phys. Rev. D*, 23:347–356, Jan 1981.

[41] R. Allahverdi, R. Brandenberger, F.-Y. Cyr-Racine, and A. Mazumdar. Reheating in inflationary cosmology: Theory and applications. *Annual Review of Nuclear and Particle Science*, 60(1):27–51, Nov 2010.

[42] J. Martin and C. Ringeval. First CMB Constraints on the Inflationary Reheating Temperature. *Phys. Rev. D*, 82:023511, 2010.

[43] A. Riotto. Inflation and the Theory of Cosmological Perturbations. 2018.

[44] Planck Collaboration, Y. Akrami, F. Arroja, and et al. Planck 2018 results - x. constraints on inflation. *A&A*, 641:A10, 2020.

[45] A. D. Sakharov. Violation of CP Invariance, C asymmetry, and baryon asymmetry of the universe. *Pisma Zh. Eksp. Teor. Fiz.*, 5:32–35, 1967.

[46] A. G. Cohen, D. B. Kaplan, and A. E. Nelson. Baryogenesis at the weal phase transition. *Nuclear Physics B*, 349(3):727–742, 1991.

[47] I. Affleck and M. Dine. A New Mechanism for Baryogenesis. *Nucl. Phys. B*, 249:361–380, 1985.

[48] R. Allahverdi and A. Mazumdar. A mini review on affleck–dine baryogenesis. 14(12):125013, dec 2012.

[49] K. Enqvist, S. Kasuya, and A. Mazumdar. Adiabatic density perturbations and matter generation from the minimal supersymmetric standard model. *Physical Review Letters*, 90(9), Mar 2003.

[50] D. J. Gross, J. A. Harvey, E. Martinec, and R. Rohm. Heterotic string. *Phys. Rev. Lett.*, 54:502–505, Feb 1985.

[51] F. Bazzocchi, S. Bertolini, M. Fabbrichesi, and M. Piai. The little flavons. *Physical Review D*, 68(9), Nov 2003.

[52] F. Bazzocchi, S. Bertolini, M. Fabbrichesi, and M. Piai. Fermion masses and mixings in the little flavon model. *Phys. Rev. D*, 69:036002, Feb 2004.

[53] A. Martin and F. Halzen. *Quarks and Leptons: An Introductory Course in Modern Particle Physics*. Wiley, Michigan University, 1984.

[54] R. Barbier, C. Bérat, M. Besançon, and et al. R-parity-violating supersymmetry. *Physics Reports*, 420(1-6):1–195, Nov 2005.

[55] M. Kawasaki, T. Sekiguchi, and T. Takahashi. Differentiating cdm and baryon isocurvature models with 21 cm fluctuations. *Journal of Cosmology and Astroparticle Physics*, 2011(10):028–028, Oct 2011.